Universidade do Minho
Escola de Engenharia

Álvaro José Gonçalves da Cunha

Use of Vanadium Redox Flow Batteries to Store energy for Fast Charging Electric Vehicles in Gas Stations

dezembro de 2013

Use of Vanadium Redox Flow Batteries to Store energy for Fast Charging Electric Vehicles in Gas Stations

Álvaro José Gonçalves da Cunha

UMinho | 2013

Universidade do Minho
Escola de Engenharia

Álvaro José Gonçalves da Cunha

Use of Vanadium Redox Flow Batteries to Store energy for Fast Charging Electric Vehicles in Gas Stations

Tese de Mestrado
Ciclo de Estudos Integrados Conducentes ao
Grau de Mestre em Engenharia Mecânica

Trabalho efetuado sob a orientação do
Professor Jorge Martins
(Universidade do Minho)
Professor Francisco P. Brito
(Universidade do Minho)
Engenheiro Nuno Rodrigues
(Petrotec, Inovação e Industria)

dezembro de 2013

ACKNOWLEDGMENTS

Firstly I want to show my gratitude towards my supervisor, Professor Jorge Martins and my co-supervisor, Professor Francisco Brito from the Department of Mechanical Engineering. Their high scientific and pedagogic qualities contributed decisively to the realization of this work.

To Nuno Rodrigues, my supervisor from Petrotec, Inovação e Industria SA, for the help provided during the realization of this work. It was his great industrial knowledge that allowed this work to be conceived.

To Professor João Luiz Afonso and Vitor Monteiro from the Department of Industrial Electronics for all the help in field of power electronics and for sharing their knowledge.

To Paulo Remísio and Julio Campos from Petrotec, Inovação e Industria SA. for all the help and for the precious knowledge that they shared with me concerning technical questions of gas stations.

ABSTRACT

The expansion of car traffic and the expected growth of population for the next years have created serious environmental concerns about the dependence on fossil fuels, air pollution and emission of greenhouse gases. In this context, the electric mobility seems to be a good solution for minimize these problems. However, the actual time required to charge the batteries of these vehicles raises other questions about their usefulness. In order to reduce this time, the fast charge method is already available but a high contracted power is needed. On the other hand, the places where it is possible to allocate those chargers is also limited. So, in this work the use of fast charging stations in conjunction with Vanadium Redox Flow Batteries (VRFBs) is assessed. These batteries are charged during low electricity demand periods (at cheap rates) and then supply electricity for the fast charging of Electric Vehicles during electricity peak demand. They may be installed inside deactivated underground gas tanks at gas stations, which are normally located in practical and accessible locations for vehicles.

Firstly, a thorough review of the current State of the Art of VRFBs has been done, detailing their genesis, the basic operation of the various existing designs and the current and future prospects of their application. Flow batteries have unique characteristics which make them especially attractive when compared with conventional batteries, such as their long life and their ability to decouple rated maximum power from rated energy capacity, as well as their greater flexibility of shape.

Subsequently, a preliminary project of a VRFB system using the philosophy previously described, as well as its economic analysis has been performed. A sensitivity analysis showing the variation of the main output parameters as a function of the input parameters was also presented.

Voltage, Current, Power and Pumping Power were predicted and an efficiency around 92% was obtained for a system to charge 26 cars per day. The economic analysis estimated parameters such as the Net Present Value and the Payback Time which have been predicted to be 33 806€ and 9,5 years, respectively, for a lifetime of 20 years.

RESUMO

O aumento do tráfego automóvel e o crescimento populacional previsto para os próximos anos tem gerado preocupações ambientais sobre a dependência dos combustíveis fósseis, poluição do ar e emissão de gases de efeito de estufa. Neste contexto a mobilidade elétrica parece ser uma boa opção para minimizar estes problemas, no entanto atualmente o elevado tempo necessário para carregar as baterias destes veículos levanta questões sobre a sua utilidade. O método de carregamento rápido, que tem como objetivo de reduzir este tempo, já está disponível, no entanto é necessária uma elevada potência contratada, sendo os locais onde é possível colocar esses carregadores ainda limitados. Assim, neste trabalho é avaliado o uso de estações de carregamento rápido em conjunto com Baterias de Fluxo Vanádio Redox (VRFBs). Estas baterias são carregadas durante períodos de pouco consumo (a baixas taxas) para posteriormente fornecerem energia para carregar Veículos Elétricos durante horas de maior consumo de eletricidade. Estas baterias podem ser instaladas dentro de tanques de combustível subterrâneos desativados existentes nos postos de abastecimento de combustível, os quais estão normalmente situados em locais de fácil acesso a veículos.

Em primeiro lugar, realizou-se uma revisão do estado da arte das VRFBs, detalhando a sua génese, o modo de operação de várias configurações existentes e as perspectivas atuais e futuras da sua aplicação. As baterias de fluxo possuem características que as tornam especialmente atrativas em comparação com as baterias convencionais, como o longo ciclo de vida, a independência entre potência máxima e capacidade, assim como a sua grande flexibilidade de forma.

Realizou-se ainda um projeto preliminar de uma VRFB de acordo com o conceito anteriormente descrito, que incluiu a sua análise económica. Apresenta-se ainda uma análise de sensibilidade que mostra a variação dos principais parâmetros de *output* em função da variação dos parâmetros de *input*.

A tensão, potência, corrente e potência de bombagem foram simuladas, tendo-se obtido um rendimento de 92% para um sistema que permite carregar 26 carros por dia. A análise de custos incluiu a estimativa de parâmetros como o Valor Atual Líquido (33 806€) e o Tempo de Recuperação (9,5 anos), para um ciclo de vida considerado de 20 anos.

CONTENTS

FIGURE LIST

TABLE LIST

NOMENCLATURE

Acronyms

VRFB	Vanadium Redox Flow Batteries (G1 and G2 technologies)
RFB	Redox Flow Battery
G1	All vanadium redox flow batteries
G2	Vanadium bromide redox flow battery
ZBB	Zinc/Bromine technology
ZCB	Cerium/Zinc technology
PSB	Polysulfide/Bromide technology
ZNB	Zinc-Nickel Battery
SSFC	Semi-Solid Flow Cell
SoC	State of Charge
DoD	Depth of discharge
EV	Electric Vehicle
PHEV	Plug-In Hybrid Electric Vehicles
UPS	Uninterruptible power supply
GHG	Greenhouse gases
ICE	Internal Combustion Engine
PANI	Polyaniline
THD	Total Harmonic Distortion
PDVF	Polyvinylidene Fluoride
GMG	Graphene-Modified Graphite
GO	Graphite Oxide
Tris	Trishydroxymethyl aminomethane
TEOS	Tetraethoxysilane
DEDMS	Diethoxydimethylsilane
N-sDDs	Nafion-sulfonated diphenyldimethoxysilane
UNSW	University of New South Wales
MIT	Massachusetts Institute of Technology
NASA	National Aeronautics and Space Administration
REDT	Renewable Energy Dynamics Technology Ltd.
GEFC	Golden Energy Fuel Cell Co., Ltd.
GEC	Golden Energy Century Ltd

Variables

η_C	Coulombic efficiency	-
η_E	Energy efficiency	-
η_V	Voltage efficiency	-
η_{Ch}	ChadeMo charger efficiency	-
$\eta_{AC\text{-}DC}$	VRFB charger with an efficiency (AC/DC)	-
η	Efficiency of the VRFB without pumping losses	-
$\eta_{total\ VRFB}$	VRFB efficiency with pumping losses	-
η_{system}	Overall system efficiency	-
ρ	Specific mass of the liquid electrolyte	kg/m^3
P_{Leaf}	Power consumption of the Nissan Leaf during charge	kW
P_r	Real discharge power	kW
P_{out}	Power output	kW
P_{in}	Input power	kW
Er	Real discharged energy	W
E_a	Available stored energy	W
V_{disch}	Voltage output of stack during discharge	V
V_{chg}	Intput voltage of the stack during charge	V
OCV_{disch}	Open circuit voltage of the stack during discharge	V
OCV_{chg}	Open circuit voltage during charge	V
R	Internal resistance	Ω
I	Current	A
N	Number of cells	-
E^*	Equilibrium potentials	V
E	Equilibrium potentials	V
r	Universal constant of ideal gases	8,31447 $J.mol^{-1}.k^{-1}$
T	Temperature	K
F	Faraday constant	9.64853399 x 10^4 $C.mol^{-1}$
t	Time	s
t_{chg}	Defined time to charge VRFB	s
t_{disch}	Defined time to discharge VRFB	s
SoC_{min}	Minimum state of charge of VRFB during cycle	-
V	Volume of liquid stored	m^3

E	Energy density of the liquid electrolyte	W
C_{in}	Concentration of vanadium in the solution before the cell	mol/L
C_{out}	Concentration of vanadium in the solution after the cell	mol/L
P_{pump}	Pumping power	kW
Δp	Total pressure loss	Pa
Δp_{stack}	Pressure loss in the Stack	Pa
Δp_{pipe}	Pressure loss in the pipes	Pa
P	Permeability of the electrodes	m^2
l	Permeated specimen length of the electrode	m
A_{cs}	Permeated cross section area of the electrodes	m^2
Re	Reynolds number	-
f	Coefficient of friction	-
k	Coefficient of head loss	-
D	Internal diameter of the pipe	m
Le	Equivalent piping length	m
H	Head loss	m
V	Velocity of the fluid	m/s
L	Length of the section	m
g	Gravitational acceleration	m/s^2
μ	Dynamic viscosity	$N.s/m^2$
v	Cinematic viscosity of the fluid	m^2/s
ε	Roughness	mm
NPV	Net present value	€
Pt	Payback time	$years$
p	Electrical energy purchasing price	€
s	Electrical energy selling price	€
i	Inflation rate	-
i'	Real interest rate	-
TOG	Taxes over gain	-
$MARR$	Minimum acceptable rate of return	-
A	Amortizations	€
CF	Cash-Flows	€
S	Gain from sales	€
C	Costs associated	€
Nd	Number of cars per day	-
$EBITDA$	Earnings before interest, taxes, depreciation and amortization	€
A_r	Amortization rate per year	-
Inv	Investment	€
RBT	Results before taxes	€
Tax	Taxes	€
LR	Liquid result	€

Subscripts

chg	Charge
disch	Discharge
in	Input
out	Output
n	Year

1. INTRODUCTION

1.1. MOTIVATION

Transportation sector sustainability issues

The disruptive proliferation of urban traffic along the last decades, is posing serious sustainability concerns mainly those related to urban air quality and greenhouse gases (GHG) emissions, as well as the excessive dependency of developed economies on fossil fuels. It is expected that in 2030 the transportation sector will be responsible for 55% of total oil consumption [1]. It is also expected that the population will grow 1,7 times and the number of cars even more (3,6 times) between 2000 and 2050 [2]. In this context, the current policies promoting emissions reduction and the improvement of the energy efficiency of Internal Combustion Engines (ICE) are contributing to palliate these issues [3]. Various strategies have been explored along time, such as engine downsizing achieved with turbo-charging [4], the strategy of over expansion used in several efficient hybrid powertrains [5, 6] or waste energy harvesting such as exhaust thermal energy recovery in form of Organic Rankine Cycle or Seebeck effect thermoelectric generators [7, 8].

Electric mobility

Nevertheless, the increase of the overall efficiency of conventional powertrains does not seem sufficient by itself to achieve the efficiency and emissions goals set by national and international agreements, nor does it improve the desired diversity of energy sources. Nowadays, the main alternatives to the traditional ICE are the Plug-In Hybrid Electric Vehicles (PHEVs) and the full Electric Vehicles (EV) [9]. These alternatives allow the reduction of the global fossil fuels consumption that is allocated to the traditional transports systems and are a key technology to the future smart grids [10]. Some of these alternatives are now available in the market with substantial success [11], such as Toyota Prius (PHEV) or the Nissan Leaf (EV). These vehicles are globally more efficient than ICE vehicles, mainly under urban traffic since they have no idling losses, they have good low end torque without the need for inefficient clutching, and they can recover some of the kinetic energy lost during the braking [3, 11]. In [12] a comparative environmental life cycle comparison between conventional and electric vehicles has been

presented. As an example, using EVs, the global GHG emissions can decrease from 10% to 24% when compared with conventional diesel or gasoline vehicles. In [13] a study highlighted the EV as a means to contribute to the overall reduction of the fossil sources and energy used for transportation, although certainly this will depend on the electricity production performance.

Vehicle energy storage and charging

Unfortunately, the success of PHEVs and EVs is currently hampered by some notable disadvantages, mostly related with energy storage and grid charging [14]. Their main disadvantages are their typically low autonomy (usually up to 150 km) which results from the low energy density of current battery technologies and the long time required to perform standard battery charging processes (typically, a full charge will require around 8 hours to complete) [11, 15]. The combination of these two factors is known to induce the so-called range anxiety phenomenon which, along with the high cost of batteries, is preventing the wide adoption of electric mobility [16]. A range extender unit may be added to the powertrain to prevent this, and the merits was confirmed on a Life Cycle basis, of efficiency-oriented range extenders [17], but the use of such systems increases design complexity and cost, as the price tag of some existing models incorporating range extenders indicate.

In order to minimize the aforementioned shortcomings, some EVs allow to perform the battery charging process using the fast charging mode, namely through the ChadeMo protocol [18], which displays a maximum power output of 50 kW. With this charging mode the battery of many existing models can be charged up to 80% of their State-of-Charge (SoC) in less than half an hour [19]. However, the high power output required by these chargers is especially demanding in terms of infrastructure and power grid integration. A high power consumption plan must be contracted with the electric grid service provider, representing a substantial cost even without any energy consumption. Moreover, EV charging demand will normally occur at daytime, coinciding with costly electrical peak demand periods [20].

Intermediate stationary storage

Fortunately, many of the aforementioned disadvantages of fast charging may be averted by decoupling grid consumption and the consumption due to vehicle charging by means of stationary energy storage systems. In fact, the energy needed for high power vehicle charging may be stored previously and more gradually (with lower average power) at off-peak demand

schedules than in the case of direct grid vehicle charging. This allows reducing both the contracted power consumption limit and the average cost of electricity. Also, power quality problems associated with power grid voltage, stability and frequency are minimized [21].

In this context, the present work explores the use of a specific energy storage technology to perform EV fast charging during daytime but without the energy costs associated with electric consumption during those peak demand periods. Moreover, the proposed energy storage technology could also be integrated into microgrids, to store the energy produced by nearby intermittent renewable power sources contributing to smooth their output and adapt it to power demand [22].

Both the load leveling and peak shaving processes rely on the storage of electrical energy during low demand periods releasing that energy when the electrical load is high. In peak shaving the stored energy is discharged solely to remove the load peaks, while in the case of load leveling, the aim is to stabilize the electrical load avoiding fluctuations [23].

The comparison between peak shaving and load leveling is illustrated in Fig. 1.

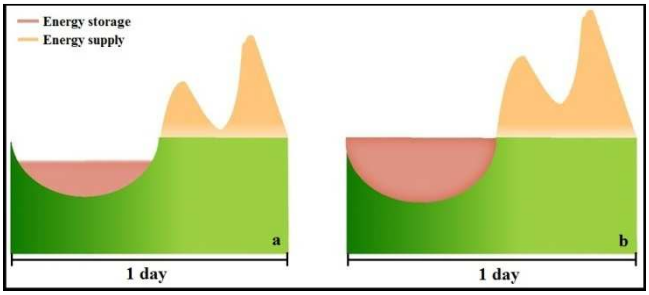

Fig. 1 - Comparison between peak shaving (a) and load leveling (b) (adapted from: [23]).

Typically, these two processes are implemented in low output power applications, such as domestic grids or small factories with a few kW of power. They have several advantages, the first of all being the reduction of the maximum power consumed from the power grid and consequently the reduction of the contracted power, which results in lower prices [20]. Secondly it permits a better management of the energy demanded from the power grid, taking into account the different energy prices depending of the schedule, because it is possible to buy cheaper

power during off-peak periods, such as during nighttime [20]. Thirdly it permits a greater incorporation into the grid of energy derived from renewable sources like solar and wind, which are unpredictable sources, often with the peak power generation occurring in counter-cycle with demand. This means that the availability of an energy storage buffer will avoid wasting the energy produced during low demand periods storing it and releasing it later during high demand events. This will enable a real substitution of fossil fuel derived energy production by renewable energy sources [24, 25].

Existing stationary storage solutions

Today, reversible hydroelectric power plants are being often used since they can use the excess of energy produced by renewables (generally the wind energy produced during night hours) to pump water back to the hydroelectric dam, which creates a gravitational energy storage. However, this resource is not always available or sufficient to solve the problem and so, the integration of large scale batteries systems in the electrical power grid seems to be a good solution for complement this energy storage system.

There are several energy storage technologies that can be used for load leveling and peak shaving processes besides the pumped hydro storage. They are compressed air storage and batteries. Regarding for batteries, many groups have been studied the use of lead acid [26, 27], sodium sulfur (NaS) [23], lithium ion [28] and also redox flow batteries [29] for this applications.

Flow Batteries

Many of the aforementioned systems have requirements not easily achieved for the application proposed in this work. Among the various battery technologies, the Redox Flow Batteries (RFB) have several advantages over the remainders, mainly because they have total independence between the energy capacity and rated power [30]. Other advantages of these batteries are related with their liquid nature and their storage (in tanks), which can be of any shape. In [31]the recent developments and studies of RFB concerning electrolytes, electrodes, membranes, and aqueous and non-aqueous systems have been reviewed. There are many types of RFB with various redox couples used, however, the Vanadium Redox Flow Battery (VRFB) is currently among the most studied and promising technologies of this kind. These batteries have the advantage of using the same material in both half cells. Thus, in the case of the cross mixing of the electrolytes there is no damage of the battery (as in the case of other RFBs) but only a self

discharge [32]. This is one of the main reasons for their fairly extended life even when comparing with the latest Li-ion battery chemistries. As main disadvantage, complete VRFB systems are still expensive, although the growing maturity of this technology and its attractiveness as an enabler for the wide adoption of intermittent renewable sources is likely to decrease its cost in the midterm [33-35].

Energy source shift in transportation and gas station business model

The recent economic crisis affecting several western economies was accompanied by a reduction in the demand of transportation fuel [36], this reduction is showed in Fig. 2and it can be seen that in the European Union the fuel consumption dropped by almost 4% of between 2007 and 2011. In the same period, the most pronounced reductions occurred in the Ireland and Spain which reduced around 23% and 15% respectively. Other sharp reductions can be also observed, like in Greece which reduced about 17% between 2009 and 2011 and in case of Portugal there was a sharp decline between 2010 and 2011 of about 7%.

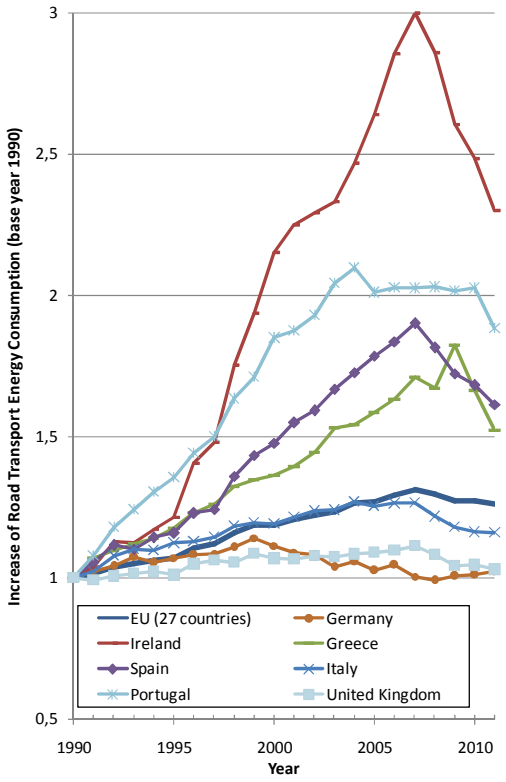

Fig. 2 - Variation of road transport energy consumption between 1990 and 2011 in some countries of European Union [36].

As an alternative to the costly and laborious deactivation/disposal of surplus large fuel storage tanks in gas stations, a retrofit of these deposits could be performed, adapting them for VRFB electrolyte storage and using the storage system for EV fast charging with the strategy explained before. One merit of such an approach would be to easily obtain EV fast charging spots in places which are already strategically located for vehicle traffic, optimizing otherwise wasted space and infrastructures and complementing the ICE vehicle fuel supply business with the emerging plug-in vehicle charging business in one place.

1.2.SCOPE OF THE PRESENT WORK

The present work aims to perform a preliminary project of a VRFB system installed in gas station environment taking advantage of its existing infrastructures. It is intended to store electric energy during low demand periods and use it for the fast charging of two electric vehicles simultaneously.

Given the lack of information concerning the emerging technologies involved, as well as the novelty of this topic within the UMinho research team, the present work starts with a detailed literature survey (Chapter 2), which carefully describes the operating principles of a vanadium redox flow battery, and analyzes in detail the existing VRFB technologies (G1 and G2). It provides a description of their major components, operation principles, performance, development over time, as well as the most recent developments, manufacturers and future prospects for the technology. After this, a preliminary project of the system is performed and analyzed in terms of energy efficiency, performance and economic viability, ending with a sensitivity analysis of the main parameters (Chapter 3). These two main chapters of the work have been based on two different articles submitted to the International Journal of Energy Research.

The principal motivation of the present work is based on the fact that, although the flow batteries are an emerging technology with a lack of available information in the literature, there is a real market need for such systems. This is so because there are currently no other technologies available for large scale energy storage applications displaying the same versatility and long-term reliability. On the other hand, to the author's knowledge, this work is of a pioneering nature even in international terms and for the company Petrotec it is considered as a future business opportunity which accompanies the slow, but steady shift of the petroleum-based

automotive economy towards the electric mobility paradigm. Moreover, it takes advantage of the vast network of existing infrastructure for supplying of conventional vehicles, a network which has the advantage of being located in places of easy and fast access for vehicles.

2. STATE OF ART OF VANADIUM REDOX FLOW BATTERIES

A battery is an electrochemical system, which is capable of storing chemical energy and generating electricity by a reaction of oxidation and reduction between two active materials.

A redox flow battery works on a principle similar to that of conventional batteries, but has the distinction of having the active materials separated from the region where electric current is generated (cell) [37]. Thus, it can be said that in a redox flow battery the active materials are not permanently sealed inside the container where electric current is produced (the cell) as in a conventional battery, but are stored separately and pumped into and across the cell according to the energy demand [32].

There are many types of redox flow batteries which can be classified by their active species, their solvent (aqueous or non-aqueous) and by the form of their active materials (liquids, solids, gaseous) [38].

There are also Hydrogen-based systems, also called “Fuel Cells” which take a fuel and an oxidant (typically hydrogen as a fuel and air as an oxidant) and produces electric energy and water [38]. However, normally a fuel cell is not considered a redox flow battery but if it could be designed in such a way that it would work in both charge and discharge directions, then a fuel cell could also be considered as a redox flow battery [38].

A typical redox flow battery incorporates two liquid electrolytes which are stored in two separate tanks (one being the positive electrolyte and the other one the negative), and they are pumped into the cell to produce energy, as depicted in Fig. 3. When the liquid electrolytes are injected into the cell (central part of Fig. 3), an electrochemical reaction (oxidation-reduction or redox) occurs, with movement of electrons along the electric circuit, as there is an exchange of ions through the membrane to maintain charge neutrality between the different ionic solutions [30].

In this chapter several types of flow battery technologies are described, and a full review of the state of art of the VRFBs is presented, including the types of VRFBs, the battery configuration, single cell configuration, the description of the circulation of the liquid electrolytes, the

configuration of storage tanks, the characteristics and performance, the components, and a comparison with conventional batteries. The typical applications and the current manufacturers are also presented in this chapter.

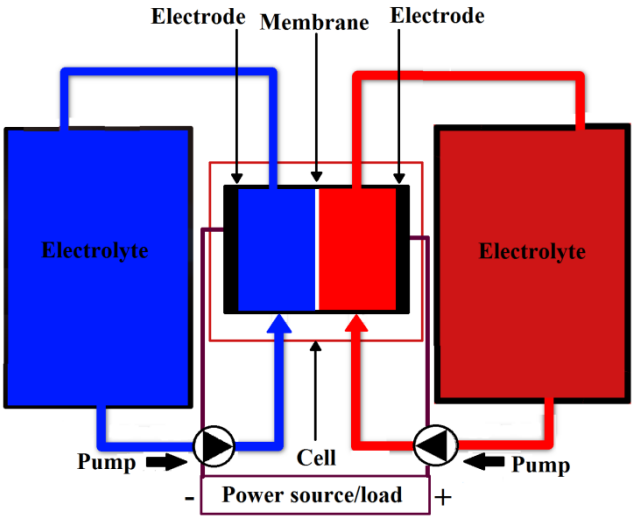

Fig. 3 - Operating principle of a redox flow battery.

2.1.TYPES OF REDOX FLOW BATTERIES

The first developed technology of flow batteries was the iron/chromium (Fe/Cr) one, developed by National Aeronautics and Space Administration (NASA) in 1970´s for photovoltaic applications [39, 40]. The positive reactant of this system is an aqueous solution of ferric-ferrous (Fe^{2+}/Fe^{3+}) redox couple and the negative reactant is a solution of chromous-chromic redox couple acidified with hydrochloric acid [41]. However, this system displayed low output voltage and efficiency and it was prone to crossover between iron and chromium ions [38].

The Polysulfide/Bromide technology (PSB) was patented in 1984 by Remick [42] and has been developed under the brand name Regenesys by Regenesys Technologies Ltd. a wholly owned subsidiary of RWE Innogy plc [43]. However, Regenesys is not considered a truly a redox system because both the positive and negative reactions involve neutral species, unlike a true redox system, which only involves dissolved ionic species [43]. This technology uses cation-exchange membranes [43-45] to separate the two liquid electrolytes in the compartments of

each cell and to provide a passage of ions to maintain electro-neutrality [44]. However, in case of rupture of the membrane in one of the cells, it will cause the mixing of both electrolytes and trigger the precipitation of sulfur [43].

The Zinc/bromine technology (ZBB) is called by Weber et al. [38] a hybrid redox flow battery because it does not store all the active material solely in liquid or gaseous form. In the ZBB technology, zinc is solid in the charged state and dissolved during the discharge, while the bromine is always dissolved in the aqueous electrolyte [43].

This technology utilizes $ZnBr_2$ as electrolyte in both half cells [43, 46] and these two electrolytes only differ in the concentration of elemental bromine and should have the same concentration of zinc and bromide ions at any given time during the charge/discharge cycles [43]. So, it is necessary to use an ion exchange membrane as the separator, which will allow the passage of zinc and bromide ions without allowing the passage of bromine or polybromine [43]. However, due to the high cost and low durability of the ion exchange membranes, this system generally uses nonselective micropourous membranes [43].

Comparing with other flow battery technologies, ZBB have a higher energy density, cell voltage and lower cost [47]. However, the low working current density results in a low power density (product of current density and cell voltage) [47], which means that bigger cells will have to be used for a given power output. But there are other problems with this technology, namely: bromine is highly dangerous for the environment [46], and presents problems associated with material corrosion, dendrite formation (which results in electrical shorting), high self discharge and short cycle life [38].

The Cerium/Zinc (ZCB) technology was patented by Plurion Limited Company [48] and it is described by Weber et al. [38] like a non aqueous redox flow battery, since it uses a methanesulfonic acid. This acid is used as a solvent for both electrolytes since it has conductivity comparable to hydrochloric acid but it has lower corrosion compared with sulfuric acid and it is more stable [49]. However, ZCB technology is at an early stage of development and there are still a few challenges that must be overcome [50], such as the low solubility of Cerium in methanesulfonic acid, the inefficiencies in the cerium discharge reaction in the early cycles and the increase of negative electrolyte acidity which is a result of the migration of protons from the positive electrolyte and also to the proton generation by the zinc electrodeposition [49]. An

advantage of this technology is its high current density compared with other redox flow batteries (successful operation of a cell at current densities as high as 400 – 500 mA/cm^2 has been claimed) [41]. Some authors reported an energy density of 12 - 20 Wh/L [51] but others have reported totally dissimilar values in the range to 37,5 – 120 Wh/L [38]. It is not clear the reasons for the differences found between the two works.

Recently single flow redox battery technologies based on lead acid batteries were proposed and studied by Pletcher et al. [52-60]. A single flow battery is different from the traditional redox flow battery because it has only a single liquid electrolyte which reacts with solid active materials, not needing an ion exchange membrane [46]. A soluble lead acid flow battery is represented in Fig. 4 and it can be seen that for a single flow redox battery system only one electrolyte tank and pump is needed. Zhang et al. [61] compared the soluble lead acid flow battery with a static lead acid battery and concluded that the soluble lead acid is more indicated for large scale energy storage systems, like a load leveling and smoothing with renewable energy systems. They also observed that the soluble lead acid exhibits a charge/discharge performance as good as a static lead acid battery and has the advantage of using methanesulfonic acid as electrolyte, which is biodegradable and environmentally friendly. However soluble lead acid batteries have disadvantages such as a lower cycle life and cell voltage.

Other single flow technologies have been proposed, such as the zinc-nickel battery (ZNB) suggested by Cheng et al. [62], which has good energy and coulombic efficiency (86% and 96% respectively, see chapter 6 for definition of coulombic efficiency) and also have high power and energy density (83 W/kg and 65 Wh/kg) when compared with other flow battery technologies [63].

The single flow acid Cu–PbO_2 battery developed by Pan et al. [64] uses low cost materials (PbO_2 as the positive electrode), and shows good coulombic and energy efficiencies (97% and 83% respectively) with a cell voltage of 1,29 V.

The single flow acid Cd–chloranil battery developed by Xu et al. [65] and employs solid organic material chloranil as the positive electrode, depositional cadmium as the negative electrode active substance and flowing H_2SO_4–$(NH_4)_2SO_4$–$CdSO_4$ solution as the electrolyte. This technology offers a discharge voltage of approximately 1,0 V and coulombic and energy efficiencies of 99% and 82% respectively.

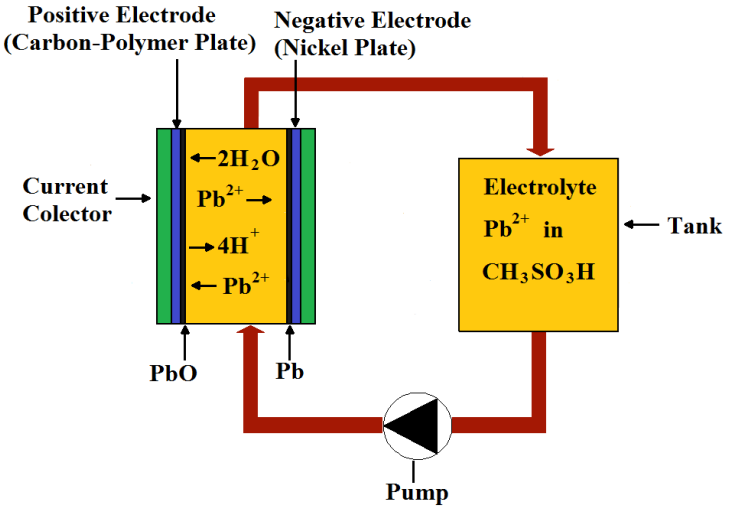

Fig. 4 - A soluble lead acid technology (adapted from:[61])

There is also a Zinc-Bromine single flow battery technology, first proposed and fabricated by Lai et al. [46] which involves a positive liquid electrolyte with a storage tank and pump system, and a semi-solid negative electrode. This technology has coulombic and energy efficiencies comparable to typical ZBB technology as well as improved energy density [46].

More recently, a single flow zinc/polyaniline battery was proposed by Zhao et al. [66]. Polyaniline (PANI) has received much attention due to its high conductivity, low cost and good redox reversibility, making it very attractive for electrode materials for use in batteries [66].

With the single flow technology it is possible to make Li-Redox flow batteries, which combines the high energy density of the lithium batteries with the advantages of the redox flow systems [67]. The use of a solid anode lithium metal with an aqueous cathode electrolyte was proposed by two groups independently, Goodenough et al. [68] and Wang et al. [69].

Another study combining redox flow batteries with lithium batteries was made by Duduta et al. [70] from Massachusetts Institute of Technology (MIT), who demonstrated a semi-solid lithium redox flow battery (they called it a semi-solid flow cell "SSFC"). This technology has inherent advantages when compared to other redox flow batteries, such as higher energy density (they use suspensions of dense active materials in a liquid electrolyte) and it can operate with very low flow rates which means very low mechanical energy dissipation. They estimate that SSFC

systems could achieve energy densities of 300 - 500 Wh/L (130 – 250 Wh/kg) something which could be satisfactory to use in electric vehicles [70].

Apart from the technologies previous described, there are also the systems which are highlighted in the present work. There are two main systems, the all vanadium system (in literature this is normally called the more recent vanadium bromide system (also called G2 technology). various redox flow battery technologies is performed in

Table 1.

One promising approach to improve the energy density of the all-vanadium system is to replace the positive electrolyte with an air electrode. Such system thus becomes, properly speaking, a new type of fuel cell, called vanadium-oxygen redox fuel cell. It was firstly proposed by Kaneko et al. in 1992 and firstly evaluated by Menictas and Skyllas-Kazacos in 1997 [75]. In a recent study, Menictas and Skyllas-Kazacos [75] have built a 5-cell stack assembly and tested it for a continuous period surpassing 120 h. This study demonstrated that a vanadium-oxygen redox fuel cell stack could be successfully constructed with a significant reduction of weight and volume. They also suggested the replacement of the sulfuric acid electrolyte by HCl or HCl/H_2SO_4 mixtures to improve the energy density, enabling the vanadium-oxigen fuel cells to have the triple or the quadruple of the energy density of the original all-vanadium system. However, in that study this technology was used only in fuel cell mode, which means that no recharging stage was considered. This technology might be a good solution for use in EVs in the future, since it has only one liquid electrolyte, and the regeneration (“recharging”) of the solution can be done outside of the vehicle in a separated cell optimized for charging the solution and without weight/size limitations. This operation consists on the reduction of the V^{3+} ions contained in the discharged (used) electrolyte to V^{2+} at the negative electrode, while producing gaseous oxygen at the positive electrode.

Table 1 - Comparison with various redox flow battery technologies

	G1	*G2*	*ZBB*	*ZCB*	*Regenesys*	*Fe/Cr*
Energy density (Wh/L)	20 – 33 [72]	35 - 70 [72]	50 [76]	12 – 20 [51] 37,5 – 120 [38]	20 – 30 [77]	-
Energy density (Wh/kg)	15 - 25 [72]	25 - 50 [72]	65 - 70 [46, 78]	-	20 [78]	<10 [78]
Nominal Voltage	1,4 V [37]	1 V [38]	1,8 V [43]	2,1 V [79]	1,35 V [80]	1,18 V [78]
Operational temperature	5 – 40 ºC [74]	0 – 50 ºC [74]	20 – 50 ºC [43]	20 - 60 ºC [49, 81]	20 – 40 ºC [77]	65 ºC (Optimal) [78]
Reported energy efficiency (η)	80 – 85 % [77]	60 - 70 % at 40 ºC [72]	75 % [77]	75 % [50, 82]	60 – 65 % [43-45, 77]	70 - 80 % [78]

2.2.DESCRIPTION OF THE VARIOUS TECHNOLOGIES OF VANADIUM REDOX FLOW BATTERIES

The use of a single metal in both half-cells was firstly proposed by N.H. Hagedorn [32], a solution which addressed the cross-contamination problem. Thus, the G1 was first patented in 1978 by Pellegri and Spaziante [71], which involves solely vanadium species in both half cells at different valence states. The G2 technology was first proposed by the University of New South Wales (UNSW) in 2001 [72] and employs a vanadium bromide solution in both half-cells [73] and

shares all the benefits of the G1 technology, including the fact that the cross contamination is eliminated [74]. In this subchapter the operating principles of these two technologies are described.

2.2.1. All-vanadium redox flow batteries (G1 technology)

A G1 operates in an electrochemical couple based on two different reactions of vanadium ions in a dilute acid solution. This is possible because vanadium is a stable material in four different oxidation states (V^{2+}, V^{3+}, V^{4+}, V^{5+}) [83].

The cathodic and anodic reactions can be represented as follows [84]:

$$VO_2^+ + 2H^+ + e^- \leftrightarrow VO^{2+} + H_2O \qquad E° = 1{,}00\ V$$

$$V^{2+} \leftrightarrow V^{3+} + e^- \qquad E° = -\ 0{,}26\ V$$

And the overall reaction is [84]:

$$VO_2^+ + 2H^+ + V^{2+} \leftrightarrow VO^{2+} + H_2O + V^{3+}$$

The separation of the redox couples in this system is usually made using a cationic exchange membrane, which allows the transport of H^+ protons while avoiding fluid mixing. This operation is depicted in Fig. 5 [33].

In a G1, the open circuit voltage is 1,6 V at 100 % State of Charge (SoC) and 1,4 V at 50 % SoC [84]. However there are notable obstacles in the development of cells for all-vanadium redox battery [32]. The first obstacle is the stability of the species V^{4+} and V^{5+} in some electrolytes, e.g., V^{5+} is unstable in solutions of HCl, and V^{4+} is unstable in solutions of NaOH [32]. The second impediment is the solubility of compound V^{5+} as V_2O_5 and Maria Skyllas-Kazacos and Robert Robins discovered that the rate of dissolution of V_2O_5 is very slow at room temperature, taking hours to dissolve completely [32].

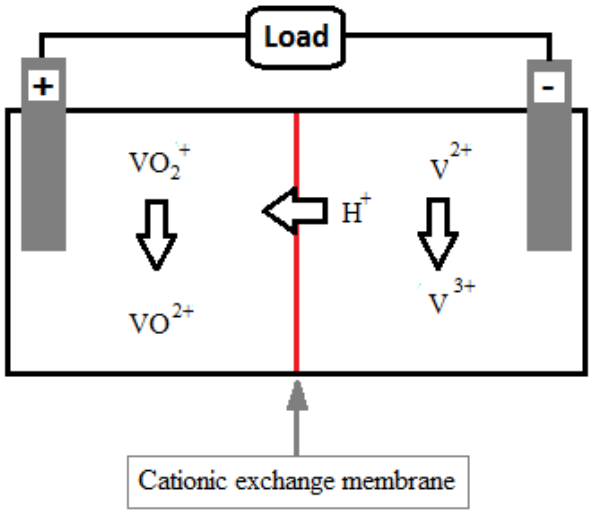

Fig. 5 - Operation of a G1 during discharge using a cation exchange membrane (adapted from:[33]).

Lather, these authors further discovered that pentavalent and tetravalent vanadium ions are stable in electrolytes such as aqueous H_2SO_4 and at least 2 M pentavalent vanadium be prepared in a solution such as 2 M H_2SO_4 electrolyte.

The main advantage of a G1 is that, in the event of a cross mixing between the two liquid electrolytes, the regeneration of the solution may be performed simply by recharging the fluids, unlike systems with different metals in which the mixed liquids would have to be replaced or removed and treated externally [32].

2.2.2.Vanadium bromide redox flow battery (G2 technology)

The G2 technology employs a vanadium bromide solution in both half-cells and since the bromide/polyhalide couple has lower positive potential than the V^{4+}/V^{5+} couple, the bromide ions will preferentially oxidize at the positive electrode during the charging [73].

The cathodic reactions of this technology are as follows [85]:

$ClBr_2^- + 2e^- \leftrightarrow 2Br^- + Cl^-$

or

$BrCl_2^- + 2e^- \leftrightarrow Br^- + 2Cl^-$

And the anodic reaction as follows [85]:

$V^{2+} \leftrightarrow V^{3+} + e^-$

Thus, while the negative half cell utilizes the same V^{2+}/V^{3+} redox couple as the G1 technology, the G2 technology uses the $ClBr_2^-/Br^-$ and/or $BrCl_2^-/Cl^-$, or even redox couples in reaction [85].

The G2 technology shares all the benefits of the G1 technology, mainly the fact that the cross contamination is eliminated because the same electrolyte is used in both half cells, resulting in electrolytes with virtually unlimited lifetime [74].

Other advantages of the G2 technology are the possibility of achieving concentrations of V^{2+} or/and V^{3+} ion species up to 4 M in hydrochloric acid supporting electrolyte [86]. This allows the doubling of the energy density potential of the G1 and enables the operation of the system at broader temperatures ranges (0° C to 50 °C), than those of G1 technology (5 °C to 40 °C, for 2 M of vanadium ion concentration) [74]. The extended lower temperature range is due to the higher solubility of vanadium bromide [72].

A typical electrolyte for a G2 includes 7 - 9 M HBr with 1,5 - 2 M HCl and 2 - 3 M Vanadium [72]. Furthermore, by utilizing a higher amount of bromide ions in positive electrolyte during charging, the volume of positive reservoir can be reduced by 50%. Thus, the total electrolyte volume can be reduced by 25% when compared to the G1 technology [72].

One disadvantage of the G2 technology is the risk of formation of bromine vapors during charging. Therefore, it is necessary to employ bromine complexing agents, although their high cost is a limiting factor for the commercialization of the G2 technology [73].

2.3.VANADIUM REDOX FLOW BATTERY CONFIGURATION

A vanadium redox flow cell is constituted by two half cells, each one having a solid electrode in contact with the liquid electrolyte. The separation between the half cells is made through a membrane [83], as shown in Fig. 3.

In a redox flow battery the cells are connected in series to form the cell stack, with the number of cells stacked depending on the nominal required output voltage.

In a cell stack the separation between cells is made by interposing bi-polar plates between them. Thus, a bi-polar plate is in contact with the negative electrode of one cell on one side, while on the opposite face it is in contact with the positive electrode of the next cell [83]. The constitution of a typical cell stack is shown in Fig. 6.

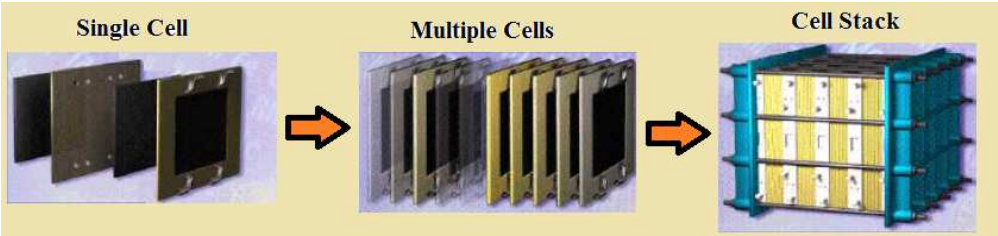

Fig. 6 - Constitution of a cell stack of a VRFB [83].

2.4.SINGLE CELL CONFIGURATION

Pertaining the configuration of single cells there are basically two options, one being the typical configuration with only the porous flow-through electrodes and the other including a flow channel to evenly distribute the electrolyte along the electrode [87].

A single cell constructed by Noack et al. [88] is presented in Fig. 7, where it is possible to identify the inlet channel of the electrolyte in the flow frame (d) which enables its circulation across the porous electrode (e). It is possible to observe that the flow frame enfolds the electrode when the cell is assembled in order to ensure a perfect sealing. On the other hand, it ensures the same prescribed compression of each electrode.

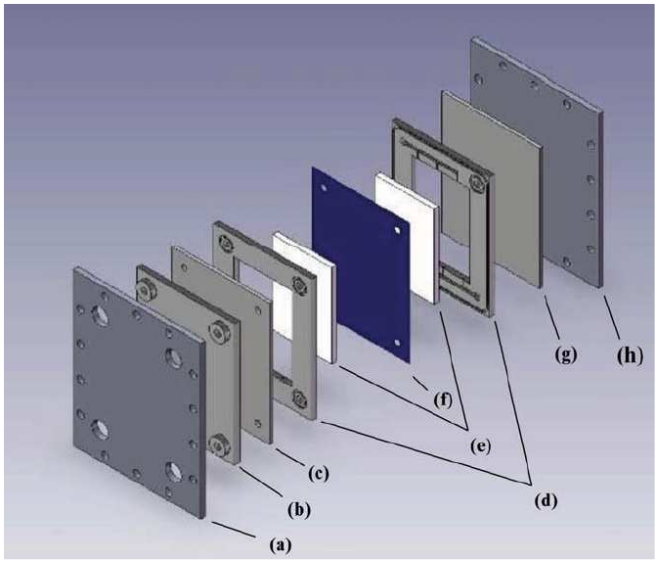

Fig. 7 - VRFB test-cell constructed by Noack et al. [88]; a) Steel plate, b) Isolation plate, c) Flow-through graphite electrode, d) Flow frame, e) Graphite felt, f) Membrane, g) Graphite electrode, h) Steel plate

However it is possible to use another configuration with a porous electrode in contact with a graphite plate in which a flow channel has been machined for electrolyte circulation, in Fig. 8 is represented a test cell made by Aaron et al. [87] which is possible to see the flow field used. In this test was demonstrated the all vanadium redox flow battery with the peak power density of 557 mW/cm^2 at 60% SOC, which apparently was the highest value reported until the date of the publication. This improvement of the energy density can reduce the quantity of material needed, which means a reduction of the cost of the system.

One way to improve the VRFB efficiency is minimize the contact resistances, so it must be used a “no gap” configuration which means that the electrodes, membranes and bi-polar plates must be in direct contact with no gap between electrode and membrane for the electrolyte flow.

In this configuration the flow into the electrode occurs due to diffusion and convection perpendicular of the flow channel [87].

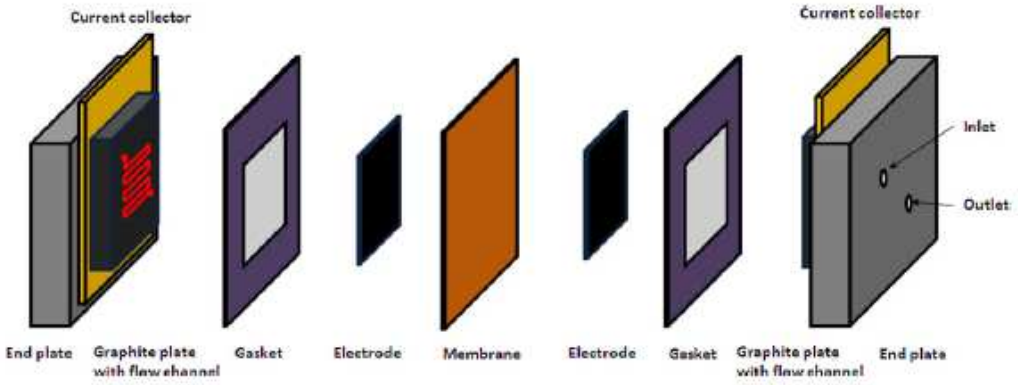

Fig. 8 - Cell test made by Aaron et al. [87].

Later, Xu et al. [89] proposed a tree dimensional numerical model to study the flow channel designs for VRFBs. In this study, they considered VRFBs with no flow channel, with serpentine flow channel (Fig. 8) and with parallel flow channel designs. In this work the maximum overall VRFB efficiency including the pumping power ($\eta_{total\ VRFB}$) was obtained for VRFB with serpentine flow channel design.

2.5.CIRCULATION OF THE LIQUID ELECTROLYTES

The US patent "Redox flow battery system and cell stack" [90] by Alberto Pellegri contains a fairly complete account on the configuration of a typical redox flow battery, so this subchapter and the subsequent one rely extensively on this publication.

The circulation of the liquid electrolytes across the cell stack can be done in two ways. A first option is to perform this circulation in parallel (represented in Fig. 9), that is, across all the cells, both towards the negative and positive electrodes, through the inlet and outlet manifolds. However, this solution might become critical when made in high voltage batteries due to the appearance of an electric current by-pass along the electrolytes contained in the manifolds. This would result in the lowering of the coulombic efficiency of the battery.

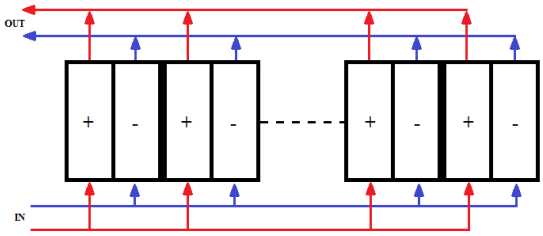

Fig. 9 - Cell Stack in parallel mode

The second mode of electrolyte circulation is called the cascade or sequence mode. In this mode, the positive and negative electrolytes flow sequentially across all cells, flowing from the enclosure of one cell to the enclosure of the next cell, down to the last one. It seems that in this way the electric by-pass currents will be significantly reduced and only a residual cell-to-cell by-pass current will remain.

This solution will certainly increase the energy required for circulating the liquid electrolytes, but, apparently this increase in energy consumption will be compensated by the coulombic efficiency improvement of the electrochemical processes of charging and discharging.

There are two modes for the circulation of the liquid electrolytes in cascade, the equicurrent mode (as shown in Fig. 10a), and the countercurrent mode (as shown in Fig. 10b), patented by Pellegri and Broman [90]. In the equicurrent mode the inlet of the negative and positive electrolytes are at the same side, while the outlets of the electrolytes are located at the opposite side of the cell stack (Fig. 10a). In the countercurrent mode (Fig. 10b) the inlet of the positive electrolyte is at the same side as the outlet of the negative electrolyte, so the inlet of the positive and negative electrolytes are on opposite sides.

The countercurrent mode is more advantageous than the equicurrent mode because the operating conditions of the various cells are reasonably uniform. In other words, it allows a similar drop of electrolyte charge within each cell: the first cell located at one end of the stack works with a substantially charged negative electrolyte and with a relatively discharged positive electrolyte, while the last cell located at the opposite end of the stack works with opposite charge conditions of the two electrolytes

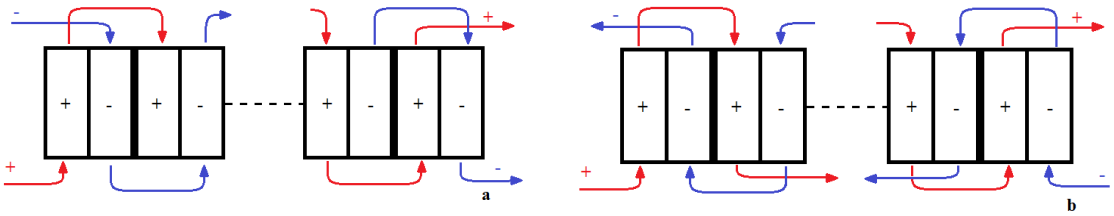

Fig. 10 - Cell Stack in equicurrent mode (a) and countercurrent mode (b) (adapted from [90])

So the magnitude of variation of the nominal cell voltage across the various cells of the stack during the cycle is reduced. Another advantage is the significant reduction of the phenomenon of water transfer unbalance through the ion exchange membranes that separate the negative and positive half-cell electrolytes in each individual cell.

2.6. CONFIGURATION OF THE STORAGE TANKS

For the configuration of the tanks, there are two possible options. Typically two tanks are used to store the liquid electrolytes separately, one tank storing the positive electrolyte and the other the negative one and each tank has its own circulation system (pump). This configuration was named “recirculation mode”, as each electrolyte is pumped from the tank to the stack and then returns back again into the same tank like is represented in Fig. 3.

There is another possible configuration called the batch mode showed in Fig. 11. This configuration works typically with four tanks, two for the positive electrolyte and two for the negative electrolyte. The charged liquids are pumped from a tank to the stack where they are discharged, and then they are directed to another tank. Therefore, in batch mode when switching from the charging phase to the discharging phase (or vice versa) the direction of the liquid flow is reversed.

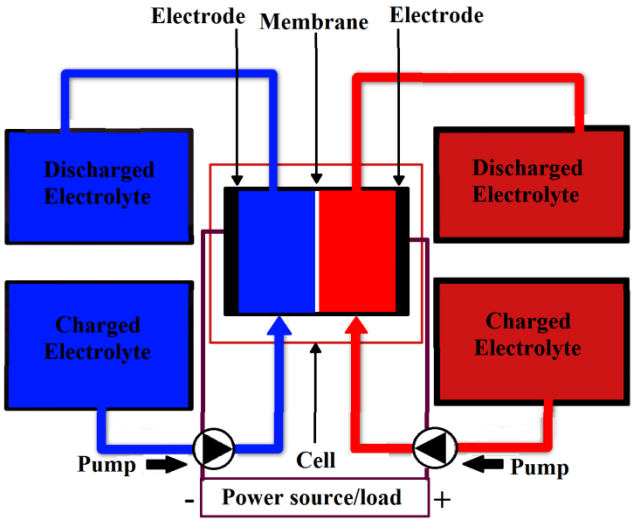

Fig. 11 - Batch mode configuration in discharge cycle.

There are advantages for each configuration. In the case of the batch mode the volume occupied in each tank is an indicator of the state of battery charge, and the two liquid electrolytes stored in the charged electrolytes tanks are maintained during the entire discharge in a state of full charge. In the recirculation mode, having only one tank for each liquid electrolyte makes it possible to store a larger quantity of energy for a given volume, but there will be a charge dilution over time.

In systems operated in batch mode in a battery operated according to a cascade and counter current mode, when there is complete discharge of the negative and positive half-cell electrolyte solutions, these discharged electrolytes can be stored in a single tank. During charging the electrolyte is pumped into the two half-cells where they are charged and then they are sent to the respective separate tanks. This system of three tanks has the advantage of allowing an equalization of the volumes of negative and positive liquid electrolyte, which in other systems are affected by unwanted water transport through the membrane.

If the three tank philosophy is applied to a vanadium redox flow battery in parallel mode, or in cascade mode in equicurrent, the mixing of the two discharged liquids into the same tank will result in decreased efficiency of the battery. This happens as in the case of all-vanadium flow battery complete discharges typically have only V^{4+} and none V^{5+} in the positive electrolyte, while only V^{3+} and not V^{2+} exist in the negative electrolyte. Thus, the mixing of the two fluids will result in

a solution with half of V^{4+} and half V^{3+} which will enter the positive and negative half-cells during the charging process, yielding an additional consumption of energy to re-oxidize V^{3+} to V^{4+} in the positive electrolyte, while at the same time it is necessary to reduce the V^{4+} to V^{3+} in the negative electrolyte.

However it is possible to use the system of three tanks with only a residual impairment of the efficiency of the battery. This is possible if a vanadium redox flow battery operates in counter current mode since in the process of discharge it is possible to over-reduce the vanadium in the positive half-cell, while it is possible to over-oxidize the vanadium in the negative half-cell being a mixture of V^{3+} and V^{4+} in the two half cells.

2.7.VRFB CHARACTERISTICS AND PERFORMANCE

This chapter is a summarized overview of the current state of the G1 and G2 vanadium redox flow batteries in terms of efficiency, charge and discharge characteristics and cycle life.

Firstly, it is necessary to make an energy balance of the system. The total efficiency of this system ($\eta_{totalVRFB}$) will be influenced by the energy losses due to the cooling system (when necessary), the control system, the circulation system and also by the coulombic and voltage efficiencies corresponding to both the charging and the discharging processes [91].

The coulombic efficiency (η_C) can be described as the ratio between the capacity input during charge and the capacity output during discharge, as shown in Eq. 1, knowing that I_{chg} is the constant current during charging, t_{chg} is the charging time, I_{disch} is the constant current during discharging and t_{disch} is the discharging time [92].

$$\eta_C = \frac{I_{dis}\ t_{disch}}{I_{chg}\ t_{chg}} \tag{1}$$

The coulombic losses are related to factors such as the irreversible reactions, diffusion of ions through the membrane, and shunt current losses [91].

The voltage efficiency (η_v) can be described as the ratio of the average voltage during discharging (V_{disch}) and the average voltage during charging (V_{chg}) as described in Eq. 2 [92].

$$\eta_V = \frac{\overline{V_{disch}}}{\overline{V_{chg}}} \tag{2}$$

The product of the voltage efficiency by the coulomb efficiency is known as cell energy efficiency (η_E), as described in Eq. 3 [92].

$$\eta_E = \eta_V \ \eta_C \tag{3}$$

These efficiencies depend on factors such as cell components (e.g. membrane), and cell design or cell stack type (e.g. countercurrent vs equicurrent modes). Moreover, the efficiency of a given cell might vary depending on the charge/discharge cycles the system has been subjected, or more importantly, depending on the actual current density (in mA/cm^2), which is the current intensity per unit area of the membrane.

In the Fig. 12, is represented the coulombic, voltage and energy efficiencies (respectively) reported by Vetter et al [93] of a vanadium redox G1 technology with 700 cm^2 of active area, measured with different current densities using a 1 kW test system.

As can be seen in the Fig. 12, for very low current densities (10mA/cm^2) there is a low coulombic efficiency, which is due to the high charging time, whilst for higher current densities (80mA/cm^2) there is a high coulombic efficiency but a lower energy efficiency (Fig. 12) due to over-voltages at the electrodes during the charge and discharge, which reduces the voltage efficiency [93].

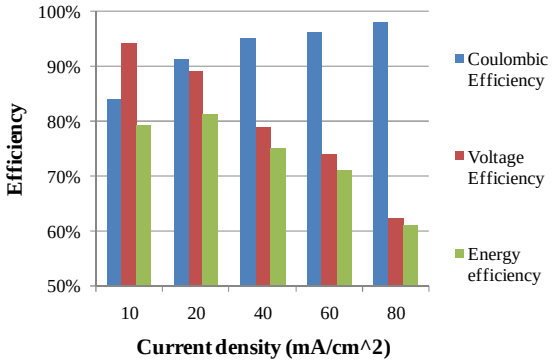

Fig. 12 - Reported Coulombic, Voltage and Energy efficiencies of a G1 (adapted from: [93]).

The voltage of each cell unit during discharge and during charge depends on the redox couples that are used. However, the potential of the cell during discharge will be below the potential during charging due to energy losses associated to the internal resistance, over-voltage losses due to the finite kinetic half-cell reactions (activation overvoltage) and mass transport limitations(concentration overvoltage) [90]. A typical difference between the charge and discharge voltages is shown in Fig. 13.

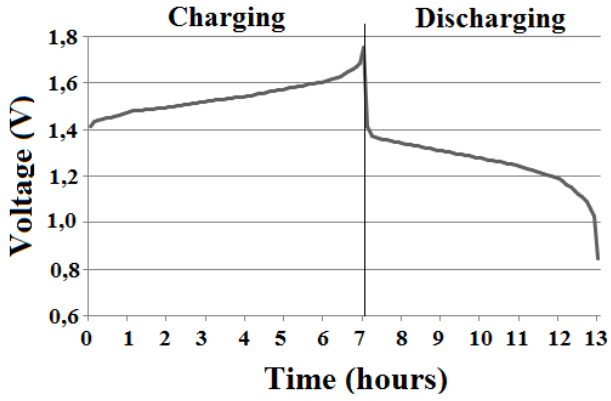

Fig. 13 - Typical charge/discharge cycle of a single cell (G1 technology) for a current density of 40 mA/cm^2 (adapted from [94]).

An advantage of the vanadium redox flow batteries is their long life cycle and consistently stable performance. A cycle life test was made by Sumitomo Electric Industries, Ltd [95] to a 20 kW G1 battery system with 60 cells in series, each one with an electrode area of 0,5 m^2, with a voltage of 75,2 V and current of 250 A system. The battery capacity was 9,4 kWh and they used an electrolyte of vanadium in a 1 mol/L sulfuric acid solution. They tested that battery with continuous charge/discharge cycles for approximately 2 years and the results showed no visible deterioration after over 12 000 cycles (Fig. 14).

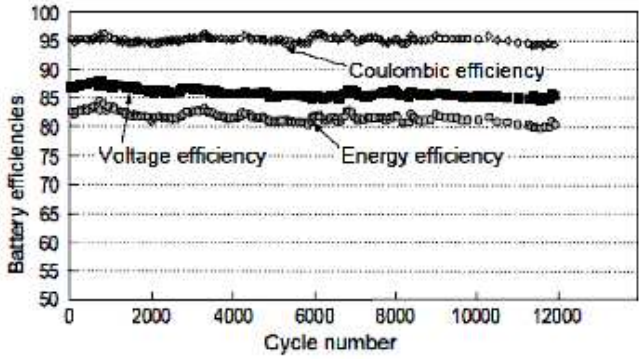

Fig. 14 - A 20 kW G1 technology battery system cycle life test by Sumitomo Electric Industries, Ltd [95].

A typical charge/discharge curve for a G2 technology vanadium redox cell with a charge/discharge current density of 20 mA/cm^2 is shown in Fig. 15 [86]. It can be seen that these values are lower than those corresponding to the G1 technology (recall Fig. 13).

Skyllas-Kazacos et al. [72] tested a G2 technology vanadium redox flow battery and they determined the various cell efficiencies for temperatures ranging from 10 to 40 °C. Fig. 16 and Fig. 17 show the coulombic and voltage efficiencies as a function of temperature and current density [72]. It can be seen that the trends of the coulombic and voltage efficiencies with the current density in G2 technology is similar to the G1 technology (Fig. 12)

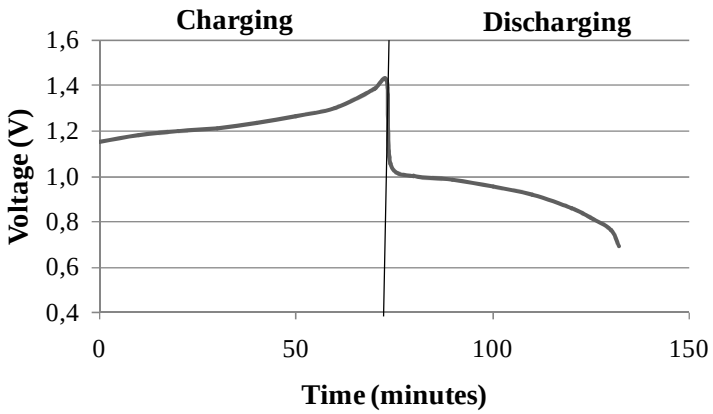

Fig. 15 -Typical charge/discharge curve for a vanadium redox G2 cell at current density of 20 mA/cm² (adapted from: [86]).

The energy efficiency of the VRFB (η) is shown in Fig. 18 and it is possible to verify that a value of 70% can be obtained for 20 mA/cm².

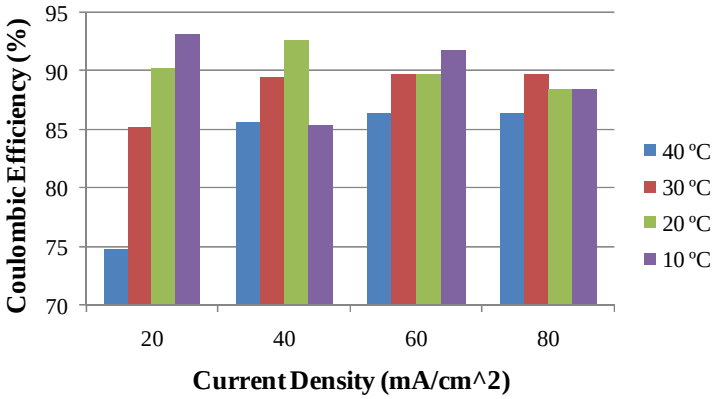

Fig. 16 - Coulombic efficiency as a function of current density and temperature for a G2 technology vanadium redox cell (adapted from: [72]).

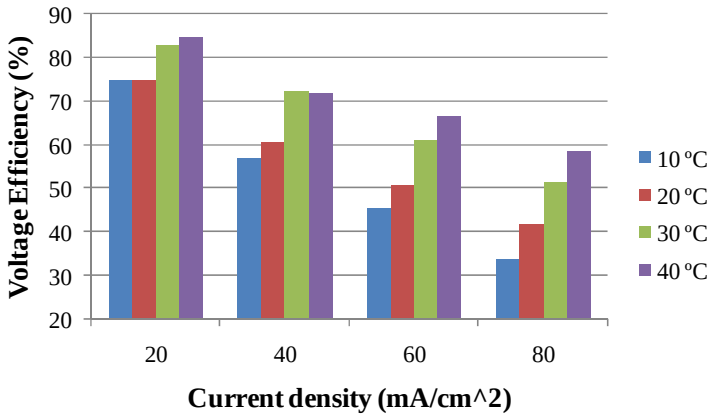

Fig. 17 - Voltage efficiency as a function of current density and temperature for a G2 technology vanadium redox cell (adapted from: [72]).

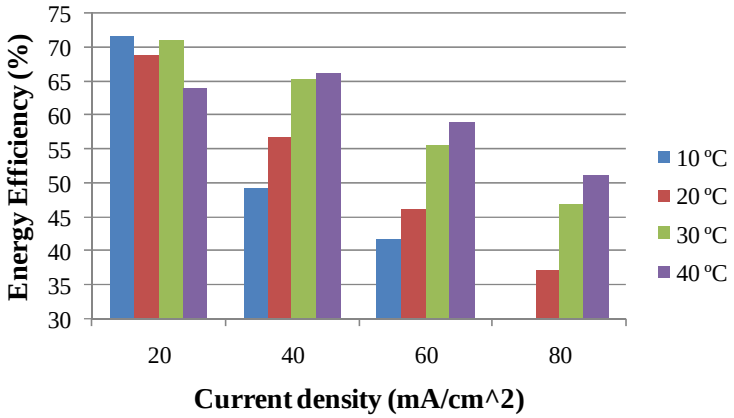

Fig. 18 - Energy efficiency as a function of current density and temperature for G2 technology vanadium redox cell (adapted from: [72]).

A chemical comparison between the G1 and G2 technology batteries is presented in Table 2 and it can be seen that the G2 has a higher concentrations of active materials. Other properties have been already summarized in Table 1.

Table 2 - Comparison between G1 and G2 technologies.

	G1	*G2*
Electrolyte	1,5 – 2 M V dissolved in H_2SO_4 aqueous solution in both half-cells [72]	2 – 3 M V/Br dissolved in aqueous solutions of HBr, HCl, NaCl, KCl, NaBr, KBr, or mixtures thereof, in both half-cells [72, 85]
Negative couple	V^{3+} / V^{2+} [72]	V^{3+} / V^{2+} [72, 85]
Positive couple	V^{4+}/ V^{5+} [72]	$Br^-/ClBr_2^-$ or $Cl^-/BrCl_2^-$ [72, 85]

An important characteristic of a VRFB is the flow rate which the corresponding pumping system can provide, because the maximum power output is a function of the flow rate. For a certain VRFB system, the theoretical flow rate will be a function of the current [93, 96], the direction of the current (charge or discharge) [96] and also on the SoC [93, 96] (considering a typical recirculation mode configuration, in case of the batch mode the flow rate depends only on the current). This may prove impractical when using the system for small values of SoC.

Typically, a higher flow rate induces higher voltages due to the lower resulting concentration (on average) of the reaction products within the cells at each side of the membranes during the operation [97]. However there is an extra consumption of energy due to the extra pumping power required. If excessive, this would eventually reduce the overall energy efficiency, so it is necessary to find the optimal value which will maximize the efficiency of the system. For the aforementioned reasons, the availability of a variable pumping strategy is an important factor to optimize the overall efficiency of the system [93, 96]. It is therefore normal to operate with flow rates larger than the theoretical [93, 98]. Furthermore, the liquid electrolytes also remove the heat from the cell stack in way similar to a dedicated cooling circuit [98].

Ma et al. [99] studied the effect of electrolyte flow rate on a kilowatt class VRFB. They observed that the VRFB energy efficiency and discharge capacity increased for higher flow rates,

but the increase of the pumping losses reduced the overall system efficiency, as it can be seen in Fig. 19.

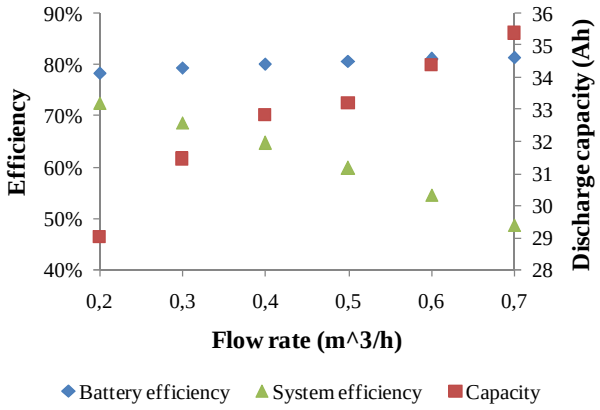

Fig. 19- Variation of battery efficiency, discharge capacity and overall system efficiency as a function of flow rate (adapted from: [99]).

They did tests with various flow rates, and defined an optimal strategy of flow rate for a current density of 75 mA/cm^2, through which it is possible to obtain a high efficiency battery with a high discharge capacity as well as a high overall system efficiency. This strategy consists on charging with a low flow rate (0,2 m^3/h) and later increasing it to a higher value (0,71 m^3/h) when the voltage of the battery exceeds 23,1 V. The same happens in the discharge, with the flow rate being maintained at 0,2 m^3/h until the cell reaches 16,8 V and then the flow rate is increased to 0,71 m^3/h until the end of discharge. This strategy is illustrated in Fig. 20 and proved to be optimal for the tested battery with a current density of 75 mA/cm^2. However, for other VRFB systems with other configurations and other current densities different flow rate values should be used in order to obtain an optimal system efficiency.

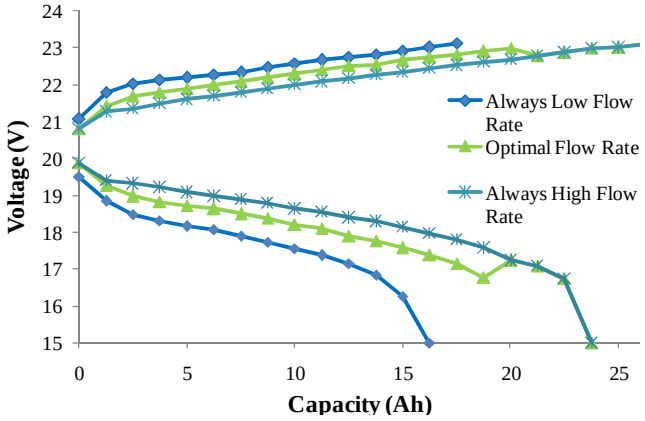

Fig. 20 - Optimal charge-discharge strategy proposed by Ma et al. (adapted from: [99]).

2.8.VRFB COMPONENTS

It can be seen in the previous subchapters that the VRFB performance is affected by several parameters, like the configuration of the system, and the charge/discharge conditions. However, the various components have a key role in the performance of the VRFBs.

In this subchapter a review of the various VRFB components is presented as well as various studies made by several groups around the world to improve the VRFB characteristics.

2.8.1. Liquids electrolytes

In a redox flow battery, there are two different electrolytes separated by an ion exchange membrane. But first it is necessary to define the difference between the "supporting electrolyte" and the "electrolyte".

The electrolyte is a solution that conducts the current through ionization [85]. The supporting electrolyte is an electrolyte that supports the reduced and oxidized forms of a redox couple. It also supports the corresponding cations and anions in order to balance the charge of the redox ions in solution during the oxidation and reduction of the redox couple [85]. The supporting electrolyte also supplies additional ions which increase the solution conductivity and

support the flow of the current [85]. Thus, the energy is stored in two different electrolytes in the active materials [100].

In order to increase the energy density of the electrolytes, reduce the volume of the tanks needed for a given amount of energy and reduce the flow rate required to maintain a given power output it is desirable to increase the concentration of the active materials, such as vanadium ions in a G1 [100]. Typically, the maximum vanadium ion concentration that can be dissolved in the supporting electrolyte (2 M or less) which results in an energy density of 25 Wh/kg and 33 Wh/L [72]. That concentration is limited by the stability of the V^{5+} ions at temperatures above 40 °C and the solubility limit of V^{2+} and V^{3+} ions in supporting electrolyte at temperatures below 5 °C [74].

In order to reduce the cell resistivity it is desirable to increase the hydrogen ion concentration in the supporting electrolyte. This reduces the resistance of the ionic conduction through the membrane. This is why generally the supporting electrolyte contains sulfuric acid [100]. On the other hand, higher H^+ and sulfate concentrations are required for stabilization of the V^{5+} species at high temperatures [101].

Typically, the two liquid electrolytes (anolyte and catholyte) of a G1 are prepared by dissolving 0,1 M to 2 M $VOSO_4$ (vanadyl sulphate) in 0,1 M to 5 M H_2SO_4 in aqueous solution, to form tetravalent vanadium ions [32]. These tetravalent vanadium ions can be electrochemically oxidized to form the catholyte, which is a solution of pentavalent vanadium ions. Conversely, the tetravalent vanadium ions can be electrochemically reduced to form anolyte, which is a solution of a divalent vanadium ions [32].

The reactions during the initial charging are the following [32]:

Positive half-cell: $V^{4+} \rightarrow V^{5+} + e^-$

Negative Half-Cell: $V^{4+} + 2e^- \rightarrow V^{2+}$

As it can be realized from the above equations, during the initial charge stage it is necessary twice the number of coulombs for the positive electrolyte to make a full charge of the negative electrolyte. Therefore, a higher flow rate of the positive electrolyte should exist.

In this technology it is preferable that the negative and positive compartments are air-tight and the electrolytes are de-aerated [32]. When this is not possible (for example in a batch mode configuration), it is frequent to bubble nitrogen through the negative half-cell solution, which allows the removal of dissolved oxygen and stop diffusion of air into the compartment, preventing the oxidation of V^{2+} [32, 102].

Recent studies suggest the use of mixed electrolytes. For instance, Li et al. [103] demonstrate that by using a mixed H_2SO_4/ HCl supporting electrolyte it is possible to dissolve 2,5 M vanadium, increasing the energy density up to 39,2 Wh/L. They also proved that it is possible to dissolve 3 M vanadium with a resulting energy density of 43,1 Wh/L, but with stabilization problems for temperatures below -5 °C [103]. With this mixed electrolyte the operational temperature can range from -5 °C to 50 °C and the resulting viscosity will be lower, reducing pumping losses [103].

Kim et al. [96] also studied the use of these mixed electrolytes in a prototype of 1kW/1kWh vanadium redox flow battery system. They demonstrated that more than 1,1 kW of power and 1,4 kWh of energy content could be obtained with this modification, in an operational range between 15% - 85% SoC (with a current density of 80 mA/cm^2). They obtained an energy efficiency of 82% and this system operated stably at temperatures in excess of 45 °C [96].

Recently, Peng et al. [104] tested the mixture of acids CH_3SO_3H / H_2SO_4 as the positive supporting electrolyte for G1 with a vanadium concentration of 2 M V^{4+}, and discovered that V^{4+} / V^{5+} redox reaction with this acid mixture is more electrochemically reversible and that the energy density increased to 39,9 Wh/L [104]. However, the higher cost of CH_3SO_3H relatively to H_2SO_4 renders this solution less attractive [105, 106].

One affordable and effective way of stabilizing the electrolytes is to incorporate additives which inhibit precipitation. Peng et al. studied the use of trishydroxymethyl aminomethane (Tris) as an additive for the positive electrolyte in a G1 [106]. They discovered that the addition of 3% of the Tris additive in the positive vanadium electrolyte increases the charge and discharge capacities, as well as the electrochemically reversibility. Additionally, the discharge capacity fade rate is reduced [106].

Liang et al. [105] investigated the thermal stability and electrochemical activity of the L-Glutamic acid when used as an additive for the positive electrolyte in a G1. They found that this additive (at 4% concentration) can significantly reduce the precipitation of V^{5+} from the positive electrolyte, as well as improve the redox electrochemical reversibility, the redox kinetics and the overall cell performance. In fact, the G1 with 4% L-Glutamic acid additive in the positive electrolyte exhibited a higher capacity and an improved coulombic and energy efficiencies. The coulombic efficiency for a G1 with additive was around 95%, nearly the same as the G1 without additive, but in this latter case after 40 cycles the coulombic efficiency slightly decreased while the coulombic efficiency of the G1 with additive stays almost unchanged. The energy density for the G1 with additive was around 74% and the maximum discharge capacity was around 4500 mAh, while for the G1 without additive it was around 73% with the maximum discharge capacity being around 4000 mAh.

Chang et al. [107] studied the use of a coulter dispersant as a positive electrolyte additive for a G1 and concluded that the addition of a proper dosage of coulter dispersant can retard the precipitation of V^{5+} ions in the positive electrolyte at 45 - 60 °C, whereas the energy efficiency is increased but the coulombic efficiency is not significantly affected.

Other studies [108, 109] have reported the use of organic additives on positive electrolytes for a G1. Li et al. [108] studied the addition of Fructose, mannitol, glucose and D-sorbitol in the positive electrolyte. The D-sorbitol showed better results with higher concentrations of V^{5+} at 60 °C in the electrolyte when compared with the electrolyte without any additive. Thus, a G1 with D-sorbitol additive in the positive electrolyte exhibited a higher capacity, an improved reversibility of the electrochemical reaction and as slightly higher energy efficiency [108]. Wu et al. [109] studied the influence of adding inositol and phytic acid to the positive electrolyte in a G1. They observed that the thermal stability of the V^{5+} electrolyte and the reaction kinetics were increased by using both additives [109]. However, the phytic acid caused a decrease of the capacity of the G1, while the G1 employing the electrolyte with inositol exhibited better charge-discharge characteristics and less discharge capacity fade rate with cycles, in comparison with a G1 with conventional electrolyte without additives [109].

Regarding the G2 technology, the positive redox couple is a polyhalide/halide in the positive electrolyte and the negative redox couple is a V^{3+}/V^{2+}, in the negative electrolyte [85]. The

supporting electrolyte in each half cell can be different but, in order to minimize the cross-contamination problems, it is preferable to use the same electrolyte in both half-cells [85]. This supporting electrolyte can be composed by aqueous solutions of HBr, HCl, mixtures of HBr and NaBr, mixtures of KCl and HCl, mixtures of NaCl and HCl, mixtures of HBr and KBr, or mixtures thereof [85].

Skyllas-Kazacos et al. [72] used 2,6 M vanadium ions (50:50 of V^{3+}: V^{4+} mixture) in 7,5 M HBr plus 1,5 M HCl as the initial electrolyte.

During the initial charge, in the negative half-cell, the V^{3+} and V^{4+} ions are reduced to V^{2+} according to the following reaction [72]:

$$V^{3+} + VO^{2+} + 2H^{+} + 3e^{-} \rightarrow 2V^{2+} + H_2O$$

The initial charge reaction in the positive half-cell involves firstly the oxidation of V^{3+} to VO^{2+} and then the oxidation of the Br^- and Cl^- ions (halide ions) to $ClBr_2^-$ (polyhalide ions), according to the following reaction [72]:

$$V^{3+} + VO^{2+} + H_2O + 2Br^{-} + Cl^{-} \rightarrow 2VO^{2+} + 2H^{+} + ClBr_2^{-} + 3e^{-}$$

The subsequent charge-discharge reactions only involve the V^{2+} / V^{3+} couples in the negative half-cell and $ClBr_2^-$ / Br^- couples in the positive half-cell [72].

The concentration of the polyhalide in the positive electrolyte, is typically 1 - 3 M when the redox flow battery is fully charged, and the negative electrolyte comprises typically 1 - 4 M of V^{2+} and/or V^{3+} dissolved ions [85].

2.8.2.Membranes

The membrane is a component that separates the two half-cells, preventing the mixture of the two electrolytes and the passage of electrons, while allowing the transport of ions to complete the circuit during the passage of a current [83].

Typically, the membranes are classified into anion exchange membranes or cation exchange membranes according to the type of ionic groups attached to the membrane matrix. So, the anion exchange membranes allow the passage of anions while the cation exchange membranes allow the passage of cations [110].

Membranes can also be classified by the material, and there are several categories of membrane materials such as: Perfluorinated ionomers, partially fluorinated polymers, non-fluorinated hydrocarbons, and so on. Among these, the perfluorinated (eg. Nafion®, Flemion®, NEOSEPTA-F®, Gore Select®, etc) are generally preferred because of their good chemical stability, high conductivity and mechanical strength [74].

To evaluate and test a membrane for use in a vanadium redox battery, it is common to apply a range of test procedures, which include various types of measurements such as vanadium ion permeability [73, 74, 111-115], ion exchange capacity [74, 111, 112, 115, 116], ionic conductivity [74, 116], area resistance [74, 111, 114, 115], chemical stability [74], thermal stability [116], water transport [74, 111, 115, 117, 118] and cell performance [74, 111-115]. These test procedures are vital for membrane characterization. For example, the vanadium ion permeability will allow the transport of vanadium ions from one half-cell to the other during operation, which leads to an accumulation of vanadium ions in one half-cell and a dilution in the other [119]. This will reduce the capacity of the battery over time. However, this accumulation can be eliminated by periodically re-mixing the solutions of the two half-cells. The required frequency of this re-mixing process will depend on the membrane properties and on the system operation [119].

On the other hand, the membranes must also resist to the highly oxidative V^{5+} ions used in the G1 technology, or to the bromine, used in the G2 technology [73].

Another issue associated with the ion exchange membranes is the water transfer from one half-cell to another, which causes the precipitation of vanadium salts in one half-cell and their dilution in the other. It seems that the direction of water transfer is dependent upon the nature of the membrane. For a cell with an anion exchange membrane the water transfer is from the positive to the negative half-cell, while for a cell with a cation exchange membrane the opposite will happen [118]. An alternative to partially solve this problem seems to be the alternating and

consecutive use of an anion followed by a cation exchange membrane in the same multi-cell stack [73, 90].

More recent studies on the transfer of water as a function of state of charge (SoC) to a cation-exchange membrane have been made. They showed that the preferred direction of water transport is dependent on the SoC. For example, for SoC between 50% and 100%, water transfer takes place preferentially from the negative half-cell to the positive, whereas for values of SoC less than 50% the opposite happens [117].

The membrane is a key component in a vanadium redox flow battery system because it defines the performance and economic viability of the system and it may weigh up to 20% of the overall system cost, so it may be an obstacle to the commercialization of many redox flow batteries [74]. So, in the development of specific redox flow battery cell solutions, special care should be taken in order to choose the membrane that yields the best compromise between cost and performance.

The cationic membrane Nafion® (manufactured by DuPont) is widely used in redox flow batteries and it has also been used as a separator in fuel cells [83]. Despite their high cost, the Nafion® membrane has been one of the most studied membranes and several works [112-116, 120-125] have been reported in which modifications to improve their electrochemical characteristics have been made.

More recently, Vijayakumar et al. [113] investigated the use of Nafion–SiO_2 composite membranes and observed a reduction on V^{4+} ion diffusivity which resulted in a slightly higher coulombic efficiency but, according to their research, these composite membranes still do not represent a feasible solution to suppress the transport of vanadium ions through membrane in VRFBs for long times of operation.

Luo et al. [121] made a surface modification on a Nafion exchange membrane using interfacial polymerization. The results of the tests showed that the permeation of vanadium ions across the membrane decreased, the area resistance increased and the water transfer across the membrane decrease dup to 50%, comparing with a standard Nafion membrane. As a result, the self-discharge of the G1 decreased and the coulombic energy efficiency increased but, due to

the increase of the area resistance, the voltage efficiency decreased, which resulted in a overall energy efficiency similar to that of a G1 with a standard Nafion membrane [121].

Zeng et al. [122] studied the modification of a Nafion 117 membrane with polypyrrole by three different methods: electrolyte soaking, oxidation polymerization and electrodeposition. The best results were for the electrodeposition method, which allowed the decrease of V^{4+} ions permeability by more than 5 times and a reduction of water transfer in more than 3 times [122].

Schwenzer et al. [114] studied the transport properties of Nafion/polyaline and Nafion/polypyrrole and concluded that for the Nafion/polypyrrole membrane, despite the reduction of the transport of vanadium ions across the membrane, the resulting membrane resistance was higher. This result is consistent with the studies made by Zeng et al. [122]. However, for a Nafion/polyaline membrane there is a enhanced reduction of transport of vanadium ions across the membrane and a lower increase of membrane resistance, comparing with the Nafion/polyaline membrane [114].

Xi et al. [120] employed a Nafion/SiO_2 hybrid membrane as the separator in a G1. They concluded that the hybrid membrane had a lower vanadium ion permeability compared to the conventional Nafion membrane. Also they noticed that the G1 with the hybrid membrane showed higher coulombic and energy efficiencies and lower self discharge rates compared to the conventional Nafion membrane system.

Later, the same team, with Xiangguo Teng and Yongtao Zhao [125] prepared a Nafion/organically modified silicate (ORMOSIL) hybrid membrane via *in situ* sol–gel reactions for mixtures of tetraethoxysilane (TEOS) and diethoxydimethylsilane (DEDMS). The results indicated a dramatic reduction in cross-contamination of vanadium ions compared to a conventional Nafion membrane. The cell tests showed that the G1 with Nafion/ORMOSIL hybrids membrane has a higher coulombic efficiency (η_c) and energy efficiency (η_E) than a G1 with Nafion and Nafion/SiO_2 hybrid membrane. A maximum η_c of 95,8% at 80 mA/cm^2 was obtained with the G1 with Nafion/ORMOSIL hybrids membrane. For a G1 with Nafion membrane and the G1 with Nafion/SiO2 membrane the maximum η_c and η_E were 92,1% and 93,1% respectively, for the same current density.

The maximum obtained η_v of the G1 with Nafion/ORMOSIL hybrid membrane was 96,5% with a current density of 10 mA/cm^2, while the maximum η_v of the G1 with Nafion membrane and Nafion/SiO_2 membrane was 94,4% and 94,7%, respectively, for the same current density. The same team [115] prepared a Nafion/organic silica modified TiO_2 composite membrane via in situ sol-gel reactions and tested it in a G1. This resulted in a reduction of vanadium ions cross-contamination and water transport and an increase of the area resistance. Due to the higher area resistance, the voltage efficiency decreased from 84,8% to 82,2%, but the coulombic efficiency increased from 90,8% to 94,8%, which resulted in an overall increase of energy efficiency from 77,0% to 77,9%.

Wang et al [123] fabricated a Nafion/TiO_2 hybrid membrane by a hydrothermal method. They observed that the permeation of the vanadium ions was significantly reduced when comparing with a conventional Nafion, and the coulombic and energy efficiencies were 88,8% and 71,5%, respectively, at 60 mA/cm^2. For a conventional Nafion membrane these efficiencies were 86,3% and 69,7% respectively, for the same current density.

Mai et al. [112] employed Nafion/Polyvinylidene fluoride (PDVF) blends to prepare the ion exchange membranes to use in a G1 single cell with various blending ratios. The results showed better vanadium ion permeability, reduced self-discharge and an increase of the energy efficiency in aN0.8P0.2 sample (denoted as NxPy where x and y are the mass ratios of Nafion and PVDF respectively).

Teng et al [124] prepared a Nafion-sulfonated diphenyldimethoxysilane (N-sDDS) composite membrane and employed it in a VRFB. The VRFB with this membrane exhibited nearly the same coulombic efficiency than a VRFB with a conventional Nafion membrane, but the energy efficiency increased up to 91,5% (81,9% for conventional Nafion membrane) and the self discharge was reduced. They concluded that the N-sDDS membrane is a promising candidate for use in VRFB systems.

However, most of commercial ion exchange membranes are still very expensive and Mohammadi and Skyllas-Kazacos [111, 126] studied the modification of low cost separators (eg. Daramic) to improve their electrochemical properties and make them a cheaper option for use in vanadium redox flow batteries. These authors studied the modification of a Daramic microporous separator by incorporating an anion exchange resin (Amberlite CG 400) and further crosslinking

with divinylbenzene [126]. Analyzing the results of their experiments, they concluded that the procedure used was not able to incorporate any ion exchange capability into the membranes. However, the slight difference in vanadium ion permeability and sheet resistance suggests that the resin may have some catalytic effect on the polymerization reaction [126]. Later, these authors [111] studied the incorporation of ion-exchange groups in a Daramic micropourous separateor using polyelectrolyte. The composite membrane was tested and the results showed that this alteration reduces the capacity loss and reservoir flooding while improving the performance characteristics of the redox flow cell, halving the area resistance, increasing diffusivity and causing a 3% increase in the overall energy efficiency (with values up to 77%) [111].

2.8.3.Electrodes

The positive and negative electrodes in vanadium redox flow batteries are typically carbon based materials, such as carbon or graphite felts, carbon cloth, carbon black, graphite powder and so on [127]. These electrodes have shown a good potential in terms of operation range, a good stability and a high reversibility.

Similarly to other battery technologies, the electrodes are a very important component on the performance of the vanadium redox flow batteries. In order to increase the electrochemical activity of the electrodes, the electrode material should have a low bulk resistivity and a large specific area [128]. The improvement of the electrochemical activity of the electrode is expected to increase the energy efficiency of the battery systems [127]. So, in order to improve the performance of the vanadium redox flow batteries, surface modification of the electrodes has been studied by several groups [128-131].

Coating graphite and carbon felts with metal is a method for improvement of the conductivity of the electrode and also to improve the stability for the flowing electrolyte [128]. Wang et al. [129] studied the use of iridium-coated carbon felt electrodes in a G1 and found that the resistance of the cell decreased by 25% while the energy efficiency increased from 56,8% to 62%.

Tsai et al. [132] studied the use of graphene-modified graphite (GMG) composite electrodes and concluded that the use of GMG may improve the reversibility and the current density of a G1. Therefore, an electrode of this type shows a considerable potential for use in G1s.

Liu et al. [102] studied the use of carbon paper and showed that it generally performs better than carbon felt as an electrode material in vanadium redox flow batteries with no-gap design.

Li et al. in a different work [127] prepared a novel Graphite/Graphite Oxide (GO) composite electrode for G1, which can be used as a positive and a negative electrode. In comparisons with single graphite electrodes, this composite electrode exhibits better performances, higher peak current density and a lower charge transfer resistance of the electrode reactions. This improved electrochemical performance of the electrode is due to the existence of oxygen functional groups and extra specific surface areas induced by the GO [127].

2.8.4.Bipolar plates

In a redox flow battery, the output power is determined by the number of single cells connected in series, and by the current passing through them. So, in order to obtain a system with high power output it is necessary to connect several single cells in series forming a cell stack. Bipolar plates are a key component in redox flow batteries and fuel cells by allowing the series connection of the single cells like is showed in Fig. 21. These components have a high cost, accounting for 30 to 50% of the total cost of a fuel cell stack [133].

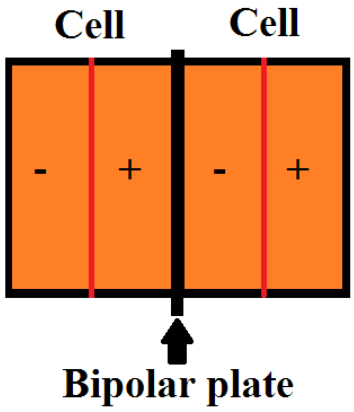

Fig. 21 - Series connection of two cells.

Typically, the bipolar plates are made of graphite, carbon, carbon plastic, etc. These materials must have high electrical conductivity in order to reduce the internal resistance of the cell stack and have the right mechanical properties to support the contact pressure to which they are subject when pressed against the electrode plates in order to prevent leakage of the liquid electrolyte [134]. The contact pressure between the electrodes (in carbon or graphite felt) and the bipolar plates is essential to prevent the leakage of the liquids. On the other hand if the contact forces are too low, there will be a high electric contact resistance between the electrode and the bipolar plate [94]. In order to solve this problem, Qian et al. [94], proposed the use of a novel electrode-bipolar plate assembly which consists on a graphite felt and a flexible graphite bipolar plate connected to each other through an adhesive conducting layer. The tests showed that this novel electrode-bipolar plate assembly offered a drop in the resistivity and guaranteed the impermeability, also allowing a good energy efficiency of 81% for a current density of 40 mA/cm^2 [94].

Graphite is one of the most used materials for bipolar plates because it has high electrical conductivity, low density and it is easy to machine [135]. However, it also has a few disadvantages because it is a brittle material, which hampers the assembly of the stack, increases the cost of machining and being porous it requires the use of thick bipolar plates [135]. To improve the performance of bipolar plates in fuel cells, several groups [136, 137] developed graphite composites by preparing a bulk molding compound material followed by a hot pressing process. Unfortunately the vanadium redox flow batteries operate at stronger grades of

acidity so the bipolar plates developed for the use in fuel cells could not be adapted for use in VRFB [135].

Recently, Lee et al. [138] developed a carbon composite bipolar plate for VRFBs using graphite, carbon black and resin, by a compression molding method, and concluded that the electrochemical stability was improved, with good electrical conductivity and performance.

More recently Sumitomo Electric Industries, Ltd. [134] patented a new type of bipolar plate for redox flow batteries constituted by an electrical conductive composite material with liquid sealant properties displaying higher conductivity, better mechanical strength and plasticity than conventional plates. This composite material was prepared by mixing a thermoplastic resin, a carbonaceous material (graphite or carbon black) and carbon nano-tubes [134].

2.8.5.Cell stack frame and storage tanks

The high acidity found in vanadium redox flow batteries makes the use of acid corrosion resistant materials a requirement [83]. Typically, the cell stack frame and the storage tanks are made of PVC or polyethylene [37, 95, 139, 140].

Stainless steel pins and bolts are generally used to make the cell stack assembly and to join the single cells, while suitable sealants (e.g. silicone rubber) are laid between joints to prevent leakage of liquid electrolytes [115, 139].

Recently, Sumitomo Electric Industries, Ltd. [95] reported the use of a flexible storage rubber tank to take advantage of the fluid battery characteristics to insert the storage tanks in underground spaces (eg. underground deposits) through the manholes.

2.9.COMPARISON WITH CONVENTIONAL BATTERIES

A comparison with conventional battery technologies is required to assess the potential of flow batteries. As there are many conventional battery technologies [141, 142], this work will only consider the lead acid and lithium ion batteries as the framing technologies for the comparison.

Conventional batteries have an obvious major advantage over flow batteries as they are completely sealed and do not require circulation systems. However, flow batteries have higher design flexibility due to the intrinsic conformability of liquids, which allows an extreme flexibility in terms of storage tank geometry flexibility [30]. Moreover, the power and energy storage capacity are independent, making it very easy to scale up the capacity of the system simply by increasing the storage of liquid electrolyte. Furthermore, these batteries have a high cycle life as the liquid electrolytes suffer low deterioration over time, even at the event of electrolyte crossover [93]. Moreover, the fact that the power production unit is physically separated from the energy storage unit can be an additional advantage because the storage tanks can be placed in underground tanks or in the basement of a building, while the cell stack can be located at a location where it is easier to dissipate the heat. This means that the auxiliary cooling system may be simpler to design and install. Also the circulation of the fluid helps the cooling of the cell stack.

As already mentioned, among the various existing flow battery technologies, VRFBs seem currently to be the most advantageous and commonly used, but they have a much lower energy density than conventional battery technologies [142]. Of course, this will be the greatest limitation for applications where packaging is important, namely mobile applications.

When comparing the energy density of different batteries, it is important to note that the values reported for conventional batteries (e.g., lithium ion, lead-acid) refer to the volume of the battery in its entirety, while for a flow battery the energy density is computed based solely on the volume occupied by the liquid electrolyte, not including the cell stack, the pumps and the pipings, which still occupy a considerable volume and weight. But this was done so because there are different cell stacks which can be attached to a system with a given amount of energy stored.

A comparison of VRFB, lead acid and lithium ion batteries is presented in Table 3.

Table 3 - Comparison between VRFBs and conventional batteries.

	Lithium ion [141]	***Lead acid (stationary) [141]***	***VRFB G1***	***VRFB G1 with mixed acid***	***VRFB G2***
Open circuit voltage	4,1	2,1	1,4 [94]	1,4 [103]	1,0 [86]
Energy density (Wh/kg)	150	20	25 [72]	-	50 [72]
Energy density (Wh/L)	400	70	33 [72]	43,1 [103]	70 [72]

Analyzing the results of Table 3 it is possible to conclude that for a lithium ion battery, an equivalent lead acid battery will be 7,5 times heavier and almost 6 times bigger. However, a VRFB G1 will be only 6 times heavier but 12 times bigger than a Li-ion battery, while a VRFB G2 will be only 3 times heavier and almost 6 times bigger. At a first glance one would think that the VRFB G2 technology is similar in terms of volume and better in terms of weight than a stationary lead acid technology. However, it was already mentioned that in the case of VRFBs these energy densities refer solely to the liquid electrolytes. The inclusion of the stack, pumps and pipes would significantly increase their volume and weight.

However care should be also taken when analyzing the values concerning the Li-ion batteries for specific applications, say, in electric mobility. For example, the 90 kW and 24 kWh lithium ion battery pack developed by Ikezoe et al. [143] and used in the Nissan Leaf electric vehicle, is comprised of 48 modules, each one with 4 cells, and each module having an energy density of 132 Wh/kg and 213 Wh/L.

However, these energy densities are computed based on modules of 4 cells, thus including the support materials for four cells. Each cell has as dimensions 290x216x 7,1 mm and 799 g of mass, with a capacity of 33,1 Ah and an average voltage of 3,8 V. This means that in reality each Leaf battery cell will have an energy density of 157 Wh/kg or 283 Wh/L. The total mass of the

Leaf battery is 153 kg and the total volume is 85 liters without including the structure and control system. With these systems, the total mass of the battery system accounts to a total of 300 kg.

In Table 4 are showed the characteristics of the lithium ion battery of the Nissan Leaf compared against lead-acid batteries and VRFBs with equivalent power/capacity. In the case of VRFBs, the weight and the volume of the cell stack was calculated using Nafion N117 membranes (trademark of DuPont), SIGRACELL GFA3EA electrodes and SIGRACET TF6 bipolar plates (trademark by SGL group). Considering a maximum current density of 100 mA/cm^2 and knowing that the Nissan Leaf Battery has a power of 90 kW and a voltage of 400V, their maximum current is 225 A, which means that the area resistivity of the equivalent VRFB will be around 0,225 m^2.

So, knowing that the aforementioned membranes have a thickness of 183 microns and a mass of 360 g/m^2 [144], the electrodes have a thickness of 3 mm (but should be compressed 20% down to a final thickness of 2,48 mm each) and a mass of 300 g/m^2 [145], each cell will be 5,143 mm thick and with a mass of 216 g. Between each two cells will be located a bipolar plate, with a thickness of 0,6 mm and a mass of 229,5 g (1020 g/m^2) [145].

The results of Table 4 are graphically represented in Fig. 22. As it can be seen, although VRFBs are lighter than lead acid batteries for the same output, they are much bulkier, occupying from 850 to 1100 liters of volume, depending on the technology. Therefore, this technology is not suited for electric vehicle applications, being more indicated for local storage applications. These results are consistent with other published studies [146].

Table 4 – Characteristics of lead-acid batteries and VRFBs equivalent to lithium ion battery of the Nissan Leaf.

	Leaf battery (Li-ion)	***Lead acid (stationary)***	***VRFB G1***	***VRFB G1 with mixed acid***	***VRFB G2***
Number of cells (serial connection)	192	190	286	286	400
Volume of cell stack (L)	-	-	370	370	517
Weight of cell stack (kg)	-	-	127	127	178
Volume of liquid electrolyte (L)	-	-	727	558	343
Weight of liquid electrolyte (kg)	-	-	960	-	480
Total volume (L)	85	343	1097	928	859
Total weight (kg)	153	1200	1087	-	657

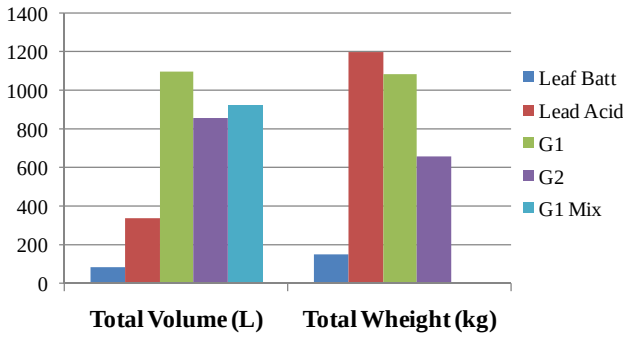

Fig. 22 - Comparison between the lithium ion battery of the Nissan Leaf EV and their VRFB and lead-acid battery equivalents.

2.10.TYPICAL APPLICATIONS FOR VRFBS

VRFBs are already being used in various stationary electrical storage applications along with other conventional battery technologies. But given their specificity, they are most used in applications having low power/energy ratios [83]. More than 20 G1 demonstration projects have already been made around the world, with various applications [72]. In these applications VRFBs benefit from their independence between rated power and stored energy, an advantage which will eventually overshadow their limitations in energy density and added complexity. Typically, the applications for VRFBs include:

- Load leveling;
- Peak Shaving;
- Uninterrupted power supply (UPS);
- Combination with renewable energies (wind/solar power generation).

A load leveling battery is used in order to provide a more leveled consumption of electric energy over time. It stores electricity in periods of low electricity cost and subsequently supplies electricity during premium tariff, minimizing cost [147]. An example of this application was the one made in 1996 by Mitsubishi Chemicals, who installed a 200 kW/800 kWh G1 system for load leveling at the Kashima-Kita Electric Power in Japan [29].

Sometimes, in certain industries there are some periods of very high power consumption during a relatively short period of time. This would usually require the increase of the electrical peak power contracted with the electricity supply company. To avoid this additional cost it is frequent to use high power batteries that work only briefly during peak power events reducing ("shaving") the instantaneous power peaks demand to the electrical grid and allowing for a lower contracted peak power [148]. As an example, in 2001, a 1,5 MW/1,5 MWh G1 system was installed at Tottori Sanyo Electric, in Japan, by Sumitomo Electric Industries Ltd, for a peak shaving application [149].

Uninterruptible power supply (UPS) technologies can guarantee a continuous supply of electric energy and/or provide a clean output voltage with low total harmonic distortion (THD) [150]. VRFBs are able to perform this task with a long cycle life. In 2003, a 500 kW/90 kWh G1

system was installed by Sumitomo Electric Industries Ltd in a Japan factory for UPS and peak shaving application [149].

Another application for VRFBs is their combination with renewable energy sources. These are often of an intermittent nature (namely, wind and solar energy), something which is not good for grid stability. Also their power generation often does not match power demand and so there is need for some kind of energy buffer which stores excess energy for later release during periods of higher demand. This is especially useful in the case of wind turbines, which typically have peak production at night time, when power demand is lowest. While many hydropower plants are able to reverse and store energy through pumping, wind turbines are frequently located in remote locations, needing for local storage to optimize output [33]. The energy storage is also important for buildings lacking an electrical grid connection, outside populated areas, which can use a photovoltaic, micro hydraulic or wind power system to produce electricity, and store it in a battery for later consumption along the day.

For all the aforementioned situations the VRFBs seem to be a valid option. In fact, there are several studies analyzing the use of VRFBs in photovoltaic and wind generation systems [93, 151-156]. Vetter et al. [93] have compared the use of lead acid batteries and one G1 for a small mountain restaurant in the black forest which has an hybrid photovoltaic system and stores the energy in a battery. They concluded that for a large energy storage, with high autonomy time, the G1 is the best option with the lowest annualized life cycle costs because their specific investment cost (€/kWh) decreases with increasing capacity, while for a lead acid battery the specific investment cost is constant and independent of the capacity.

2.11.CURRENT MANUFACTURERS

Today, there are several manufacturers of VRFBs worldwide. The Renewable Energy Dynamics Technology Ltd. (REDT), formerly RE-fuel Technology, was founded by Camco Clean Energy in 2000 with the purpose of developing VRFBs. They developed the ENIFY, a VRFB system with a range of power/energy stored from 5 kW/20 kWh to 20 kW/100 kWh [157].

Golden Energy Fuel Cell Co., Ltd. (GEFC) is a Chinese company established in 2003 which commercializes materials and components for VRFBs including electrodes, membranes, electrolyte and also cell stacks, as well as whole systems with output ranges between 2,5 kW/3,75 kWh and 4 MW/32 MWh [158].

V-Fuel is an Australian company established in January 2005 which has an exclusive worldwide license for commercializing the VRFB G2 technology. They commercialize VRFBs with a range of power outputs from 5 kW to 50 kW [159].

Prudent Energy operates since 2007 in the design and manufacture of VRFB systems. They maintain corporate offices in Bethesda, Maryland and Beijing, China, with research, development, and assembly of VRFBs facilities in the United States, Canada and Asia [160].

Cellenium (Thailand) Company Ltd was founded in 2000, being the sole licensee to commercialize in Thailand a number of inventions associated with VRFBs. Their first commercial system was placed in operation in 2008 [161].

Gildemeister is a German engineering company and machine tool builder founded in 1870. In 2010 Gildemeister entered into the market of energy storage with the “CellCube”, a commercial vanadium redox flow battery solution with powers and capacities ranging from 10 kW/40 kWh to 1 MW/4 MWh. They promote a variety applications, from energy storage for buildings without grid connections, to stabilization of energy production and fluctuation [162].

Golden Energy Century Ltd (GEC) is a Chinese company founded in 2011 commercializing electrolyte and membranes for VRFBs, as well as cell stacks and whole VRFB systems with power/energy capacity ranging from 2,5 kW/40 kWh to 5 kW/40 kWh [163].

Ashlawn Energy provides energy storage solutions with its “VanCharg” system. The company’s developing and manufacturing team is located in the USA, supported by US Department of Energy SmartGrid award and a network of national laboratories [164].

2.12.CHAPTER CONCLUSIONS

The typical applications for VRFBs are those in which the volume and weight are not limiting factors, such as load leveling, peak shaving, Uninterrupted Power Supply (UPS) and support to renewable energy sources such as wind and solar. VRFBs might indeed contribute for the viability of the mass adoption of abundant, yet intermittent renewable energy sources, providing an energy buffer which allows the power output to adjust itself to the instantaneous grid demand.

The performance of VRFBs depends of various factors, namely on the technology involved, e.g. G1 or G2, based on pure Vanadium or Vanadium bromide electrolytes, respectively. It will also depend on the performance of each one of their components, which in the present study have been analyzed separately in detail.

Firstly, the cell stack may be configured in parallel or in series. When in series it can be configured in equicurrent or countercurrent mode, with the latter configuration being more advantageous.

The flow rate is also a very important factor, typically the VRFB efficiency and discharge capacity increases with the increase of the flow rate, but the energy consumed for circulating the fluid (pumping losses) also increases, so it is necessary to find the optimal flow rate which maximizes the overall system efficiency.

Unfortunately, VRFBs still have a low energy density when compared with conventional batteries. This is due to the maximum concentration of Vanadium that can currently be dissolved in the supporting electrolyte. In the case of the G1 technology, typically the maximum vanadium ion concentration is 2 M or less, which corresponds to an energy density of 25 Wh/kg or 33 Wh/L, and that concentration is limited by the stability of the V^{5+} ions at temperatures above 40 °C and the solubility limit of V^{2+} and V^{3+} ions in supporting electrolyte at temperatures below 5 °C.

The G2 technology uses a vanadium bromide solution in both half-cells and shares all the benefits of the G1 technology including the fact that the cross contamination is eliminated. One disadvantage of this technology is the risk of formation of bromine vapors during charging. To avoid this it is necessary to employ bromine complexing agents, but their high cost is a limiting

factor for its commercialization, making price the main disadvantage of the G2 relatively to the G1 technology.

The membrane is also a critical component in a VRFB because it defines the performance and economic viability of the system (it can sum up to more than 20% of the overall system cost) and it can be an obstacle to their commercialization.

Electrodes play a key role in the performance of VRFBs as the improvement of the electrochemical activity of the electrode tends to increase the energy efficiency of the system. This can be done with the use of materials having a low bulk resistivity and a large specific area. For that reason surface modifications of the electrodes have been studied by several groups.

Bipolar plates should have high electrical conductivity in order to reduce the internal resistance of the cell stack. Simultaneously, they must have good mechanical properties in order to withstand the contact pressure when they are pressed against the electrodes, preventing the leakage of the liquid electrolyte.

It is likely that the recent advances in the energy density, power density and reliability of the VRFB technology, namely the G1 technology with mixed acids and the G2 technology, will lessen the gap between VRFBs and conventional batteries in terms of performance, efficiency and energy density, while maintaining the clear advantages they have and bringing up new possibilities for applications such as small scale energy storage, namely to boost the adoption of intermittent renewable energy sources. Undoubtedly, this is presently the focus of interest of VRFB application. But perhaps, one of the most desirable application fields for flow batteries in the future will be also the growing electric mobility market. In fact, the energy capacity of a flow battery can be restored in a few minutes through replacement of the liquid electrolytes.

As proved in the present work, the energy density of VRFBs is still far from being suitable for mobile applications, particularly electric mobility. It is still unclear if this particular flow battery technology might one day achieve the needed energy density at an affordable price. But if this happens with VRFBs, or any other kind of flow battery, it will indeed prove to be a disruptive technology for the electric vehicle market because it will eliminate two of the main obstacles for the acceptance of EVs, which are their exceedingly slow charging times and the concern over battery life shorter than vehicle life.

3. PRELIMINARY PROJECT OF A VRFB SYSTEM

This work proposes an energy storage technology to be used by the electric vehicles fast charging stations to make a peak shaving process enabling the charging of various EVs at the same time with a low contracted power.

The gas stations are generally easy and fast for vehicles to access, and an electric vehicle owner can charge his vehicle in the conventional gas stations in less than an hour, enabling the electric vehicles for run for long distances. Furthermore, gas stations could adapt their business size as a function of the increase of the EVs.

3.1.PROPOSED SYSTEM LAYOUT

Fig. 23 shows a typical steel fuel tank used in gas stations [165], among the various fuel tanks available in the market. Capacities vary from 1000 liters of capacity, to the giant tanks with 100 000 liters of capacity [165, 166], but one of the most commonly used in gas stations is the 20 000 liter tank with around 2,5 m of diameter and around 4,7 m in length. The present work has considered this tank for the storage of the liquid electrolytes.

Fig. 23– Typical fuel tank used in gas stations
(courtesy of Henriques & Henriques S.A.)[165].

The shape and material of the tanks raises some difficulties. Since they are typically made from steel [165, 166], the liquid electrolytes cannot be in direct contact with them due to their acid nature. To avoid that contact, the tanks may be coated with an acid resistant material. In such case, each fuel tank can only be used for one electrolyte (positive or negative). Alternatively, one or several smaller flexible tanks (made from an acid resistant material and similar to the one depicted in Fig. 24) may be installed inside the steel tanks. In this latter case, two smaller flexible tanks, each one containing a different liquid electrolyte, may be accommodated inside one steel tank.

As can be seen in Fig. 23, the diameter of the main tank opening (only 60cm) may hamper the insertion of the flexible tanks inside it. Several small solid tanks made from PVC or other acid resistant material could also be used. However the best solution seems to be the use of flexible rubber tanks as those firstly proposed by Sumitomo Electric Industries Ltd and represented in Fig. 24. These were made specifically to take advantage of the fluidic form of these batteries and to allow their insertion in unused spaces such as underground cisterns, through manholes [95].

Fig. 24 - Rubber tank for VRFB liquids electrolytes
(courtesy of Sumitomo Electric Industries LTD) [95].

Rubber tanks with a shape which reasonably conforms to the interior of the steel tanks should be made, as illustrated in Fig. 25a, including a support structure to separate both tanks and leaving free space below the manhole to allow the entry of installation and service staff. This

structure can be done simply with Landsquare PVC beams and mounted *in loco* with stainless steel screws.

Another alternative, is to use four tanks (two for positive and two for negative electrolyte). This facilitates their introduction into the fuel tank. On the other hand, this configuration allows the existence of two VRFBs using the same gas tank so it is possible to have one battery to charge EVs and the other one being charged at low power input from the electric grid. The four tank configuration is represented in Fig. 25b.

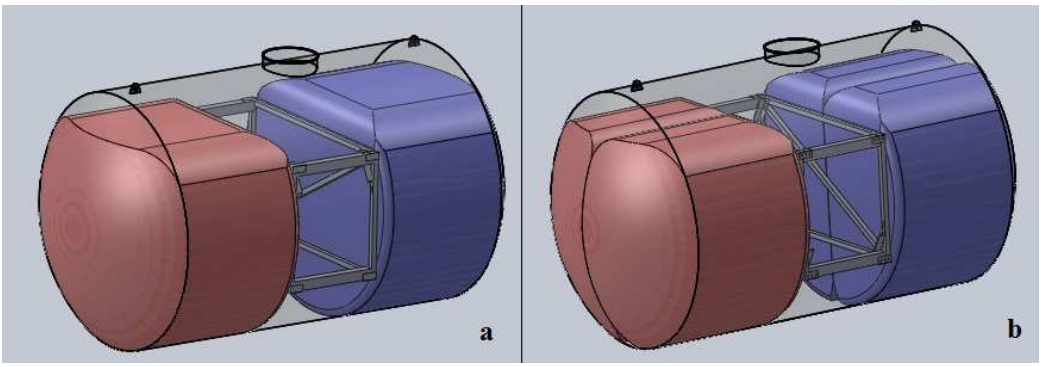

Fig. 25 - Scheme of rubber tanks for VRFBs (a - two tanks configuration; b – four tanks configuration) inside fuel tanks with support structure.

To make these tanks, the appropriate rubber should be selected. It must be highly resistant to the corrosion with sulfuric acid under the prescribed concentration. Typically, the two liquids electrolytes (anolyte and catholyte) of a G1 are prepared by dissolving 0,1 M to 2 M $VOSO_4$ (vanadylsulphate) in 0,1 M to 5 M H_2SO_4 aqueous solution, to form tetravalent vanadium ions [32], which means that the volume concentration of sulfuric acid should be between 0,005% and 27%.

Table 5 which has been compiled from references [167-169], shows the chemical resistance of the most common rubber types, and it can be seen that there are various types of rubber which are resistant of acid sulfuric for the concentrations needed, like the EPDM, Butyl and Teflon.

However, the Vanadium oxides are also corrosive [73] and their presence within the electrolyte must be considered, so a rubber which is resistant to both substances is needed. After

analyzing Table 1, as a first approximation it seems that Butyl rubber will be a good candidate material for the rubber tanks.

Table 5 - Compatibility of various types of rubber with sulfuric acid and vanadium oxides [167-169]

	Natural	***EPDM***	***Nitrile***	***Neoprene***	***Viton***	***SBR***	***Silicone***	***Butyl***	***Teflon***
Sulfuric acid dilute (10%)	C	B	C	B	A	C	D	B	A
Sulfuric acid 25%	B	A	-	-	C	-	-	A	A
Sulfuric acid 25 – 50 %	B	A	-	-	B	-	-	A	A
Sulfuric acid 50 – 98%	-	A	-	-	A	-	-	-	A
Sulfuric acid 98%	D	C	D	D	A	D	D	D	C
Vanadium Oxide	-	D	A	B	A	D	D	A	-
Vanadium Pentoxide	-	D	A	B	A	D	D	A	-

A - Recommended B - Minor to moderate effect C - Moderate to severe effect D - Not recommended

3.2.DETERMINATION OF THE SYSTEM OPERATING CONDITIONS

The determination of the system operating conditions under analysis is presented in this section. The aim is to evaluate its technological viability in order to characterize the charge/discharge cycles, the flow rate and the required pumping power. This will allow the estimation of the overall efficiency of the system. These calculations do not exclude the importance of building and testing a physical prototype to compare the theoretical and real conditions of operation in order to confirm the accuracy of the presented calculations, but show an initial approach to the design of such a system.

This project involves the use of a VRFB to store energy from the electrical grid during low demand schedules (and also from renewable sources, if required). The stored energy is then supposed to supply two ChadeMo fast chargers to charge EVs similar to the ones manufactured by Petrotec [170]. Fig. 26 outlines the architecture of the proposed system. Renewable energy sources could be present at the gas station (eg. solar or wind energy) in order to reduce the energy consumed from the grid and to benefit from the energy storage facility. However, all the energy included in the calculations is considered to come from the grid.

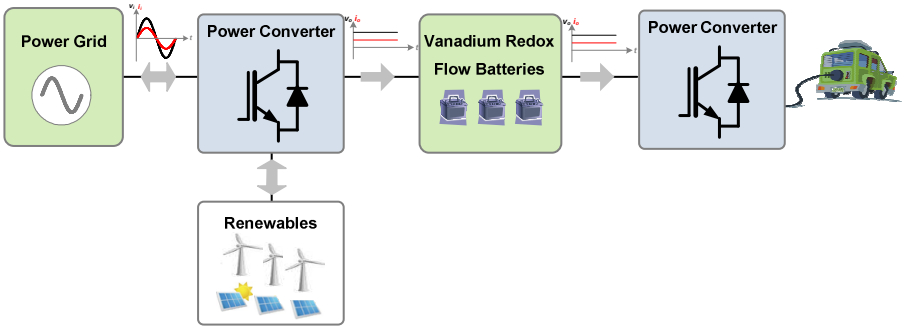

Fig. 26 – Proposed system architecture.

During the fast charge of an EV the voltage, current and power output from charger will vary, and these parameters were monitored by Bai et al. [171] for a Nissan Leaf. The evolution of the power output is represented in Fig. 27. This charging cycle was performed by a Terra 51

charger manufactured by ABB and the Nissan Leaf was charged up to 80% SoC. By integrating the power against time it can be concluded that in this particular cycle about 14,8 kWh were supplied to the car. This confirms that the vehicle was not fully discharged when the charge began. In a real case probably each car will have a different initial SoC but for the present calculations it was considered that all cars would be in the same initial conditions and would be submitted to the same charging cycle as the car monitored in Fig. 27.

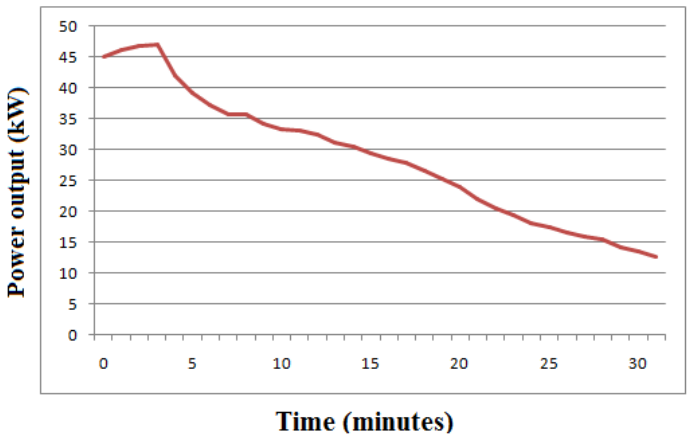

Fig. 27 - Evolution of the charging power output of a Nissan Leaf, as monitored by Bai et al. [171].

It is assumed that there will be always two vehicles charging simultaneously (two chargers connected to the VRFB) and that the ChadeMo charger efficiency (η_{Ch}) will be around 95%, so the power output (P_{out}) can be calculated for each time step by Eq. 4:

$$P_{out} = \frac{2\ P_{Leaf}}{\eta_{Ch}} \tag{4}$$

The voltage output of the stack during discharge (V_{disch}) can be calculated as a function of the open circuit voltage of the stack during discharge (OCV_{disch}), its internal resistance (R) and the discharge current (I) in each time step by the Eq. 5. In this equation only the voltage losses due to the internal resistance are considered.

$$V_{disch} = OCV_{disch} - RI \tag{5}$$

So, it is necessary to calculate the discharge current (*I*) and the open circuit voltage of the stack for each time step. The discharge current can be calculated as a function of the output power and the output voltage for each time step by Eq. 6:

$$I = \frac{P_{Out}}{\mathrm{V}_{disch}} \tag{6}$$

The open circuit voltage of the stack is a function of the number of cells (*N*), the equilibrium potentials *E+* and *E-* (which are equal to 1,004 V and -0,255V, respectively), the universal constant of the ideal gases (*r*), the temperature (*T*), the Faraday constant (*F*) and the state of charge, through Eq. 7:

$$OCV_{disch} = N\left(E^{+} - E^{-} + \frac{rT}{F}\ln\frac{SoC^{2}}{(1-SoC)^{2}}\right) \tag{7}$$

However, due to the internal resistances, the output voltage will always be lower that the open circuit voltage of the stack, which means that there are losses associated and the real discharge power (P_r) is considered to be the sum of the power output and the losses as represented in Fig. 28, and can be calculated by Eq. 8:

$$P_r = OCV_{\ disch}\, I \tag{8}$$

So, for each time step, the real discharged energy (E_r) of the stack can be calculated by multiplying the real discharge power by the time step (Δt), through Eq. 9:

$$E_r = P_r \Delta t \tag{9}$$

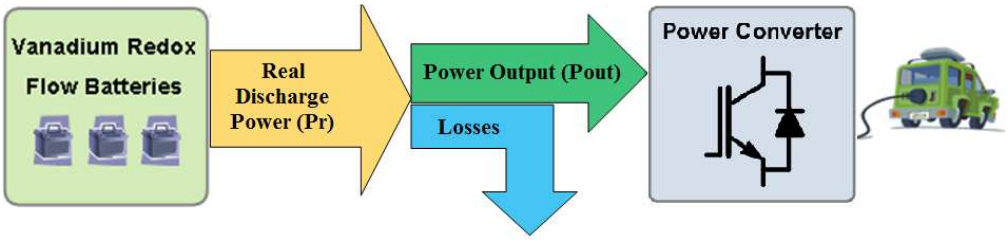

Fig. 28 - Discharging process of a VRFB.

On the other hand, the open circuit voltage of the stack depends on the state of charge (SoC) of the VRFB, which will vary during the discharge according to the real discharged energy (*Er*).

The state of charge in each time step can be calculated as a function of the energy density of the liquid electrolyte (*E*), the volume of liquid stored (*V*), the maximum state of charge of the VRFB and the real energy discharged, through Eq. 10:

$$SoC = \frac{E\ V\ SoC_{Max} - \sum E_r}{E\ V} \tag{10}$$

As a first approach, the maximum SoC of the VRFB during discharge will be considered as 100%. Using iterative calculations and providing output power (P_{out}) as a function of time as an input (profile of Fig. 27), the previous equations can be combined in order to obtain the desired parameters.

Considering a system with 250 cells and a membrane area of 0,5 m^2, the internal resistance can be calculated using the information gathered in Table 6. In the case of membranes, the area resistance is around 0,1 $\Omega.cm^2$, and the present work considers that the membranes have a square geometry, but a rectangular shape could also have been adopted.

Table 6 - VRFB stack components selected for the analysis.

	Membrane	***Electrodes***	***Bi-polar plates***
Model	Nafion 117	SGL GFA6EA [145]	SGL PPG86 [145]
Resistivity	-	15 Ωmm	1 Ωmm
Thickness	-	6 mm	3 mm
Compression ratio	-	20%	-
Resistance reduction	-	70%	-
Electric Resistance	0,02 mΩ	0,054 mΩ	0,00334 mΩ
Quantity	250	500	249

Since the electrodes proposed are carbon felts, they must be compressed in order to prevent the leakage of the liquid electrolyte and, at the same time, reduce the electric resistance.

The electrodes GFA6EA from SGL GROUP have been chosen for this project and the variation of the electric resistance with the compression ratio is showed in Fig. 29. It can be seen that for a compression ratio of 20%, the electric resistance reduces around 70% [145]. Therefore, the internal resistance (R) of this system will be around 33,5 mΩ.

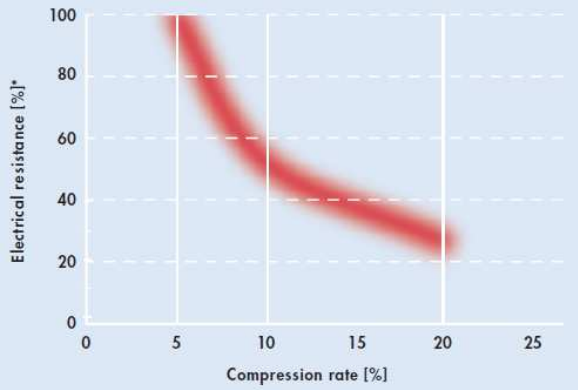

Fig. 29 - Electrical resistance as a function of the compression rate of the graphite felt electrodes of SGL GROUP [145].

Table 7 shows the specific input values used to simulate the VRFB system proposed for this project, but the analysis proposed may be used for different values.

Table 7 - Input values used to simulate the VRFB system.

Number of cells (N)	250
Energy density (E)	33 Wh/L
Volume of liquid stored (V)	14000 L
Membrane area (for each cell)	0,5 m^2
Internal resistance (R)	33,5 mΩ
Efficiency of ChadeMo fast charger (η_{ch})	95%
Temperature (T)	25 ºC
Vanadium Concentration	2 mol/L
Number of cars charging simultaneously	2
Charging time of VRFB (t_{chg})	12h

Fig. 30a and Fig. 30b represent the variation of the voltage and the current, respectively, determined for the VRFB system considered, for 14 consecutive fast charging cycles of 2 EVs simultaneously. The vehicles simulated have the characteristics of the Nissan Leaf, while the charging profile was the one represented in Fig. 27. This means that a total of 28 vehicles were charged in a 7,5 h period, with the final state of charge of the VRFB having dropped to around 1%, with no energy left to perform another vehicle charge. The rise in current observed in Fig. 30b is a natural consequence of the drop in voltage observed in Fig. 30a, to ensure the programmed power cycle. The slight ripple observed in the SoC curve is due to the non-constant power profile (Fig. 27).

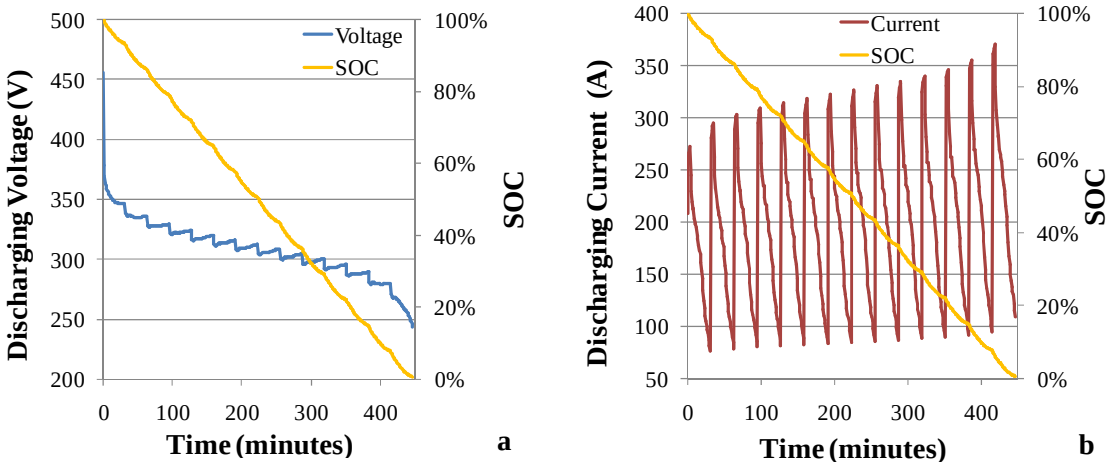

Fig. 30 - Discharging Voltage (a) and Current (b) cycles for VRFB system.

With the knowledge of the discharge profiles of Fig. 30 it is possible to define the charge cycle for the VRFB. Firstly, the available stored energy, E_a (showed in Fig. 31) coincides with the real discharged energy, calculated through Eq. 9. So, for a given SoC during charge, the available energy stored is calculated as follows:

$$E_a = E\ V\ SoC - E\ V\ SoC_{min} \tag{11}$$

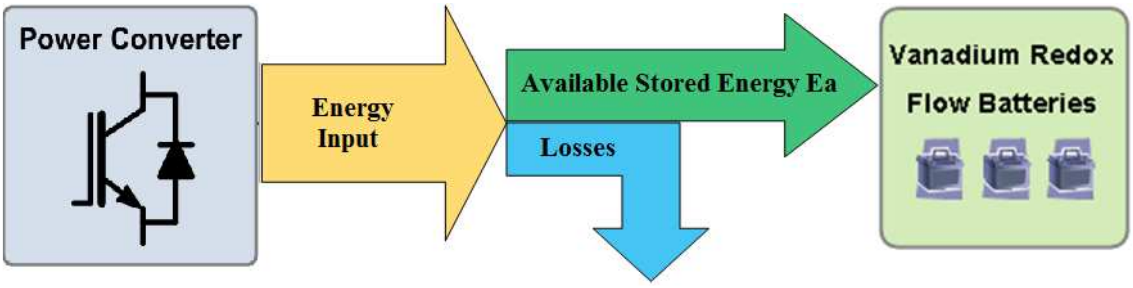

Fig. 31 - Charging process of a VRFB.

The open circuit voltage during charge (OCV_{chg}) can be calculated as a function of the *SoC,* as it was done previously for the discharge phase with Eq. 7.

Considering the real power (equal to the input power minus the losses) during a given charge time lapse (t_{chg}), (in this study, 12 hours have been always considered), the evolution of OCV_{chg} as a function of time can be estimated. In this way it is then possible to calculate the current during each time step:

$$I = \frac{\frac{\sum E_a}{t_{ch}}}{OCV_{chg}} \tag{12}$$

With this information it is possible to calculate the output voltage of the stack during charge (V_{chg}):

$$V_{chg} = OCV_{chg} + RI \tag{13}$$

Note that in this case the input voltage will be the sum of the open circuit voltage and the losses. This means that the input voltage is always higher that the open circuit voltage. This is the opposite of what happens during the discharge of the VRFB.

So, the input power (P_{in}) can be calculated as follows:

$$P_{In} = V_{chg} I \tag{14}$$

And the efficiency of the VRFB (η) can be obtained through:

$$\eta = \frac{\int_0^{t_{disch}} P_{out} t dt}{\int_0^{t_{ch}} P_{In} t dt} \quad (15)$$

The voltage and current, as a function of charge time, are showed in Fig. 32a and Fig. 32b respectively. The calculated theoretical energy efficiency was 93,7% without considering the pumping losses.

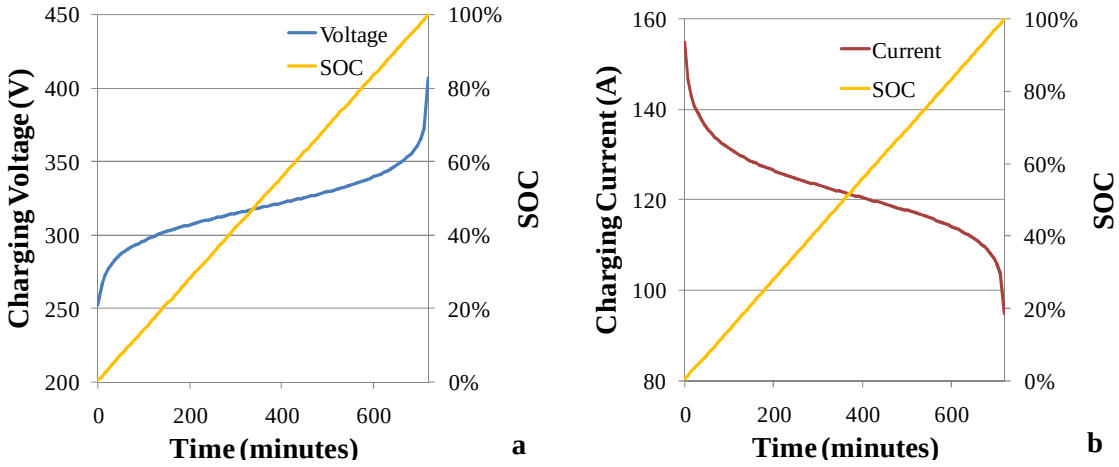

Fig. 32 - Charging Voltage (a) and Current (b) cycles for the VRFB system.

As explained in chapter 2, an important factor in the viability study of a VRFB system is the required mass flow rate, as it represents an extra energy consumption which will reduce the overall system efficiency.

It is necessary to divide the number of moles of vanadium oxidized per second by the molarity of vanadium ions in the solution in order to calculate the minimum required flow rate [172]. So, knowing the number cells (N), the current (I), and the concentration of vanadium in the solution (C_v) and the Faraday constant (F) it is possible to calculate the minimum necessary flow rate (Q) through Eq. 16 [172]:

$$Q = \frac{I\,N}{F\,C_v}\ (L/s) \quad (16)$$

Since the flow rate depends on the concentration of vanadium, it is necessary to take into account the variation of the concentration of the vanadium reactant in the solution due to the variation of the SoC of the liquid stored in tank during the charge and discharge cycles. The total concentration of vanadium is constant. However, during the discharge, the concentration of reactants decreases, while the concentration of products increases, and vice versa.

Knowing the vanadium reactant and product concentration in the solution, the *SoC* can be calculated in two ways, regarding to the concentration at the anode or at cathode respectively [93, 173]:

$$SoC = \frac{CV^{2+}}{CV^{2+} + CV^{3+}} = \frac{CVO_2^+}{CVO_2^+ + CVO^{2+}} \tag{17}$$

And the Depth of Discharge (*DoD*) can be calculated as follows [93]:

$$DoD = 1 - SoC = \frac{CV^{3+}}{CV^{2+} + CV^{3+}} = \frac{CVO^{2+}}{CVO_2^+ + CVO^{2+}} \tag{18}$$

Eq. 16 does not take into account the variation of the *SoC* through the membrane. This variation can be neglected for very high flow rates, but must be considered for the optimal flow rate [97].

So, considering the initial concentration of vanadium in the solution upstream of the cell (C_{in}) and the concentration of vanadium in the solution downstream of the cell (C_{out}), the minimum necessary flow rate (Q) can be calculated through Eq. 19 [174]:

$$Q = \frac{IN}{F(C_{out} - C_{in})} \ (L/s) \tag{19}$$

Note that when the VRFB is charging C_{out} and C_{in} of Eq. 19 refer to the concentration of V^{2+} or VO_2^+. On the other hand, when the VRFB is discharging, C_{out} and C_{in} refer to the concentration of V^{3+} or VO^{2+}. This means that the flow rate will have to vary during the operation of the VRFB. It will increase during the increase of the *SoC* (when charging) and during the increase of *DoD* (when discharging). This is consistent with the study made by Ma et al. [99].

In Eq. 19 C_{in} is considered to be equal to the actual concentration of vanadium in the storage tanks, and varies during cycle. C_{out} is equal to 0 M/L in the case of discharge (0% *SoC*) and is equal to 2 M/L in the case of charge (100% *SoC*), being constant during each cycle.

Note that the flow rate calculated by Eq. 19 is the flow rate for each electrolyte (i.e. anode and cathode solutions). However, this value represents the minimum flow rate necessary to produce the desired current if all vanadium ions existing within the solution were oxidized while flowing through cells. In practice, this does not happen and some authors suggest the use a flow rate which is higher than the one theoretically calculated.

Unfortunately, to the author knowledge, there is no sufficient information available in the literature concerning the difference between the theoretical and the real flow rate needed, so in this work it will be considered that the VRFB will operate with the theoretical flow rate calculated from Eq. 16. In this way, the calculated efficiency with pumping power might be higher than the one announced by manufacturers.

Fig. 33a and Fig. 33b display the variation of the flow rate for each liquid electrolyte during discharge and charge cycles, respectively. It can be seen that there is an exponential increase of the flow rate along time during both charge and discharge.

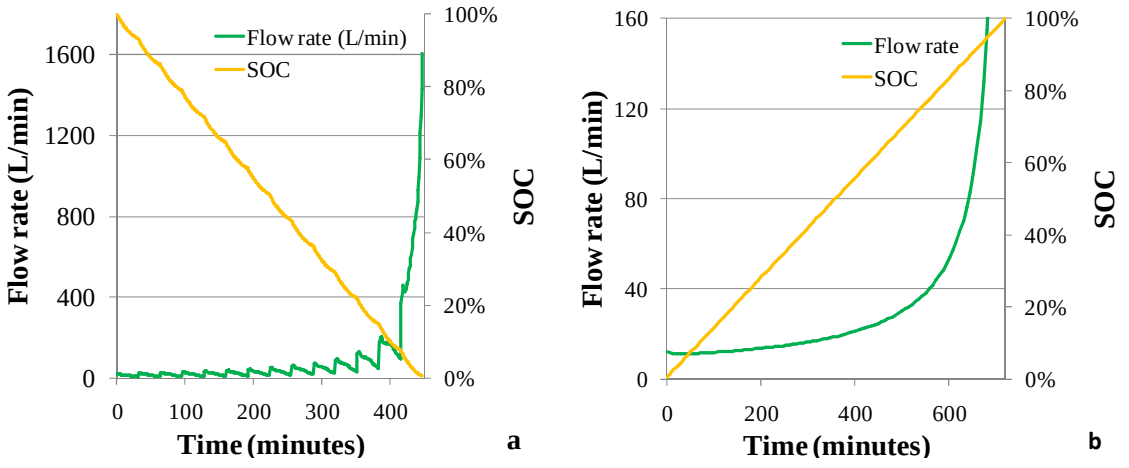

Fig. 33 - Variation of flow rate during discharging (a) and charging (b) cycles.

So, knowing the flow rate, the pumping power (P_{pump}) can be estimated by Eq. 20:

$$P_{pump} = 2Q\ \Delta p \tag{20}$$

With Δp representing the total pressure loss in the system, calculated through:

$$\Delta p = \Delta p_{pipes} + \Delta p_{stack} \tag{21}$$

The pressure loss in the Stack (Δp_{stack}) is due to the flow of the liquid through the graphite felt electrodes and can be calculated based on the flow rate, the dynamic viscosity (μ) in this case 4,93 x10^{-3} Pa.S, the permeated specimen length (l), the permeability (P) and the permeated cross section area (A_{cs}) [145]:

$$\Delta p_{stack} = \frac{Q\ \mu\ l}{P\ A_{cs}} \tag{22}$$

It is necessary to consider that the permeability of the electrodes will vary with the compression of the electrodes, according to the chart represented in Fig. 34. in the present work a compression of 20% has been considered, so the permeability of the electrodes will be around 4,7 x 10^{-11} m^2 [145].

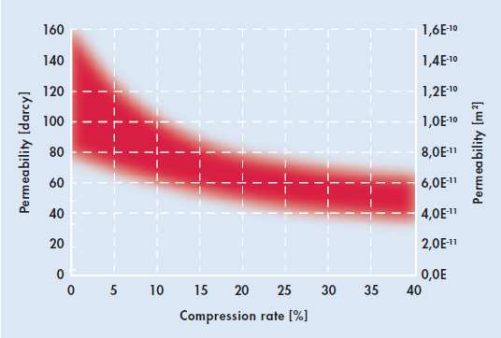

Fig. 34 - Permeability of the graphite felt electrodes SGL GFA6EA [145].

The pressure loss in the pipes (Δp_{pipe}) should also be calculated. It is considered that each liquid electrolyte has a height difference between the tank and the stack of 1 m. The tubes used are considered to be made of PVC with low roughness (ε=0,005 mm). The first section of

the piping is a circular tube with 40 mm of inner diameter, a length of 12 m and three 90° bends, which carries the liquids from the tanks to the cell. The second section of the piping is a collector with one output for each cell, with 3 mm of inner diameter and 20 cm of length. The third section is another collector attached to each output of section 2. This collector has 5 outputs, which means that the entry of the liquid into the cell is made through 5 different locations in order to uniform the flow. Each output is also a circular tube with 3 mm of inner diameter and 20 cm of length. The return circuit displays an identical circuit, symmetrical to the one just described. The pressure losses in collectors have been neglected.

Therefore, to calculate the total pressure drop, it is necessary in the first place, to calculate the Reynolds number (*Re*) in each section [175]:

$$Re = \frac{4\,Q}{\pi\,D\,v} \tag{23}$$

In which v represents the kinematic viscosity of the fluid (in this case 5 x 10^{-6} m^2/s) and D the inner diameter of the pipe. The coefficient of friction (f) can be calculated from the Colebrook expression, which is the basis for the Moody Diagram [175]:

$$\frac{1}{f} = -0{,}86 \ln\left(\frac{\varepsilon/_D}{3{,}7} + \frac{2{,}51}{Re\sqrt{f}}\right) \tag{24}$$

The localized head losses can be considered as an equivalent piping length (*Le*) calculated as a function of the coefficient of head loss (*k*), which is 0,9 for each one of the bending's [175]:

$$Le = \frac{\sum k\;\; D}{f} \tag{25}$$

So, the total head loss (*H*) for each section can be calculated function of the parameters calculated previously by Eq. 26 [175]:

$$H = f\;\frac{L + Le}{D}\frac{V^2}{2\,g} \tag{26}$$

In which V corresponds to the velocity of the fluid, L corresponds to the length of the section and g is the gravitational acceleration. The pressure drop for each section can be calculated as follows [175]:

$$\Delta p_{pipe} = \frac{H}{\rho\, g} \tag{27}$$

Where the specific mass of the liquid electrolyte (ρ) was considered to be 1320 kg/m³:

The total pipe pressure loss will be the sum of the pressure loss in each section and the pumping power can be calculated using equations 20 and 21. The result it is shown in Fig. 35a and Fig. 35b for the discharge and charge respectively.

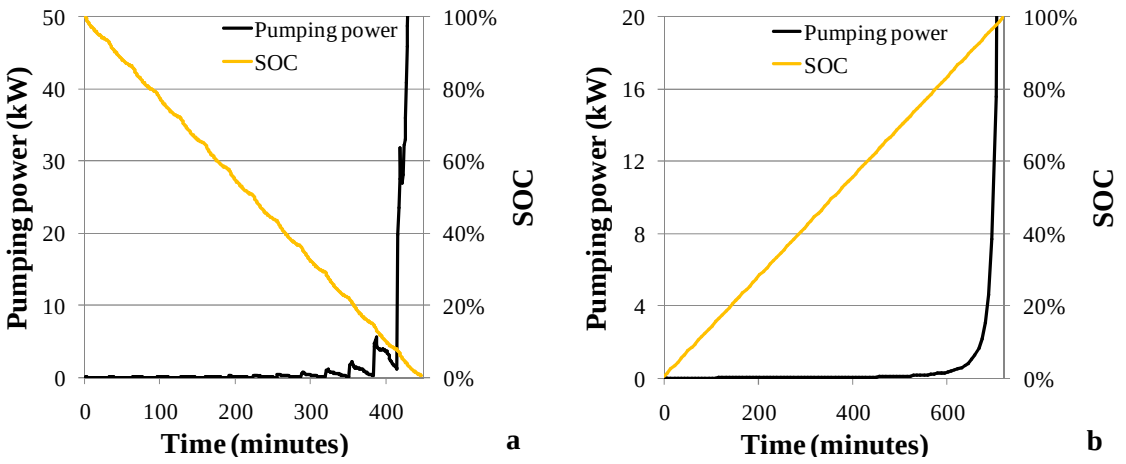

Fig. 35 - Variation of pumping power during discharging (a) and charging (b) cycles.

It can be seen that this system will have very high flow rates during the ending of the charge and it very high pumping power will be need, resulting in a very low efficiency, around 9%.

So in order to reduce the pumping power and increase the system efficiency, a reduction of the SoC interval used is proposed. A good compromise seems to be choosing a maximum SoC obtained during charge of 97% (which reduces the total number of cycles to 13). Under these conditions the minimum SoC achieved during discharge will be 4,7 %, and the VRFB efficiency considering pumping losses ($\eta_{totalVRFB}$) will be 91,7% (93,8% without pumping losses). However the reduction of the SoC range used resulted also in a reduction of the system capacity used, from

462 kWh to only 426 kWh. On the other hand, these 426 kWh available are affected by the discharge efficiency with means that in these conditions the VRFB will only provide to the fast charger around 405 kWh. This energy is sufficient to charge 26 cars.

One of the current manufacturers of VRFB systems has informed the authors that their system had an energy density of 16 Wh/L and displayed a DC-DC efficiency ($\eta_{totalVRFB}$), including pumping losses, around 80%, which is lower that the efficiency estimated for the system proposed by the authors. The differences might be attributed to several reasons. Firstly, as mentioned, the efficiency was estimated for a theoretical flow rate which will be lower than the real flow rate. Secondly, the energy density of the liquid electrolyte used by the referred manufacturer was roughly half of the one considered in the present work. This means that a lower concentration of vanadium was present and consequently a much higher flow rate for the same current output was probably needed.

Fig. 36 thru Fig. 39 shows the voltage, current, flow rate and pumping power during discharge and charge respectively, now for the SoC interval used.

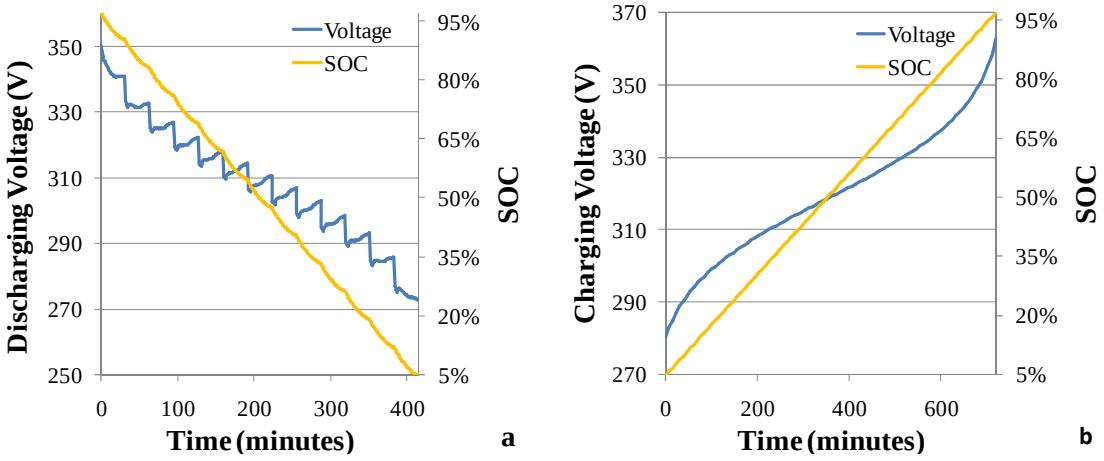

Fig. 36 – Optimized Discharging (a) and Charging (b) voltage cycles proposed for the VRFB system.

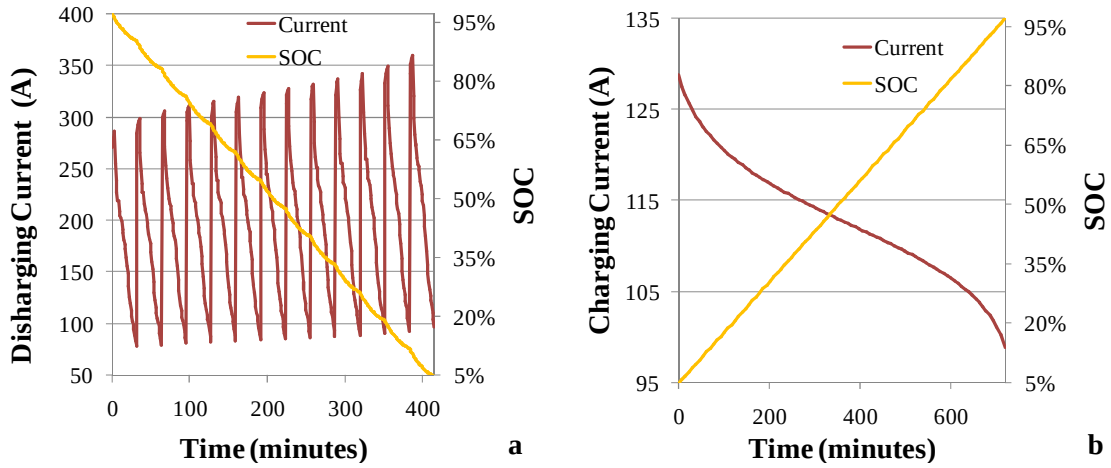

Fig. 37 - Optimized Discharging (a) and Charging (b) current cycles for the VRFB system proposed.

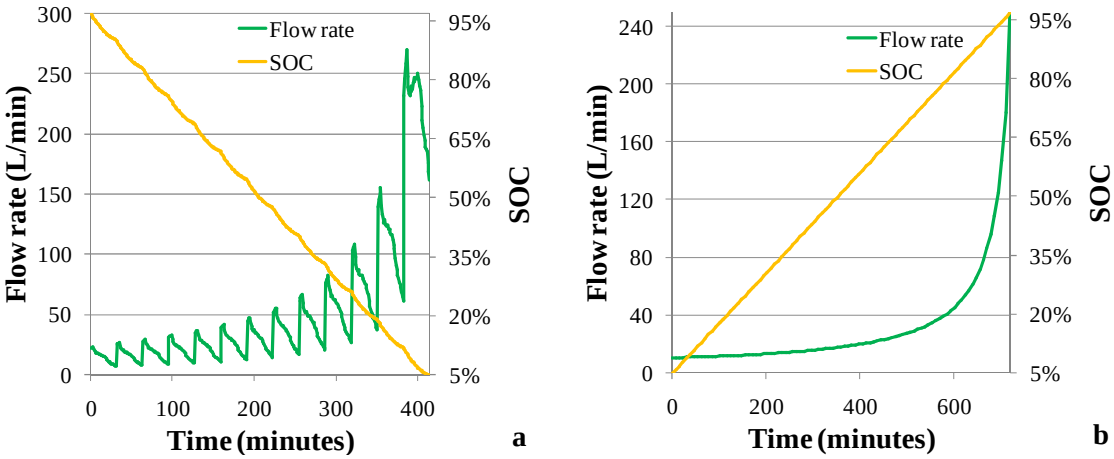

Fig. 38– Optimized Flow rate for Discharging (a) and Charging (b) cycles for the VRFB system proposed.

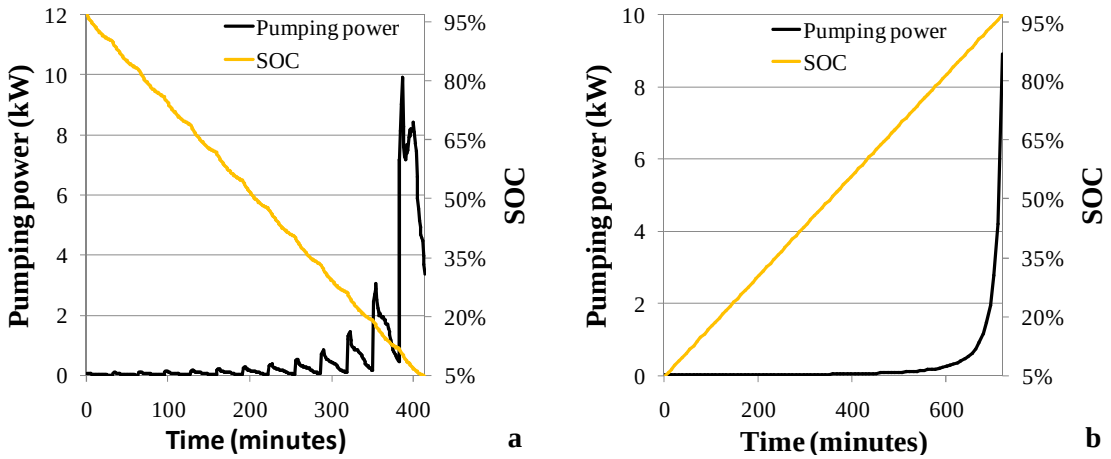

Fig. 39 – Optimized Pumping power for Discharging (a) and Charging (b) cycles for the VRFB system proposed.

3.3.ECONOMIC ANALYSIS OF THE PROJECT

The technological analysis made would be incomplete without a suitable economic analysis. Firstly it is necessary to roughly estimate the total cost of the system proposed, even if there is a substantial uncertainty degree concerning its real cost. Nevertheless, estimations based on the information obtained from the manufacturers may be done. A manufacturer has provided a price of 324 000 € for a complete system with the power and capacity similar to the values required by this project (100 kW and 405 kWh). This commercial system includes tanks, pumps, control system, cell stack and liquids electrolytes. However, this is a typical system in which all the components are sealed in a box. The present work considers that switching the solid tanks by the rubber tanks will not impact the final price of the system. The manufacturer reported the total VRFB system efficiency with pumping power ($\eta_{totalVRFB}$) to be around 80% in DC-DC. For the sake of coherence the present analysis has used this efficiency.

Firstly, it is necessary to calculate the overall system efficiency using this VRFB connected to two ChadeMo chargers each with an assumed efficiency (η_{Ch}) of 95% and one VRFB AC/DC charger with an assumed efficiency ($\eta_{AC\text{-}DC}$) of 95%. So the overall system efficiency (η_{system}) can be calculated by the following expression:

$$\eta_{System} = \eta_{AC-DC}\ \eta ch\ \eta_{total\,VRFB} = 0{,}95 \text{ x } 0{,}95 \text{ x } 0{,}8 = 0{,}722 \quad (28)$$

So, to make the economic evaluation of the project, the *NPV* (net present value) and the payback time (*PT*) criteria will be used. A 20 year life cycle is considered for the project, with 26 cars being charged per day, during 365 days for year. The electrical energy will be purchased at a price (*p*) of 0,08 €/kWh (low demand period price) and sold at a price (*s*) of 0,4 €/kWh. The inflation rate (*i*) is considered to be 3%, the tax over gain (*TOG*) 25%, and the minimum acceptable rate of return (*MARR*) 5%. The loss of value of the equipment translated into the amortizations (A), is also taken into account. It is considered that that at the end of the 20 years the value of the equipment is null, so a devaluation of the equipment around 5% year may be considered. The amortization is taken into account in the calculation of the Cash-Flows (*CF*) because it brings

advantages in taxes and it is assumed that there is no external financing requested. This economic evaluation of the project is based on [176].

So, firstly the calculation of the gains from sales (*S*) for the first year (n=1) is performed as follows: It is a function of the energy sold for the charging of each vehicle (14,8 kWh according to the charge profile of Fig. 27), the number of cars charged per day (*Nd*). The gain from sales for the first year (n=1) can then be calculated by Eq. 29:

$$S_{n=1}(€) = (14{,}8\ Nd\ s\ 365)\ (1+i) \tag{29}$$

Considering that all of the parameters assumed are constant during the whole life cycle considered, the gain from sales during the next years is calculated as follows:

$$S_{n}(€) = S_{n-1}(€)\ (1+i) \tag{30}$$

The associated costs (*C*) for the first year (n=1) are calculated as follows:

$$C_{n=1}(€) = \frac{(14{,}8\ Nd\ 365)}{\eta_{System}}\ p\ (1+i) \tag{31}$$

And the cost for the next years is calculated by the Eq. 32:

$$C_{n}(€) = C_{n-1}(€)\ (1+i) \tag{32}$$

Knowing the total values of the sales and costs for each year, the earnings before interest, taxes, depreciation and amortization (*EBITDA*) for each year can be calculated by Eq. 33:

$$EBITDA_n\ (€) = S_n - C_n \tag{33}$$

Knowing the amortization rate per year (A_r) and the investment (*Inv*), the amortization for each year is calculated by Eq. 34:

$$A\ (€) = Inv\ (€)\ A_r \tag{34}$$

The results before taxes (*RBT*) for each year can be calculated through:

$$RBT\ (€) = EBITDA\ (€) - A\ (€) \tag{35}$$

The total value of taxes (*Tax*) can be calculated by Eq. 36:

$$Tax\ (€) = RBT\ \ TOG \tag{36}$$

So, the liquid result (*LR*) for each year can be calculated by the Eq. 37:

$$LR\ (€) = RBT - Tax \tag{37}$$

And the cash flow (*CF*) for each year is calculated by Eq. 38:

$$CF(€) = LR + A - Inv \tag{38}$$

So, it is possible to analyze the project by the *NPV* criterion, calculating the total *NPV* for the whole 20 years but firstly it is necessary to calculate the real interest rate (i'), which considers the *MARR* and the inflation rate (i):

$$i' = (1 + MARR)\ \ (1 + i) \tag{39}$$

And the *NPV* can be calculated by Eq. 40:

$$NPV = \sum_{n=0}^{15} CF_n(1 + i')^{-n} \tag{40}$$

As a general rule, the project will be economically viable when the *NPV* is a positive value. Table 4 displays the input data required for the calculation of the *CF* of this project, and Table 5 shows the calculation of the *CF* for the 20 years considered.

Table 8 - Input data required for the calculation of the cash-flows of the project.

Energy charged per car	14,8 kWh
Number of cars per day	22
Days per year	365
S	0,4 €
P	0,08 €
Amortization rate	5%
Taxes over gain	25%
i	3%
MARR	5%
$\eta_{total\ VRFB}$	80%
η_{System}	72,2 %

Table 9 - Cash flows of the project for the 20 years considered.

Year	*Inv (€)*	*Sales (€)*	*Cost (€)*	*EBITDA (€)*	*A (€)*	*RBT (€)*	*Taxes (€)*	*LR (€)*	*CF (€)*
0	324 000								324 000
1		48 964	3 563	35 400	16 200	19 200	4 800	14 400	30 600
2		50 433	3 970	36 462	16 200	20 262	5 066	15 197	31 397
3		51 946	14 389	37 556	16 200	21 356	5 339	16 017	32 217
4		53 504	4 821	38 683	16 200	22 483	5 621	16 862	33 062
5		55 109	5 266	39 843	16 200	23 643	5 911	17 733	33 933
6		56 762	5 724	41 039	16 200	24 839	6 210	18 629	34 829
7		58 465	6 195	42 270	16 200	26 070	6 517	19 552	35 752
8		60 219	6 681	43 538	16 200	27 338	6 834	20 503	36 703
9		62 026	7 182	44 844	16 200	28 644	7 161	21 483	37 683
10		63 887	7 697	46 189	16 200	29 989	7 497	22 492	38 692
11		65 803	8 228	47 575	16 200	31 375	7 844	23 531	39 731
12		67 777	18 775	49 002	16 200	32 802	8 201	24 602	40 802
13		69 811	19 338	50 472	16 200	34 272	8 568	25 704	41 904
14		71 905	19 918	51 987	16 200	35 787	8 947	26 840	43 040
15		74 062	20 516	53 546	16 200	37 346	9 337	28 010	44 210
16		76 284	21 131	55 153	16 200	38 953	9 738	29 214	45 414
17		78 572	21 765	56 807	16 200	40 607	10 152	30 455	46 655
18		80 930	22 418	58 511	16 200	42 311	10 578	31 734	47 934
19		83 357	23 091	60 267	16 200	44 067	11 017	33 050	49 250
20		85 858	23 783	62 075	16 200	45 875	11 469	34 406	50 606

For the cash-flows showed in Table 5 the global *NPV* is 33 806 € which means that the project is economically viable for the conditions showed in Table 4. So, the recovery time can be calculated by successively adding the *CF* of each year (cumulative) until it becomes a positive value. The recovery time will correspond to the moment at which the cumulative crosses zero.

Table 6 shows the value of the cumulative for each year and it can be seen that the estimated recovery time is between 9 and 10 years, (around 9,5 years after interpolating).

However, for these calculations it was assumed that there would be always 22 cars charging per day, and the minimum acceptable rate of return would be 5%, which is a small value. However, the price of this system is still high because it is not yet a mature technology and

there are still not a lot of manufacturers worldwide. It is expected that during the next few years the price of this technology will decrease.

Table 10 - Cumulative value of cash-flows.

Year	*CF (€)*	*Cumulative (€)*	*Year*	*CF (€)*	*Cumulative (€)*
0	324 000	-324 000	11	39 731	60 601
1	30 600	-293 400	12	40 802	101 402
2	31 397	-262 003	13	41 904	143 307
3	32 217	-229 786	14	43 040	186 347
4	33 062	-196 724	15	44 210	230 556
5	33 933	-162 791	16	45 414	275 971
6	34 829	-127 962	17	46 655	322 626
7	35 752	-92 210	18	47 934	370 560
8	36 703	-55 506	19	49 250	419 810
9	37 683	-17 823	20	50 606	470 416
10	38 692	20 869			

3.4.SENSITIVITY ANALYSIS

In the previous subchapters the system viability was analyzed both technologically and economically. However the results of the analysis performed are specific for the input parameters assumed and presented in Table 7 and Table 8. So in this subchapter a sensitivity analysis is made in order to evaluate the effect of the variation of the main input parameters on the viability of the project.

The technological viability is mainly dependent on the efficiency of the system, which is its most important characteristic. It can be seen in Fig. 40 thru Fig. 43 that this system has a good efficiency and it is still possible to increase it by varying, on one hand, some of the construction parameters, like the number of cells and the membrane area. On the other hand, it is also possible to adjust the operational parameters, like the number of cars in simultaneous charging and the VRFB charging time. In another way, it can be seen in these figures that the efficiency

does not change abruptly with the variation of any parameter studied, which means that this system has a good flexibility of design and operation.

Another important parameter that must be studied is the maximum current in the system, since if too high currents are present, they might require the use of excessive cable sections.

The first parameter studied is the number of electric vehicles charged simultaneously. When comparing the original two cars against only one car, higher currents and flow rates will result, yielding lower efficiencies. In practice, however, the average number of cars being charged at a given moment will be somewhere between one and two, with the system efficiency being located somewhere between these two cases. This is illustrated in Fig. 40, where a total of 26 car charges were simulated for both situations.

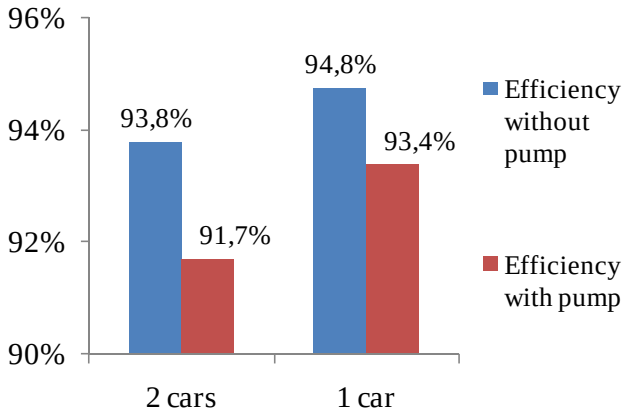

Fig. 40 - Efficiency comparison between1 and 2 cars charging simultaneously.

Another important parameter that influences the system efficiency is the number of cells used. The use of more cells will result in higher output voltages and lower currents, which will result in lower losses. On the other hand, the use of more cells will mean higher system costs. Estimating the variation of system cost as a function of the number of cells is out of the scope of the present work, but the number chosen seemed to be a good compromise between a reasonable number of cells, efficiency and maximum current during the discharge. Analyzing Fig. 41 it can be seen that for a system with 125 cells the efficiency is low (around 86%) and the current is around 800A, which is very high and would require the use of cables with high section.

250 cells seems to be a good choice because it results in reasonable values of maximum current and efficiency.

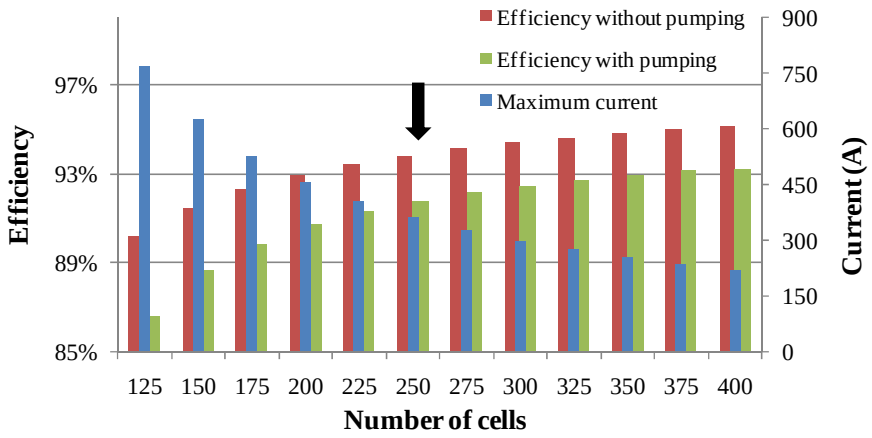

Fig. 41 - Variation of efficiency and maximum current as a function of the number of cells.

The membrane area is also an important parameter. It can be seen in Fig. 42 that the efficiency increases with the increase of the membrane area. On the other hand, the maximum current density during the discharge also decreases. However, bigger membranes means higher costs. Therefore, like in case of the choice of the number of cells, it would be also necessary to take this into account. A membrane area of 0,5 m^2 was chosen as being to be a good compromise.

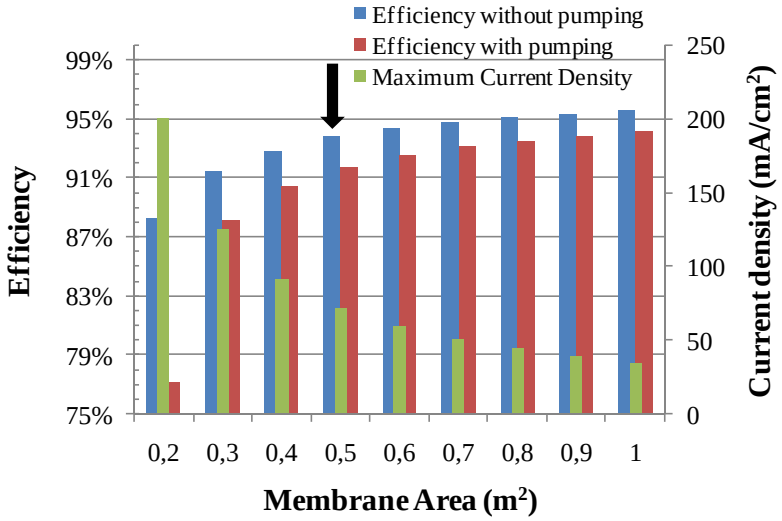

Fig. 42 - Variation of the efficiency and maximum current density as a function of membrane area.

Regarding to the technological viability, the last parameter analyzed is the VRFB charging time. Higher charging times represent a lower average charging power and therefore a higher efficiency due to the lower required flow rates and currents. But it also increases the period of unavailability of the system for EV charging. This is a key part of the economic viability of the project. When analyzing Fig. 43 it can be seen that the variation of system efficiency with varying charging time is not that significant. This work considers that the system will be charged in 12 hours, during the night, when the demand and the electricity costs will be lower.

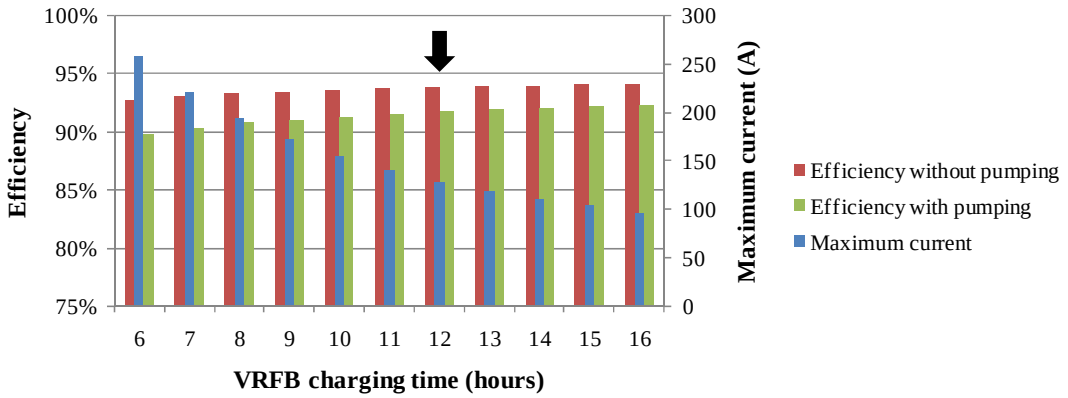

Fig. 43 - Variation of the efficiency and maximum current (during charge) as a function of VRFB charging time.

Regarding to the economic viability, it will depend on the NPV and the payback time. With a positive NPV the project can be considered as economically viable. However, long payback times might render the project unattractive.

The relationship between the technological and the economic viability is provided by the VRFB system efficiency (with pumping) which is the main parameter directly affecting the total efficiency of the system (Eq. 25). This efficiency will be translated into the relationship between the energy consumed from the grid and the energy sold to charge the electric vehicles. Therefore, the economic viability of this project will be strongly affected by the reduction of the efficiency of the system. In Fig. 44 shows the variation of the NPV and payback time as function of the VRFB efficiency (with pumping). The 80% efficiency is the value announced by a manufacturer, as previously referred. Also, the maximum and minimum efficiencies calculated in section 4.3 for one car or two cars in simultaneous charge (91,7% and 93,4%, respectively) are also presented.

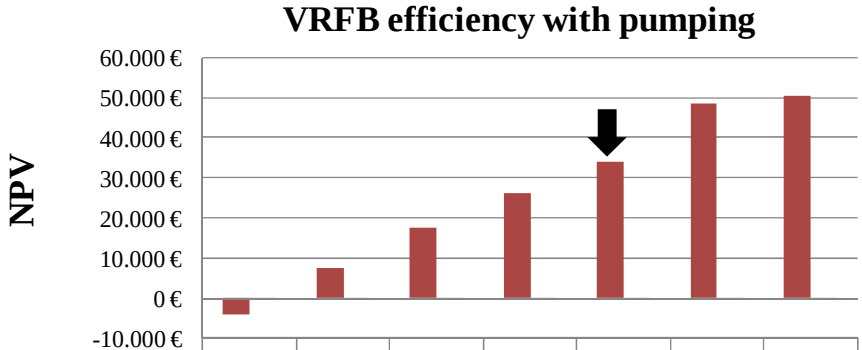

	60,0%	65,0%	70,0%	75,0%	80,0%	91,7%	93,4%
NPV	-4.129	7.544	17.549	26.219	33.806	48.327	50.134
Payback time (yearss)	10,5	10,2	9,9	9,7	9,5	9,1	9

Fig. 44 - NPV and Payback time as a function of VRFB efficiency with pumping (with 91,7% and 93,4% corresponding to the efficiency obtained by the analysis with 2 and 1 cars in simultaneous charging, respectively).

Another important factor that affects the economic viability of this project is the MARR, which has been considered to be 5% in the previous section. NPV almost doubles when decreasing MARR from 5 to 4%. However, it can be seen in Fig. 45 that for values of 7% and below the NPV is already negative, which means that this project would only be economically

viable for small values of MARR. In this case the payback time is constant and does not depend on the value of the MARR.

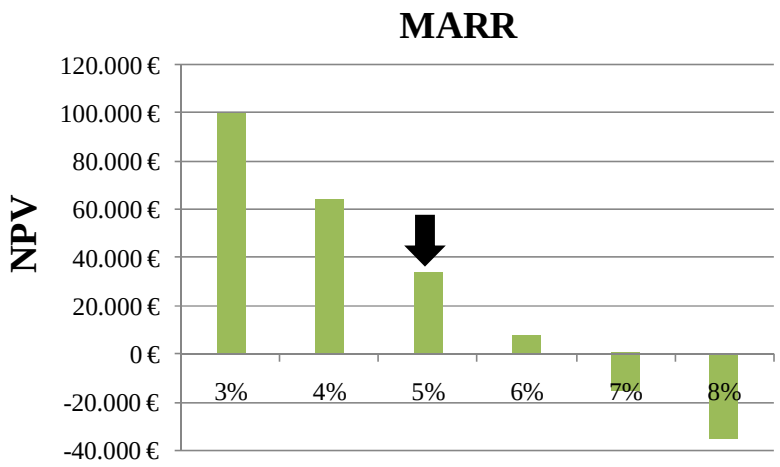

Fig. 45 – Net Present Value as a function of the Minimum Acceptable Rate of Return.

The number of cars charged per day is also an important factor and it can be seen in Fig. 46 that the NPV is positive for averages roughly above 19,5 cars per day during 20 years. The NPV nearly doubles when increasing from 22 cars (the value used in the analysis) to 24 cars per day.

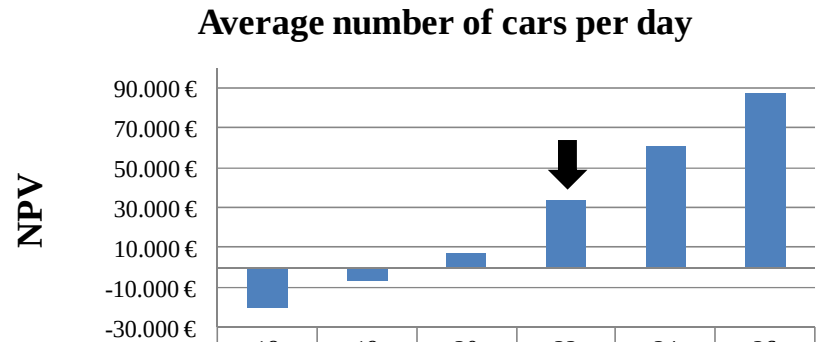

	18	19	20	22	24	26
NPV	-20.199	-6.698	6.804 €	33.806	60.809	87.812
Payback time (years)	11	10,6	10,2	9,5	8,9	8,3

Fig. 46 - NPV and Payback time as a function of the average number of cars charged per day.

As already mentioned, it is expected that the price of this kind of system will tend to decrease along time. Therefore, it is useful to analyze the variation of the NPV with the percentage of the system cost, as represented in Fig. 47. It can be seen that it is possible to triple the NPV with a 30% reduction in the system cost.

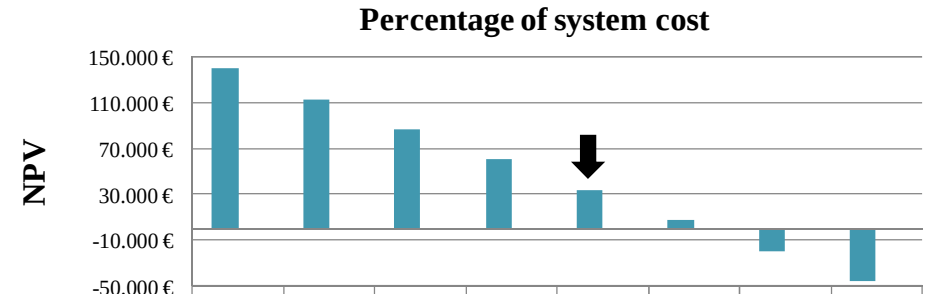

	60%	70%	80%	90%	100%	110%	120%	130%
NPV	139.096	112.773	86.451	60.129	33.806	7.484 €	-18.838	-45.161
Payback time (years)	6,2	7,1	7,9	8,7	9,5	10,2	10,9	11,6

Fig. 47 - NPV and Payback time in function of percentage of system cost.

3.5.CHAPTER CONCLUSIONS

In this chapter a preliminary project of a VRFB system to store energy in gas stations for the fast charging of electric vehicles was presented. This system should be capable of charging two electric vehicles simultaneously and to store energy for the charging of a total of 26 cars per day. A big benefit of such a solution is the possibility of taking advantage of the existing infrastructures currently used to store fossil fuels for conventional vehicles. For this effect, the use of rubber tanks inside the underground fuel tanks was proposed, with the Butyl rubber seeming to be a good choice for the construction of these tanks. However, a more detailed study should be done for the definitive selection of the most suitable rubber.

The system behavior was predicted for specific conditions and yielded an energy efficiency of 92% considering the pumping losses, and 94% without these losses.

A cost analysis of the preliminary project was also performed, in terms of Net Present Value (NPV) for 20 years (the life estimated for the system) and Payback Time. In order to improve the accuracy of the analysis the efficiency announced by one manufacturer was

considered in detriment of the theoretical value predicted in the present work. It has been concluded that for the input parameters considered and for a Minimum Acceptable Rate of Return (MARR) of 5% the project is indeed economically viable and the investment may be recovered in 9,5 years with a NPV of 33 806 €. However, the minimum rate of return considered is a small value taking into account the risk posed by the low maturity of this technology. However, it is expected that in the next years, with the increasing of the number of manufacturers, the costs will tend to decrease.

The sensitivity analysis showed that it is possible to increase the efficiency of this system by changing the operating conditions. For instance, in the case of charging only one car at a time, the system efficiency increases up to 93,4 %. It is also possible to change lightly the VRFB efficiency by varying the charging time. The major influence on the system efficiency is the design parameters of the VRFB, in this work the number of cells and the membrane area was analyzed, and it was verified that the VRFB efficiency increases with the increase of these two parameters. However, in these two cases a more in-depth study may be done considering the variation of the cost of the system.

The sensitivity analysis was also extended to issue of economic viability, and it showed that the NPV also depends of the VRFB efficiency. In the case of a system efficiency of 80% the resulting NPV will be 33806€, but that the NPV may be almost halved if the VRFB efficiency would fall to 70%. In another way, the NPV can be 48327€ or 50134€ considering the variation of the efficiencies corresponding to the simultaneous charging of two cars (91,7%) or just one car (93,4%), respectively.

It is possible to see in the sensitivity analysis that the NPV also depends on the MARR considered, and this project is still economically viable if the MARR is 6%, but for a MARR value of 7% the NPV starts being negative. On the other hand, it is possible to double the NPV by reducing the MARR from 5% to 4%, and triple it by reducing the MARR to 3%.

Another important factor analyzed is the average number of cars charged per day, and this system will be economically viable if at least an average of 20 cars per day are charged. It is important to note that in this case the NPV increases sharply with the increase of the average number of cars per day, for 22 cars per day the NPV becomes five times bigger than in case of

20 cars per day, and for 24 cars per day the NPV is the double of that corresponding to the case of 22 cars per day.

The variation of the NPV as a function of the cost of the system was also analyzed, since it is expected that the technological advances and the cost reduction of these systems will occur along the next few years, and it can be seen that the NPV could approximately double and triple, in the case of a system cost reduction of 10% and 30%, respectively. If these price drops happen, they will dramatically improve the viability of these systems for the aforementioned applications.

4. CONCLUSIONS

The proliferation of the Electric Vehicle will bring a higher demand for battery fast charge locations. Existing or recently deactivated gas stations are privileged locations for this purpose and many of them have available space and unused fuel storage tanks.

However, the high power demanded for fast charge stations is a disadvantage. The use of energy storage systems, and in particular, Vanadium Redox Flow Batteries seems to be a good solution for reducing the contracted power with a peak shaving strategy. Flow batteries also provide the possibility of taking advantage of the availability of empty fuel storage tanks.

Given the novelty of the topic and the lack of similar systems, after a full review of the literature, the preliminary design of such a system was performed in order to assess its feasibility. This full review and the corresponding conclusions are presented in the chapter 2.

This concept seems especially promising regarding the possibility of reducing electricity costs by Peak Shaving, the use of space of gas stations and as a complementary business that accompanies the gradual paradigm shift mobility from internal combustion engines to electric mobility.

In the present work a preliminary project of a Vanadium Redox Flow Battery generation 1 (G1) to be used in gas stations for supplying the energy for two ChadeMo chargers (50 kW each) working simultaneously has been performed. The VRFB is charged for 12h during off-peak power demand (at night), with the same cell stack being used for charging and discharging the liquid electrolytes. This preliminary project was made using commercially available system components.

A method for storing the liquid electrolytes in rubber tanks installed inside the fuel storage tanks normally used in gas stations has been proposed. This will prevent the corrosion of the fuel tanks which are normally made of steel, while allowing the use of the same fuel tank for the storage of the two liquid electrolytes (anode and cathode) without their mixing. On the other hand, due to the flexibility of the rubber it is possible to use large size rubber tanks which can still pass through the manhole entry in the fuel tanks.

The preliminary project was assessed in terms of voltage, current, power and efficiency (both with and without pumping losses). An efficiency around 92% (with pumping losses) has been obtained when using the VRFB system to charge 26 in one day.

On the other hand, local energy storage may help to solve the problems associated with the management of the power grid, and also allow to more easily incorporate intermittent renewable power sources which reduce fossil fuel dependency and associated emissions.

For future work, it will be interesting to build a functional prototype of a VRFB G1 system in order to evaluate its performance, and compare it with the theoerical calculations based on the methodology proposed in this work. This comparison might help to explain the differences between the efficiencies estimated in this work, and the efficiency provided by one manufacturer during the research.

On the other hand, the present calculations were made considering the theoerical flow rate needed, but in practice it is frequently to use higher flow rates, so a prototype would be useful to evaluate the diferences between the theoerical and the real flow rates needed for the output conditions established. With this information it will be also possible to improve the calculation method used in this work.

Another important study will be the analysis of heat transfer in this system, and the sizing of cooling fans and heat exchangers in order to keep the VRFB within the desired temperature limits. Since the electrolyte will be stored underground, where the heat transfer will be difficult, it might be necessary to dissipate the heat in the stack, or along the path of the liquid electrolyte between the output of the stack and tanks.

Concerning the rubber tanks, a more detailed study should be done in order to select the most suitable rubber for making the storage tanks. This rubber must be resistant to the chemical corrosion induced by the liquids electrolytes, and at the same time it must have the necessary mechanical properties to prevent the leakage of the liquids. So, an experimental test of various rubber types submersed in the liquids electrolytes used, at the various oxidation states, should be done.

REFERENCES

1. *International Energy Outlook 2009*, May 2009, Energy Information Administration Office of Integrated Analysis and Forecasting U.S. Department of Energy Washington DC

2. Zdenek, C. and Pavel, M. *Electric, hybrid electric and combustion engine driven cars and their impact on environment*. in *Power Electronics and Applications (EPE 2011), Proceedings of the 2011-14th European Conference on*. 2011.

3. Martins, J.;Brito, F.;Pedrosa, D.;Monteiro, V.; and Afonso, João L., *"Real-Life Comparison Between Diesel and Electric Car Energy Consumption"*, in *"Grid Electrified Vehicles: Performance, Design, and Environmental Impacts"* 2013, Nova Science Publishers: New York

4. Silva, Carla;Ross, Marc; and Farias, Tiago, *Analysis and simulation of "low-cost" strategies to reduce fuel consumption and emissions in conventional gasoline light-duty vehicles.* Energy Conversion and Management, 2009. 50 (2): p. 215-222.http://dx.doi.org/10.1016/j.enconman.2008.09.046

5. MARTINS, Jorge J.G.;UZUNEANU, Krisztina;RIBEIRO, Bernardo Sousa; and JASANSKY, Ondrej, *THERMODYNAMIC ANALYSIS OF AN OVER-EXPANDED ENGINE* SAE 2004-01-0617 2004

6. Ribeiro, Bernardo and Martins, Jorge, *Direct Comparison of an Engine Working under Otto, Miller and Diesel Cycles: Thermodynamic Analysis and Real Engine Performance.* SAE SP, 2007. 2093: p. 75

7. Brito, Francisco P.;Martins, Jorge;Goncalves, L.M.; and Sousa, Rui, *Temperature Controlled Exhaust Heat Thermoelectric Generation.* SAE International Journal of Passenger Cars - Electronic and Electrical Systems, 2012. 5 (2): p. 561-571.10.4271/2012-01-1214

8. F.Brito;Martins, J.;Goncalves, L.M.;Antunes, N.; and Sousa, D., *Influence of Heat Pipe Operating Temperature on Exhaust Heat Thermoelectric Generation.* SAE International Journal of Passenger Cars - Mechanical Systems 2013-01-0559, 2013. 6(2).10.4271/2013-01-0559

9. Boulanger, A. G.;Chu, A. C.;Maxx, S.; and Waltz, D. L., *Vehicle Electrification: Status and Issues.* Proceedings of the IEEE, 2011. 99 (6): p. 1116-1138.10.1109/jproc.2011.2112750

10. Galus, Matthias D.;Vayá, Marina González;Krause, Thilo; and Andersson, Göran, *The role of electric vehicles in smart grids.* Wiley Interdisciplinary Reviews: Energy and Environment, 2013. 2(4): p. 384-400.10.1002/wene.56

11. Martins, J. and Brito, F., *"Carros Elétricos"*Dez. 2011, Porto, Portugal: Publindústria

12. Hawkins, Troy R.;Singh, Bhawna;Majeau-Bettez, Guillaume; and Strømman, Anders Hammer, *Comparative Environmental Life Cycle Assessment of Conventional and*

Electric Vehicles. Journal of Industrial Ecology, 2013. 17(1): p. 53-64.10.1111/j.1530-9290.2012.00532.x

13. Camus, C. and Farias, T. *Electric vehicles as a mean to reduce, energy, emissions and electricity costs*. in *European Energy Market (EEM), 2012 9th International Conference on the*. 2012.10.1109/eem.2012.6254668

14. Cadoux, Florent and Gross, George, *Integration of Vehicles with Rechargeable Batteries into Distribution Networks*, in *Smart Grids* 2013, John Wiley & Sons, Inc. p. 243-261.10.1002/9781118562581.ch8

15. Ribeiro, B.;Brito, F.; and Martins, J., *"A Survey on Electric/Hybrid Vehicles"*. in Electric and Hybrid-Electric Vehicles - Overviews and Viewpoints, 2010: Edited by Ronald K. Jürgen, SAE International, Warrendale, USA.doi-1000092221

16. Faria, Ricardo;Moura, Pedro;Delgado, Joaquim; and de Almeida, Anibal T., *A sustainability assessment of electric vehicles as a personal mobility system.* Energy Conversion and Management, 2012. 61 (0): p. 19-30.http://dx.doi.org/10.1016/j.enconman.2012.02.023

17. Ribau, João;Silva, Carla;Brito, Francisco P.; and Martins, Jorge, *Analysis of four-stroke, Wankel, and microturbine based range extenders for electric vehicles.* Energy Conversion and Management, 2012. 58 (0): p. 120-133.http://dx.doi.org/10.1016/j.enconman.2012.01.011

18. *Role of Chademo*. 11/10/2013]; Available from: http://www.chademo.com/wp/role/challenge/

19. *http://www.chademo.com/*. ChadeMo Association - last acessed in 15/07/2013;

20. *http://www.energia.edp.pt/*. EDP energia - last acessed in 15/07/2013;

21. Sekyung, Han;Soohee, Han; and Sezaki, K., *Development of an Optimal Vehicle-to-Grid Aggregator for Frequency Regulation.* Smart Grid, IEEE Transactions on, 2010. 1 (1): p. 65-72.10.1109/tsg.2010.2045163

22. Saber, A. Y. and Venayagamoorthy, G. K., *Plug-in Vehicles and Renewable Energy Sources for Cost and Emission Reductions.* Industrial Electronics, IEEE Transactions on, 2011. 58 (4): p. 1229-1238.10.1109/tie.2010.2047828

23. Kerestes, R. J.;Reed, G. F.; and Sparacino, A. R. *Economic analysis of grid level energy storage for the application of load leveling*. in *Power and Energy Society General Meeting, 2012 IEEE*. 2012.10.1109/pesgm.2012.6345072

24. *Department of Alternative Energy Development and Efficiency - AEDP 2012-2021 - Last acessed in 07/11/2013*. Available from: http://www.dede.go.th/dede/images/stories/dede_aedp_2012_2021.pdf

25. *Notre Dame Open Course Ware - environmental philosophy - Chapter 9: Replacing fossil fuel with clean energy - Last acessed in 07/11/2013*. Available from:

http://ocw.nd.edu/philosophy/environmental-philosophy/eduCommons/philosophy/environmental-philosophy/unearthed/chapter-9-replacing-fossil-fuel-with-clean-energy

26. Carr, D. S., *Ten-megawatt load-levelling lead/acid battery project.* Journal of Power Sources, 1988. 23 (1–3): p. 183-192.http://dx.doi.org/10.1016/0378-7753(88)80063-6

27. Nakayama, Yasuhide;Takahashi, Sawako;Hirakawa, Kenji; and Yamaguchi, Yoshiaki, *Development of a long life 35 Ah capacity VRLA battery for load-leveling applications.* Journal of Power Sources, 2004. 125 (1): p. 135-140.http://dx.doi.org/10.1016/S0378-7753(03)00828-0

28. Iwahori, T.;Ozaki, Y.;Funahashi, A.;Momose, H.;Mitsuishi, I.;Shiraga, S.;Yoshitake, S.; and Awata, H., *Development of lithium secondary batteries for electric vehicles and home-use load leveling systems.* Journal of Power Sources, 1999. 81–82 (0): p. 872-876.http://dx.doi.org/10.1016/S0378-7753(98)00245-6

29. Shibata, A. and Sato, K., *Development of vanadium redox flow battery for electricity storage.* Power Engineering Journal, 1999. 13 (3): p. 130-135.10.1049/pe:19990305

30. Hagedorn, Norman H. and Thaller, Lawrence H. , *Design Flexibility of Redox Flow Systems.* National Aeronautics and Space Administration Lewis Research Center, DOE/NASA/12726-16, NASA TM-82854, 1982: p. 19

31. Wang, Wei;Luo, Qingtao;Li, Bin;Wei, Xiaoliang;Li, Liyu; and Yang, Zhenguo, *Recent Progress in Redox Flow Battery Research and Development.* Advanced Functional Materials, 2013. 23 (8): p. 970-986.10.1002/adfm.201200694

32. Skyllas-Kazacos, Maria;Rychick, Miron; and Robins, Robert, *All-vanadium redox battery.* US Pat., 4 786 567, 1988

33. Kear, Gareth;Shah, Akeel A.; and Walsh, Frank C., *Development of the all-vanadium redox flow battery for energy storage: a review of technological, financial and policy aspects.* INTERNATIONAL JOURNAL OF ENERGY RESEARCH, 2012. 36 (11): p. 1105-1120.10.1002/er.1863

34. *International Renewable Energy Agency - Energy Storage and Renewables for Island Power - A guide for decision makers - Last acessed in 07/11/2013*. Available from: http://www.irena.org/DocumentDownloads/Publications/Electricity%20Storage%20and%20RE%20for%20Island%20Power.pdf

35. *Cleantech Conference & Showcase 2013, Washington DC - Last Acessed in 07/11/2013*. Available from: http://www.techconnectworld.com/Cleantech2013/a.html?i=1574

36. *Eurostat - Energy consumption of transport - Last acessed in 07/11/2013*. Available from: http://epp.eurostat.ec.europa.eu/tgm/table.do?tab=table&plugin=1&language=en&pcode=tsdtr250

37. SHIGEMATSU, Toshio, *Redox Flow Battery for Energy Storage.* SEI Technical Review, 2011. Number 73: p. 4-13

38. Weber, AdamZ;Mench, MatthewM;Meyers, JeremyP;Ross, PhilipN;Gostick, JeffreyT; and Liu, Qinghua, *Redox flow batteries: a review.* Journal of Applied Electrochemistry, 2011. 41 (10): p. 1137-1164.10.1007/s10800-011-0348-2

39. Thaller, Lawrence H. , *Electrically rechargeable redox flow cells, .* Proc. 9th Intersoc. Energy Conv. Eng. Conf., San Francisco, CA, ; NASA TM X-71540, August, 1974: p. 26-30

40. Hagedorn, Norman H. and Thaller, Lawrence H. , *Redox storage systems for solar applications, .* NASA TM-81464; DOE/NASA/1002-80/5, 1980

41. Ponce de León, C.;Frías-Ferrer, A.;González-García, J.;Szánto, D. A.; and Walsh, F. C., *Redox flow cells for energy conversion.* Journal of Power Sources, 2006. 160 (1): p. 716-732.http://dx.doi.org/10.1016/j.jpowsour.2006.02.095

42. Remick, R.J. and Ang, P.G.P., *Electrically rechargeable anionically active reduction-oxidation electrical storage-supply system* USA Patent 4485154, November 27, 1984

43. EPRI-DOE Handbook of Energy Storage for Transmission &Distribution Applications, EPRI, Palo Alto, CA, and the U.S. Department of Energy, Washington, DC: 2003. 1001834.,

44. Scamman, Daniel P.;Reade, Gavin W.; and Roberts, Edward P. L., *Numerical modelling of a bromide–polysulphide redox flow battery: Part 1: Modelling approach and validation for a pilot-scale system.* Journal of Power Sources, 2009. 189 (2): p. 1220-1230.http://dx.doi.org/10.1016/j.jpowsour.2009.01.071

45. Scamman, Daniel P.;Reade, Gavin W.; and Roberts, Edward P. L., *Numerical modelling of a bromide-polysulphide redox flow battery. Part 2: Evaluation of a utility-scale system.* Journal of Power Sources, 2009. 189 (2): p. 1231-1239.http://dx.doi.org/10.1016/j.jpowsour.2009.01.076

46. Lai, Qinzhi;Zhang, Huamin;Li, Xianfeng;Zhang, Liqun; and Cheng, Yuanhui, *A novel single flow zinc–bromine battery with improved energy density.* Journal of Power Sources, 2013. 235 (0): p. 1-4.http://dx.doi.org/10.1016/j.jpowsour.2013.01.193

47. Zhang, Liqun;Zhang, Huamin;Lai, Qinzhi;Li, Xianfeng; and Cheng, Yuanhui, *Development of carbon coated membrane for zinc/bromine flow battery with high power density.* Journal of Power Sources, 2013. 227 (0): p. 41-47.http://dx.doi.org/10.1016/j.jpowsour.2012.11.033

48. Clarke, Robert Lewis;Dougherty, Brian;Harrison, Stephen;Millington, Peter J; and Mohanta, Samaresh, *Cerium Batteries.* US Patent 2004/0202925 A1 2004

49. Leung, P. K.;Ponce-de-León, C.;Low, C. T. J.;Shah, A. A.; and Walsh, F. C., *Characterization of a zinc–cerium flow battery.* Journal of Power Sources, 2011. 196 (11): p. 5174-5185.http://dx.doi.org/10.1016/j.jpowsour.2011.01.095

50. Xie, Zhipeng;Liu, Qingchao;Chang, Zhiwen; and Zhang, Xinbo, *The developments and challenges of cerium half-cell in zinc–cerium redox flow battery for energy storage.* Electrochimica Acta, 2013. 90 (0): p. 695-704.http://dx.doi.org/10.1016/j.electacta.2012.12.066

51. A Leung, P.K., *Development of a zinc-cerium redox flow battery*, in *University of Southampton , Faculty of Engineering and the Environment , Doctoral Thesis* (2011). p. 352

52. Pletcher, Derek and Wills, Richard, *A novel flow battery–A lead acid battery based on an electrolyte with soluble lead(II): III. The influence of conditions on battery performance.* Journal of Power Sources, 2005. 149 (0): p. 96-102.http://dx.doi.org/10.1016/j.jpowsour.2005.01.048

53. Hazza, Ahmed;Pletcher, Derek; and Wills, Richard, *A novel flow battery–A lead acid battery based on an electrolyte with soluble lead(II): IV. The influence of additives.* Journal of Power Sources, 2005. 149 (0): p. 103-111.http://dx.doi.org/10.1016/j.jpowsour.2005.01.049

54. Pletcher, Derek;Zhou, Hantao;Kear, Gareth;Low, C. T. John;Walsh, Frank C.; and Wills, Richard G. A., *A novel flow battery–A lead-acid battery based on an electrolyte with soluble lead(II): V. Studies of the lead negative electrode.* Journal of Power Sources, 2008. 180 (1): p. 621-629.http://dx.doi.org/10.1016/j.jpowsour.2008.02.024

55. Pletcher, Derek;Zhou, Hantao;Kear, Gareth;Low, C. T. John;Walsh, Frank C.; and Wills, Richard G. A., *A novel flow battery–A lead-acid battery based on an electrolyte with soluble lead(II): Part VI. Studies of the lead dioxide positive electrode.* Journal of Power Sources, 2008. 180 (1): p. 630-634.http://dx.doi.org/10.1016/j.jpowsour.2008.02.025

56. Li, Xiaohong;Pletcher, Derek; and Walsh, Frank C., *A novel flow battery: A lead acid battery based on an electrolyte with soluble lead(II): Part VII. Further studies of the lead dioxide positive electrode.* Electrochimica Acta, 2009. 54 (20): p. 4688-4695.http://dx.doi.org/10.1016/j.electacta.2009.03.075

57. Collins, John;Kear, Gareth;Li, Xiaohong;Low, C. T. John;Pletcher, Derek;Tangirala, Ravichandra;Stratton-Campbell, Duncan;Walsh, Frank C.; and Zhang, Caiping, *A novel flow battery: A lead acid battery based on an electrolyte with soluble lead(II) Part VIII. The cycling of a 10 cm × 10cm flow cell.* Journal of Power Sources, 2010. 195 (6): p. 1731-1738.http://dx.doi.org/10.1016/j.jpowsour.2009.09.044

58. Collins, John;Li, Xiaohong;Pletcher, Derek;Tangirala, Ravichandra;Stratton-Campbell, Duncan;Walsh, Frank C.; and Zhang, Caiping, *A novel flow battery: A lead acid battery based on an electrolyte with soluble lead(II). Part IX: Electrode and electrolyte conditioning with hydrogen peroxide.* Journal of Power Sources, 2010. 195 (9): p. 2975-2978.http://dx.doi.org/10.1016/j.jpowsour.2009.10.109

59. Hazza, Ahmed;Pletcher, Derek; and Wills, Richard, *A novel flow battery: A lead acid battery based on an electrolyte with soluble lead(ii) Part I. Preliminary studies.* Physical Chemistry Chemical Physics, 2004. 6 (8): p. 1773-1778.10.1039/b401115e

60. Pletcher, Derek and Wills, Richard, *A novel flow battery: A lead acid battery based on an electrolyte with soluble lead(ii) Part II. Flow cell studies.* Physical Chemistry Chemical Physics, 2004. 6 (8): p. 1779-1785.10.1039/b401116c

61. Zhang, C. P.;Sharkh, S. M.;Li, X.;Walsh, F. C.;Zhang, C. N.; and Jiang, J. C., *The performance of a soluble lead-acid flow battery and its comparison to a static lead-acid battery.* Energy Conversion and Management, 2011. 52 (12): p. 3391-3398.http://dx.doi.org/10.1016/j.enconman.2011.07.006

62. Cheng, Jie;Zhang, Li;Yang, Yu-Sheng;Wen, Yue-Hua;Cao, Gao-Ping; and Wang, Xin-Dong, *Preliminary study of single flow zinc–nickel battery.* Electrochemistry Communications, 2007. 9 (11): p. 2639-2642.http://dx.doi.org/10.1016/j.elecom.2007.08.016

63. Cheng, Yuanhui;Zhang, Huamin;Lai, Qinzhi;Li, Xianfeng;Shi, Dingqin; and Zhang, Liqun, *A high power density single flow zinc–nickel battery with three-dimensional porous negative electrode.* Journal of Power Sources, 2013. 241 (0): p. 196-202.http://dx.doi.org/10.1016/j.jpowsour.2013.04.121

64. Pan, Junqing;Sun, Yanzhi;Cheng, Jie;Wen, Yuehua;Yang, Yusheng; and Wan, Pingyu, *Study on a new single flow acid Cu–PbO2 battery.* Electrochemistry Communications, 2008. 10 (9): p. 1226-1229.http://dx.doi.org/10.1016/j.elecom.2008.06.008

65. Xu, Yan;Wen, Yuehua;Cheng, Jie;Cao, Gaoping; and Yang, Yusheng, *Study on a single flow acid Cd–chloranil battery.* Electrochemistry Communications, 2009. 11 (7): p. 1422-1424.http://dx.doi.org/10.1016/j.elecom.2009.05.021

66. Zhao, Yongfu;Si, Shihui; and Liao, Cui, *A single flow zinc//polyaniline suspension rechargeable battery.* Journal of Power Sources, 2013. 241 (0): p. 449-453.http://dx.doi.org/10.1016/j.jpowsour.2013.04.095

67. Wang, Yarong;He, Ping; and Zhou, Haoshen, *Li-Redox Flow Batteries Based on Hybrid Electrolytes: At the Cross Road between Li-ion and Redox Flow Batteries.* Advanced Energy Materials, 2012. 2 (7): p. 770-779.10.1002/aenm.201200100

68. Goodenough, J. B. and Kim, Youngsik, *Challenges for rechargeable batteries.* Journal of Power Sources, 2011. 196 (16): p. 6688-6694.http://dx.doi.org/10.1016/j.jpowsour.2010.11.074

69. Wang, Yarong;Wang, Yonggang; and Zhou, Haoshen, *A Li–Liquid Cathode Battery Based on a Hybrid Electrolyte.* ChemSusChem, 2011. 4 (8): p. 1087-1090.10.1002/cssc.201100201

70. Duduta, Mihai;Ho, Bryan;Wood, Vanessa C.;Limthongkul, Pimpa;Brunini, Victor E.;Carter, W. Craig; and Chiang, Yet-Ming, *Semi-Solid Lithium Rechargeable Flow Battery.* Advanced Energy Materials, 2011. 1 (4): p. 511-516.10.1002/aenm.201100152

71. PELLEGRI, A. and SPAZIANTE, P.M., UK Patent GB 2 030 349, 10 July 1978

72. Skyllas-Kazacos, Maria;Kazacos, George;Poon, Grace; and Verseema, Hugh, *Recent advances with UNSW vanadium-based redox flow batteries.* INTERNATIONAL JOURNAL OF ENERGY RESEARCH, 2010. 34 (2): p. 182-189.10.1002/er.1658

73. Parasuraman, Aishwarya;Lim, Tuti Mariana;Menictas, Chris; and Skyllas-Kazacos, Maria, *Review of material research and development for vanadium redox flow battery applications.* Electrochimica Acta, (0).http://dx.doi.org/10.1016/j.electacta.2012.09.067

74. Helen Prifti , Aishwarya Parasuraman , Suminto Winardi , Tuti Mariana Lim , Maria Skyllas-Kazacos, *Membranes for Redox Flow Battery Applications.* Membranes, 2012. 2: p. 32.10.3390/membranes2020275

75. Menictas, Chris and Skyllas-Kazacos, Maria, *Performance of vanadium-oxygen redox fuel cell.* Journal of Applied Electrochemistry, 2011. 41 (10): p. 1223-1232.10.1007/s10800-011-0342-8

76. Crompton, T. R., *Battery Reference Book*. Third Edition ed 2000, Oxford: Newnes.http://dx.doi.org/10.1016/B978-075064625-3/50018-4

77. Gonzalez, Adolfo;Gallachóir, Brian Ó; and McKeogh, Eamon, *Study of Electricity Storage Technologies and Their Potential to Address Wind Energy Intermittency in Ireland*, (2004), Sustainable Energy Research Group, University College Cork, Funded by the National Development Plan through Sustainable Energy Ireland's Renewable Energy Research, Development and Demonstration Grant RE/HC/03/001

78. Yang, Zhenguo;Zhang, Jianlu;Kintner-Meyer, Michael C. W.;Lu, Xiaochuan;Choi, Daiwon;Lemmon, John P.; and Liu, Jun, *Electrochemical Energy Storage for Green Grid.* Chemical Reviews, 2011. 111 (5): p. 3577-3613.10.1021/cr100290v

79. Leung, P. K.;Ponce de León, C.; and Walsh, F. C., *An undivided zinc–cerium redox flow battery operating at room temperature (295 K).* Electrochemistry Communications, 2011. 13 (8): p. 770-773.http://dx.doi.org/10.1016/j.elecom.2011.04.011

80. Zhao, Ping;Zhang, Huamin;Zhou, Hantao; and Yi, Baolian, *Nickel foam and carbon felt applications for sodium polysulfide/bromine redox flow battery electrodes.* Electrochimica Acta, 2005. 51 (6): p. 1091-1098.http://dx.doi.org/10.1016/j.electacta.2005.06.008

81. Clarke, Robert Lewis;Dougherty, Brian;Harrison, Stephen;Millington, Peter J; and Mohanta, Samaresh, *Cerium Batteries.* US Pat., 7 625 663 B2, 2009

82. Xie, Zhipeng;Zhou, Debi;Xiong, Fengjiao;Zhang, Shimin; and Huang, Kelong, *Cerium-zinc redox flow battery: Positive half-cell electrolyte studies.* Journal of Rare Earths, 2011. 29 (6): p. 567-573.http://dx.doi.org/10.1016/S1002-0721(10)60499-1

83. Vanadium Redox Flow Batteries: An In-Depth Analysis EPRI, Palo Alto, CA: 2007. 1014836.,

84. TASSIN, Noëlle, *Investigation on Storage Technologies for Intermittent Renewable Energies: Evaluation and recommended R&D strategy*, 2006

85. Skyllas-Kazacos, Maria, *Vanadium/polyhalide redox flow battery.* US Pat., 7 320 844 B2, 2008

86. Skyllas-Kazacos, Maria, *Novel vanadium chloride/polyhalide redox flow battery.* Journal of Power Sources, 2003. 124 (1): p. 299-302.http://dx.doi.org/10.1016/S0378-7753(03)00621-9

87. Aaron, D. S.;Liu, Q.;Tang, Z.;Grim, G. M.;Papandrew, A. B.;Turhan, A.;Zawodzinski, T. A.; and Mench, M. M., *Dramatic performance gains in vanadium redox flow batteries through modified cell architecture.* Journal of Power Sources, 2012. 206 (0): p. 450-453.http://dx.doi.org/10.1016/j.jpowsour.2011.12.026

88. Noack, Jens and Tübke, Jens, *A Comparison of Materials and Treatment of Materials for Vanadium Redox Flow Battery.* ECS Transactions, 2010. 25 (35): p. 235-245.10.1149/1.3414022

89. Xu, Q.;Zhao, T. S.; and Leung, P. K., *Numerical investigations of flow field designs for vanadium redox flow batteries.* Applied Energy, 2013. 105 (0): p. 47-56.http://dx.doi.org/10.1016/j.apenergy.2012.12.041

90. Pellegri, Alberto and Broman, Barry Michael, *Redox flow battery system and cell stack.* US Pat., 6 475 661 B1, 2002

91. Turker, Burak;Arroyo Klein, Sebastian;Hammer, Eva-Maria;Lenz, Bettina; and Komsiyska, Lidiya, *Modeling a vanadium redox flow battery system for large scale applications.* Energy Conversion and Management, 2013. 66 (0): p. 26-32.http://dx.doi.org/10.1016/j.enconman.2012.09.009

92. Lu, Rengui ;Yang, Aochi ;Xue, Yufeng ;Xu, Lichao ; and Zhu, Chunbo *Analysis of the key factors affecting the energy efficiency of batteries in electric vehicle.* World Electric Vehicle Journal, 2010. 4: p. 9-13

93. Vetter, Matthias ;Dennenmoser, Martin ;Schwunk, Simon;Smolinka, Tom;Dötsch, Christian;Berthold, Sascha;Tübke, Jens; and Noack, Jens, *Redox flow batteries – Already an alternative storage solution for hybrid PV mini-grids?*, in *Proceedings 5th European Conference PV-Hybrid and Mini-Grid, pp. 100-109* (2010): Tarragona, Spain. p. 100-109

94. Peng Qian , Huamin Zhang , Jian Chena , Yuehua Wen , Qingtao Luo , and Zonghao Liu , Dongjiang You , Baolian Yi, *A novel electrode-bipolar plate assembly for vanadium redox flow battery applications.* Journal of Power Sources, 2007. 175: p. 8

95. Tokuda, Nobuyuki;Kanno, Takashi;Hara, Takushi;Shigematsu, Toshio;Tsutsui, Yasumitsu;Ikeuchi, Atsuo;Itou, Takefumi; and Kumamoto, Takahiro, *Development of a Redox Flow Battery System.* SEI Technical Review, 2000. Number 50: p. 88-94

96. Kim, Soowhan;Thomsen, Edwin;Xia, Gordon;Nie, Zimin;Bao, Jie;Recknagle, Kurtis;Wang, Wei;Viswanathan, Vilayanur;Luo, Qingtao;Wei, Xiaoliang;Crawford, Alasdair;Coffey,

Greg;Maupin, Gary; and Sprenkle, Vincent, *1 kW / 1kWh Advanced Vanadium Redox Flow Battery Utilizing Mixed Acid Electrolytes.* Journal of Power Sources, (0).http://dx.doi.org/10.1016/j.jpowsour.2013.02.045

97. Spellman, Kevin;Stiles, Kendrick; and Little, Ian, *Economic Report on Vanadium Redox Flow Battery with Optimization of Flow Ratw*, in *University of Tennessee Honors Thesis Projects* 2013

98. Tang, Ao;Ting, Simon;Bao, Jie; and Skyllas-Kazacos, Maria, *Thermal modelling and simulation of the all-vanadium redox flow battery.* Journal of Power Sources, 2012. 203 (0): p. 165-176.http://dx.doi.org/10.1016/j.jpowsour.2011.11.079

99. Ma, Xiangkun;Zhang, Huamin;Sun, Chenxi;Zou, Yi; and Zhang, Tao, *An optimal strategy of electrolyte flow rate for vanadium redox flow battery.* Journal of Power Sources, 2012. 203 (0): p. 153-158.http://dx.doi.org/10.1016/j.jpowsour.2011.11.036

100. Nagashima, Ikuo;Fukui, Jun;Gotoh, Hiroshi;Kaneko, Hiroko;Nozaki, Ken; and Ozawa, Takeo, *Electrolytes for redox flow batteries.* US Pat., 4 814 241, 1989

101. Kausar, N.;Howe, R.; and Skyllas-Kazacos, M., *Raman spectroscopy studies of concentrated vanadium redox battery positive electrolytes.* Journal of Applied Electrochemistry, 2001. 31 (12): p. 1327-1332.10.1023/a:1013870624722

102. Q. H. Liu, G. M. Grim, A. B. Papandrew, A. Turhan, T. A. Zawodzinski, M. M. Mench, *High Performance Vanadium Redox Flow Batteries with Optimized Electrode Configuration and Membrane Selection.* Journal of Electrochemical Society, 2012. 159 (8): p. A1246-A1252.10.1149/2.051208jes

103. Li, Liyu;Kim, Soowhan;Wang, Wei;Vijayakumar, M.;Nie, Zimin;Chen, Baowei;Zhang, Jianlu;Xia, Guanguang;Hu, Jianzhi;Graff, Gordon;Liu, Jun; and Yang, Zhenguo, *A Stable Vanadium Redox-Flow Battery with High Energy Density for Large-Scale Energy Storage.* Advanced Energy Materials, 2011. 1 (3): p. 394-400.10.1002/aenm.201100008

104. Peng, Sui;Wang, Nan-Fang;Wu, Xiao-Juan;Liu, Su-Qin;Fang, Dong;Liu, You-Nian; and Huang, Ke-Long, *Vanadium Species in CH3SO3H and H2SO4 Mixed Acid as the Supporting Electrolyte for Vanadium Redox Flow Battery. International Journal of ELECTROCHEMICAL SCIENCE*, 2012. 7: p. 643-649

105. Liang, Xinxing;Peng, Sui;Lei, Ying;Gao, Chao;Wang, Nanfang;Liu, Suqin; and Fang, Dong, *Effect of l-glutamic acid on the positive electrolyte for all-vanadium redox flow battery.* Electrochimica Acta, 2013. 95 (0): p. 80-86.http://dx.doi.org/10.1016/j.electacta.2013.01.138

106. Peng, Sui;Wang, Nangfang;Gao, Chao;Lei, Ying;Liang, Xingxing;Liu, Suqin; and Liu, Younian, *Stability of Positive Electrolyte Containing Trishydroxymethyl Aminomethane Additive for Vanadium Redox Flow Battery.* International Journal of ELECTROCHEMICAL SCIENCE, 2012. 7: p. 4388-4396

107. Chang, Fang;Hu, Changwei;Liu, Xiaojiang;Liu, Lian; and Zhang, Jianwen, *Coulter dispersant as positive electrolyte additive for the vanadium redox flow battery.*

Electrochimica Acta, 2012. 60(0): p. 334-338.http://dx.doi.org/10.1016/j.electacta.2011.11.065

108. Li, Sha;Huang, Kelong;Liu, Suqin;Fang, Dong;Wu, Xiongwei;Lu, Dan; and Wu, Tao, *Effect of organic additives on positive electrolyte for vanadium redox battery.* Electrochimica Acta, 2011. 56 (16): p. 5483-5487.http://dx.doi.org/10.1016/j.electacta.2011.03.048

109. Wu, Xiaojuan;Liu, Suqin;Wang, Nanfang;Peng, Sui; and He, Zhangxin, *Influence of organic additives on electrochemical properties of the positive electrolyte for all-vanadium redox flow battery.* Electrochimica Acta, 2012. 78 (0): p. 475-482.http://dx.doi.org/10.1016/j.electacta.2012.06.065

110. Xu, Tongwen, *Ion exchange membranes: State of their development and perspective.* Journal of Membrane Science, 2005. 263 (1–2): p. 1-29.http://dx.doi.org/10.1016/j.memsci.2005.05.002

111. Mohammadi, T. and Skyllas-Kazacos, M., *Use of polyelectrolyte for incorporation of ion-exchange groups in composite membranes for vanadium redox flow battery applications.* Journal of Power Sources, 1995. 56 (1): p. 91-96.http://dx.doi.org/10.1016/0378-7753(95)80014-8

112. Mai, Zhensheng;Zhang, Huamin;Li, Xianfeng;Xiao, Shaohua; and Zhang, Hongzhang, *Nafion/polyvinylidene fluoride blend membranes with improved ion selectivity for vanadium redox flow battery application.* Journal of Power Sources, 2011. 196 (13): p. 5737-5741.http://dx.doi.org/10.1016/j.jpowsour.2011.02.048

113. Vijayakumar, M.;Schwenzer, Birgit;Kim, Soowhan;Yang, Zhenguo;Thevuthasan, S.;Liu, Jun;Graff, Gordon L.; and Hu, Jianzhi, *Investigation of local environments in Nafion–SiO2 composite membranes used in vanadium redox flow batteries.* Solid State Nuclear Magnetic Resonance, 2012. 42 (0): p. 71-80.http://dx.doi.org/10.1016/j.ssnmr.2011.11.005

114. Schwenzer, Birgit;Kim, Soowhan;Vijayakumar, M.;Yang, Zhenguo; and Liu, Jun, *Correlation of structural differences between Nafion/polyaniline and Nafion/polypyrrole composite membranes and observed transport properties.* Journal of Membrane Science, 2011. 372 (1–2): p. 11-19.http://dx.doi.org/10.1016/j.memsci.2011.01.025

115. Teng, Xiangguo;Zhao, Yongtao;Xi, Jingyu;Wu, Zenghua;Qiu, Xinping; and Chen, Liquan, *Nafion/organic silica modified TiO2 composite membrane for vanadium redox flow battery via in situ sol–gel reactions.* Journal of Membrane Science, 2009. 341 (1–2): p. 149-154.http://dx.doi.org/10.1016/j.memsci.2009.05.051

116. Schmidt, C.;Glück, T.; and Schmidt-Naake, G., *Modification of Nafion Membranes by Impregnation with Ionic Liquids.* Chemical Engineering & Technology, 2008. 31 (1): p. 13-22.10.1002/ceat.200700054

117. Sukkar, Theresa and Skyllas-Kazacos, Maria, *Water transfer behaviour across cation exchange membranes in the vanadium redox battery.* Journal of Membrane Science, 2003. 222 (1–2): p. 235-247.http://dx.doi.org/10.1016/S0376-7388(03)00309-0

118. Mohammadi, T.;Chieng, S. C.; and Skyllas Kazacos, M., *Water transport study across commercial ion exchange membranes in the vanadium redox flow battery.* Journal of Membrane Science, 1997. 133 (2): p. 151-159.http://dx.doi.org/10.1016/S0376-7388(97)00092-6

119. Sukkar, Theresa and Skyllas-Kazacos, Maria, *Membrane stability studies for vanadium redox cell applications.* Journal of Applied Electrochemistry, 2004. 34 (2): p. 137-145

120. Xi, Jingyu;Wu, Zenghua;Qiu, Xinping; and Chen, Liquan, *Nafion/SiO2 hybrid membrane for vanadium redox flow battery.* Journal of Power Sources, 2007. 166 (2): p. 531-536.http://dx.doi.org/10.1016/j.jpowsour.2007.01.069

121. Luo, Qingtao;Zhang, Huaming;Chen, Jian;Qian, Peng; and Zhai, Yunfeng, *Modification of Nafion membrane using interfacial polymerization for vanadium redox flow battery applications.* Journal of Membrane Science, 2008. 311 (1–2): p. 98-103.http://dx.doi.org/10.1016/j.memsci.2007.11.055

122. Zeng, Jie;Jiang, Chunping;Wang, Yaohui;Chen, Jinwei;Zhu, Shifu;Zhao, Beijun; and Wang, Ruilin, *Studies on polypyrrole modified nafion membrane for vanadium redox flow battery.* Electrochemistry Communications, 2008. 10 (3): p. 372-375.http://dx.doi.org/10.1016/j.elecom.2007.12.025

123. Wang, Nanfang;Peng, Sui;Lu, Dan;Liu, Suqin;Liu, Younian; and Huang, Kelong, *Nafion/TiO2 hybrid membrane fabricated via hydrothermal method for vanadium redox battery.* Journal of Solid State Electrochemistry, 2012. 16 (4): p. 1577-1584.10.1007/s10008-011-1560-z

124. Teng, Xiangguo;Lei, Jie;Gu, Xuecai;Dai, Jicui;Zhu, Yongming; and Li, Faqiang, *Nafion-sulfonated organosilica composite membrane for all vanadium redox flow battery.* Ionics, 2012. 18 (5): p. 513-521.10.1007/s11581-012-0694-z

125. Teng, Xiangguo;Zhao, Yongtao;Xi, Jingyu;Wu, Zenghua;Qiu, Xinping; and Chen, Liquan, *Nafion/organically modified silicate hybrids membrane for vanadium redox flow battery.* Journal of Power Sources, 2009. 189 (2): p. 1240-1246.http://dx.doi.org/10.1016/j.jpowsour.2008.12.040

126. Mohammadi, T. and Skyllas-Kazacos, M., *Characterisation of novel composite membrane for redox flow battery applications.* Journal of Membrane Science, 1995. 98 (1–2): p. 77-87.http://dx.doi.org/10.1016/0376-7388(94)00178-2

127. Li, Wenyue;Liu, Jianguo; and Yan, Chuanwei, *Graphite–graphite oxide composite electrode for vanadium redox flow battery.* Electrochimica Acta, 2011. 56 (14): p. 5290-5294.http://dx.doi.org/10.1016/j.electacta.2011.02.083

128. Kim, Hyung Sun, *Electrochemical Properties of Graphite-based Electrodes for Redox Flow Batteries.* Bull. Korean Chem. Soc., 2011. 32: p. 5.10.5012/bkcs.2011.32.2.571

129. Wang, W. H. and Wang, X. D., *Investigation of Ir-modified carbon felt as the positive electrode of an all-vanadium redox flow battery.* Electrochimica Acta, 2007. 52 (24): p. 6755-6762.http://dx.doi.org/10.1016/j.electacta.2007.04.121

130. Wei, Z. D. and Chan, S. H., *Electrochemical deposition of PtRu on an uncatalyzed carbon electrode for methanol electrooxidation.* Journal of Electroanalytical Chemistry, 2004. 569 (1): p. 23-33.http://dx.doi.org/10.1016/j.jelechem.2004.01.034

131. Haddadi-Asl, V.;Kazacos, M.; and Skyllas-Kazacos, M., *Conductive carbon-polypropylene composite electrodes for vanadium redox battery.* Journal of Applied Electrochemistry, 1995. 25 (1): p. 29-33.10.1007/bf00251261

132. Tsai, Han-Min;Yang, Shin-Yi;Ma, Chen-Chi M.; and Xie, Xiaofeng, *Preparation and Electrochemical Properties of Graphene-Modified Electrodes for All-Vanadium Redox Flow Batteries.* Electroanalysis, 2011. 23 (9): p. 2139-2143.10.1002/elan.201100181

133. Chen, Weimin;Liu, Ying; and Xin, Qin, *Evaluation of a compression molded composite bipolar plate for direct methanol fuel cell.* International Journal of Hydrogen Energy, 2010. 35 (8): p. 3783-3788.http://dx.doi.org/10.1016/j.ijhydene.2010.02.004

134. Maeda, Shuhei;Sugawara, Jun; and Hayami, Hiroshi, *Bipolar plate for redox flow battery.* US Pat., 2013/0037760 A1, 2013

135. Dihrab, Salwan S.;Sopian, K.;Alghoul, M. A.; and Sulaiman, M. Y., *Review of the membrane and bipolar plates materials for conventional and unitized regenerative fuel cells.* Renewable and Sustainable Energy Reviews, 2009. 13 (6–7): p. 1663-1668.http://dx.doi.org/10.1016/j.rser.2008.09.029

136. Yen, Chuan-Yu;Liao, Shu-Hang;Lin, Yu-Feng;Hung, Chih-Hung;Lin, Yao-Yu; and Ma, Chen-Chi M., *Preparation and properties of high performance nanocomposite bipolar plate for fuel cell.* Journal of Power Sources, 2006. 162 (1): p. 309-315.http://dx.doi.org/10.1016/j.jpowsour.2006.06.076

137. Liao, Shu-Hang;Hung, Chih-Hung;Ma, Chen-Chi M.;Yen, Chuan-Yu;Lin, Yu-Feng; and Weng, Cheng-Chih, *Preparation and properties of carbon nanotube-reinforced vinyl ester/nanocomposite bipolar plates for polymer electrolyte membrane fuel cells.* Journal of Power Sources, 2008. 176 (1): p. 175-182.http://dx.doi.org/10.1016/j.jpowsour.2007.10.064

138. Lee, Nam Jin;Lee, Seung-Wook ;Kim, Ki Jae;Kim, Jae-Hun;Park, Min-Sik;Jeong, Goojin;Kim, Young-Jun; and Byun, Dongjin, *Development of Carbon Composite Bipolar Plates for Vanadium Redox Flow Batteries.* Bulletin of the Korean Chemical Society, 2012. 33(11).10.5012/bkcs.2012.33.11.3589

139. M. R. Mohamed , S. M. Sharkh , H. Ahmad , M. N. Abu Seman , F. C. Walsh, *Design and development of unit cell and system for vanadium redox flow batteries (V-RFB).* Journal of the Physical Sciences, 2012. 7: p. 15.10.5897/IJPS11.1555

140. Ping Zhao , Huamin Zhang , Hantao Zhou , Jian Chen , Sujun Gao , Baolian Yi, *Characteristics and performance of 10kW class all-vanadium redox-flow battery stack.* Journal of Power Sources, 2006. 162: p. 5

141. Linden, David and Reddy, Thomas B. , *HANDBOOK OF BATTERIES*. 3º ed 2002: McGraw-Hill. 1454

142. Bradbury, Kyle, *Energy Storage Technology Review*, in *Duke University*22 August 2010. p. 34

143. Ikezoe, Michinori;Hirata, Norihiko;Amemiya, Chika;Miyamoto, Takeshi;Watanabe, Yasuharu;Hirai, Toshiro; and Sasaki, Tetsuo *Development of High Capacity Lithium- Ion Battery for NISSAN LEAF.* SAE Technical Paper 2012-01-0664, 2012. 10.4271/2012-01-0664

144. Dupont. *Nafion PSFA Membranes*. last acessed in 12/06/2013]; Available from: http://www2.dupont.com/FuelCells/en_US/assets/downloads/dfc101.pdf

145. Group, SGL. *SIGRACET and SIGRACELL Components for Flow Batteries*. last acessed in 12/06/2013]; Available from: http://www.sglgroup.com/cms/_common/downloads/products/product-groups/nm/Mobility/NMM_Components_for_Flow_Batteries.pdf

146. Mohamed, Mohd R;Sharkh, Suleiman M; and Walsh, Frank C, *Redox Flow Batteries for Hybrid Electric Vehicles: Progress and Challenges.* Vehicle Power and Propulsion Conference, 2009. VPPC'09. IEEE, 2009: p. 551-557

147. Wagner, R., *Large lead/acid batteries for frequency regulation, load levelling and solar power applications.* Journal of Power Sources, 1997. 67 (1–2): p. 163-172.http://dx.doi.org/10.1016/S0378-7753(97)02509-3

148. Johnson, Matthew P.;Bar-Noy, Amotz;Liu, Ou; and Feng, Yi, *Energy peak shaving with local storage.* Sustainable Computing: Informatics and Systems, 2011. 1 (3): p. 177-188.http://dx.doi.org/10.1016/j.suscom.2011.05.001

149. Shigematsu, T.;Kumamoto, T.;Deguchi, H.; and Hara, T., *Applications of a vanadium redox-flow battery to maintain power quality.* Transmission and Distribution Conference and Exhibition 2002: Asia Pacific. IEEE/PES, 2002. 2: p. 1065-1070.10.1109/tdc.2002.1177625

150. Zhan, Yuedong;Wang, Hua; and Zhu, Jianguo, *Modelling and control of hybrid UPS system with backup PEM fuel cell/battery.* International Journal of Electrical Power & Energy Systems, 2012. 43 (1): p. 1322-1331.http://dx.doi.org/10.1016/j.ijepes.2012.03.046

151. Rydh, Carl Johan and Sandén, Björn A., *Energy analysis of batteries in photovoltaic systems. Part I: Performance and energy requirements.* Energy Conversion and Management, 2005. 46 (11–12): p. 1957-1979.http://dx.doi.org/10.1016/j.enconman.2004.10.003

152. Rydh, Carl Johan and Sandén, Björn A., *Energy analysis of batteries in photovoltaic systems. Part II: Energy return factors and overall battery efficiencies.* Energy Conversion and Management, 2005. 46 (11-12): p. 1980-2000.http://dx.doi.org/10.1016/j.enconman.2004.10.004

153. Ch. Fabjan , J. Garche , B. Harrer , L. Jorissen , C. Kolbeck , F. Philippi , and G. Tomazic , F. Wagner, *The vanadium redox-battery: an efficient storage unit for photovoltaic systems.* Electrochimica Acta, 2001. 47: p. 7

154. *The Multiple Benefits of Integrating the VRB-ESS with Wind Energy - Case Studies in MWH Applications*, (2007), VRB Power Systems Inc. p. 14

155. *The VRB Energy Storage System (VRB-ESS TM) An Introduction to Wind & the Integration of a VRB-ESS*, (2007), VRB Power Systems Inc

156. Joerissen, Ludwig;Garche, Juergen;Fabjan, Ch; and Tomazic, G., *Possible use of vanadium redox-flow batteries for energy storage in small grids and stand-alone photovoltaic systems.* Journal of Power Sources, 2004. 127(1–2): p. 98-104.http://dx.doi.org/10.1016/j.jpowsour.2003.09.066

157. http://www.poweringnow.com/. *REDT (Renewable Energy Dynamics Technology Ltd.) - last acessed in 12/06/2013*.

158. http://www.gefc.com/en/. *Golden Energy Fuel Cell Co., Ltd. - last acessed in 12/06/2013*.

159. http://www.vfuel.com.au/. *V-Fuel - last acessed in 12/06/2013*.

160. http://www.pdenergy.com/. *Prudent Energy - last acessed in 12/06/2013*.

161. http://vanadiumbattery.com/. *Cellennium (Thailand) Company Limited - last acessed in 12/06/2013*.

162. http://www.gildemeister.com/de. *Gildemeister - last acessed in 12/06/2013*.

163. http://www.gec.cn/en/. *Golden Energy Century Ltd - last acessed in 12/06/2013*.

164. *http://www.ashlawnenergy.com/index.php . Ashlawn Energy - last acessed in 19/06/2013*.

165. *http://www.heh.pt/*. Henriques & Henriques S.A - last acessed in 15/07/2013;

166. *www.citergaz.com*. Citergaz - last acessed in 15/07/2013;

167. http://mykin.com/. *Mykin Inc. - last acessed in 07/08/2013*.

168. http://www.customadvanced.com/, *Custom Advanced Connections, Inc. - last acessed in 07/08/2013.*

169. http://www.ingersollrandproducts.com/_downloads/ChemGuide_8677-P.pdf, *Ingersoll Rand - last acessed in 07/08/2013.*

170. *Petrotec - Notícias; Last acessed in 07/11/2013*. Available from: http://www.petrotec.pt/index.php?id=52&tbl=noticias

171. Sanzhong, Bai and Lukic, S. M., *Unified Active Filter and Energy Storage System for an MW Electric Vehicle Charging Station.* Power Electronics, IEEE Transactions on, 2013. 28(12): p. 5793-5803.10.1109/tpel.2013.2245146

172. Moore, Mark A.;Counce, Robert M.;Watson, Jack S.;Zawodzinski, Thomas A; and Kamath, Haresh, *A Step by Step Methodology for a Base Case Vanadium Redox Flow Battery*, in *University of Tennessee, Knoxville* 2012

173. Dumanic, Dominic and Wallin, Fredik, *Flow Batteries Status and Potential*, in *Malardalens Hogskola - Institutionen for Samhallsteknik* 2011

174. Lutes, Katie, *Study Level Design of a Vanadium Redox Flow Battery*, in *University of Tennessee Honors Thesis Projects* 2013

175. Streeter, Victor L. and Wylie, E. Benjamin, *Mecanica dos Fluidos*. 7ª ed 1982

176. Abecassis, F. and Cabral, N., *Análise Económica e Financeira de Projetos*. 3rd ed, ed. F.C. Gulbenkian 1991